# Universitetet i Stavanger

# DET TEKNISK-NATURVITENSKAPELIGE FAKULTET

# MASTEROPPGAVE

| Studieprogram/spesialisering:<br>Offshore Technology – Offshore systems | Vår semesteret, 2009<br><br>Konfidensiell |
|---|---|
| Forfatter: Eivind Hvidsten | …………………………………………<br>(signatur forfatter) |

Faglig ansvarlig Professor Ove Tobias Gudmestad, Universitetet i Stavanger

Veileder(e): Professor Ove Tobias Gudmestad, Universitetet i Stavanger
        Per Richard Nystrøm, IKM Ocean Design

Engelsk tittel:

    Pipelaying on uneven seabed

Studiepoeng: 30

| Emneord:<br><br><br>Pipelines, S-lay, span length ,strain, OrcaFlex, experiment | Sidetall: 99<br>+ vedlegg/annet: 42 + CD<br><br><br>Stavanger, 15.06.09 |
|---|---|

# Preface

This thesis has been written during the spring of 2009. The thesis is the final part of achieving my master degree in Offshore Technology – Offshore Systems at the University of Stavanger.

The work has been done in cooperation with IKM Ocean Design.

The written part of the thesis has taken place at IKM Ocean Design's offices at Forus, Stavanger, as well as at the University. The laboratory experiments were performed in Professor Ove Tobias Gudmestad's barn at Nærbø, Hå.

Many people have been involved in this project, helping, contributing with ideas and making the project possible to accomplish.

Special thanks go to;

Employees at the University of Stavanger;

- Professor Ove Tobias Gudmestad for supervising me during the project. He has given me great help and guidance and contributed with many ideas during the project. Gudmestad also made this project possible by lending us his barn.

- John Grønli, chief of the laboratory at the University. I would like to thank him for letting me use the laboratory at the University when constructing and doing tests before the real experiments could start. He also provided me with funds for the material used.

- Ahmad Yaaseen Amith, teacher at the University of Stavanger. I would like to thank Amith for teaching me how to use the strain gauges and the related measuring equipment. He also lent me this equipment. I also want to thank him for his quick ordering of the strain gauges needed.

Employees at IKM Ocean Design;

- Per Nystrøm, engineering manager. Nystrøm has been of great help and has contributed with many good ideas on how to execute the laboratory tests. I would also like to thank him for providing me with an office space at IKM's offices as well as providing funds for parts of the material used in the experiments.

- Loic Meignan, engineer. A special thank goes to Meignan for introducing me into the software OrcaFlex.

# Table of Contents

# Nomenclature and abbreviations

| | |
|---|---|
| ASD | = Allowable stress design |
| CSF | = Concrete Stiffness Factor |
| FPSO | = Floating Production Storage and Offloading |
| SMYS | = Specified Minimum Yield Stress |
| TDP | = Touchdown Point |
| VIV | = Vortex Induced Vibrations |

| | |
|---|---|
| $\Delta T$ | = Temperature increase |
| $\mu$ | = Friction coefficient |
| $A$ | = Cross-sectional area of steel |
| $A_e$ | = External cross-sectional area |
| $A_i$ | = Internal cross-sectional area |
| $C_1$ | = Boundary condition |
| $C_3$ | = Boundary condition |
| $D$ | = Outside pipe steel diameter |
| $D_1$ | = Water depth |
| DF | = Design factor |
| $D_{max}$ | = Largest measured inside or outside diameter of the pipeline. |
| $D_{min}$ | = Smallest measured inside or outside diameter of the pipeline |
| $E$ | = Young's Modulus of the pipeline |
| $f$ | = Natural frequency |
| $F_f$ | = Friction force |
| $f_o$ | = The ovality of the pipeline |
| $F_s$ | = Shedding frequency |
| $f_y$ | = Yield stress |
| $f_{y,temp}$ | = Derating value due to temperature |
| $H$ | = Distance from sea surface to top of pipeline/Horizontal pull |
| $I$ | = Moment of inertia |
| $K$ | = Factor proportional to the tension force and opposite proportional to the radius of curvature |
| $L$ | = Horizontal length |
| $L_{eff}$ | = Effective span length |
| $M$ | = Bending Moment |
| $m_e$ | = Effective mass |
| $N$ | = Pipe wall force |
| $o$ | = Buoyancy of the stinger per unit length |
| $p_c$ | = Collapse pressure |
| $P_{cr}$ | = Critical buckling load |
| $p_e$ | = External pressure |
| $p_i$ | = Internal pressure |
| $p_{min}$ | = Minimum internal pressure |
| $R$ | = Bending radius of pipeline |
| $r$ | = radius of the pipeline |
| $s$ | = Distance along pipe span |

| | |
|---|---|
| $S$ | = Length of the free spanning pipeline |
| $S_0$ | = Quantity for calculation of free span |
| $S_a$ | = Axial stiffness |
| $S_b$ | = Bending stiffness |
| $S_{eff}$ | = Effective axial force |
| $S_t$ | = Strouhal number |
| $T$ | = Tension force |
| $T$ | = Natural period |
| $t_1$ | = Pipe wall thickness factor |
| $t_2$ | = Pipe wall thickness factor |
| $T_h$ | = Horizontal force |
| $U$ | = Current velocity |
| $v$ | = Poisson's ratio |
| $w_1$ | = Submerged weight of the pipeline per unit length |
| $w_2$ | = Weight of pipeline in air per unit length |
| $x$ | = horizontal axis |
| $z$ | = Height above seafloor |
| $Z_1$ | = Height from seabed to surface |
| $Z_2$ | = Height of the pipeline above surface |
| $\alpha$ | = Horizontal angle of the stinger |
| $\alpha_u$ | = Material strength factor |
| $\gamma_{cc}$ | = Safety factor for concrete |
| $\gamma_m$ | = Material resistance factor |
| $\gamma_{sc}$ | = Safety class resistance factor |
| $\delta$ | = Pipe deflection |
| $\varepsilon$ | = Bending strain |
| $\varepsilon_0$ | = Accepted strain |
| $\varepsilon_{axial}$ | = Axial strain |
| $\varepsilon_{cc}$ | = Concrete crushing strain |
| $\varepsilon_{mean}$ | = Mean overbend strain |
| $\eta$ | = Usage factor |
| $\rho$ | = Density of seawater |
| $\sigma_0$ | = Minimum specified yield stress |
| $\sigma_{eq}$ | = Equivalent stress |
| $\sigma_h$ | = Hoop stress |
| $\sigma_l$ | = Longitudinal/axial stress |
| $\tau_{hl}$ | = Tangential shear stress |
| $\theta$ | = Angle of pipeline |

# Summary

The first part of this thesis outlines some theoretical aspects of pipeline installation. The reader is introduced to some of the issues and parameters involved when installing subsea pipelines.

The main objective of this thesis was to construct a test rig to be used for performing several investigations regarding S-laying of a pipeline. The test rig was made of a stinger mounted to a lift. Tension force was applied to the pipeline by attaching calibrated weights by a wire system.

Several of the investigations are also analysed in the software OrcaFlex and a comparison has been made of the results from OrcaFlex and the experiments.

Many tests were performed during this thesis, and the most important results, presented in this report, are;

- OrcaFlex does not take the friction force from the stinger into consideration. This will cause the applied tension force in the OrcaFlex simulation to be larger than the tension force acting on a real pipeline laying on a stinger with friction. The bending radius of the pipeline in the sagbend will therefore be larger in the OrcaFlex model, resulting in smaller strains. This means that for installation analyses of pipelines, the strains calculated in the sagbend by OrcaFlex are not necessarily conservative.

- If a scenario should occur where there is a failure in the laying vessels' positioning system or there is a slip of the anchor system, the consequence for the pipeline could be fatal.

- In order for low tension force to result in plastic deformation in the free spans created by an uneven seabed, the unevenness/obstacle has to be substantial.

# 1    Introduction

## Heading for deeper water

Until quite recently most existing oil and gas fields have been developed in limited water depths. All oil companies' dream is to find large fields in shallow water. Many of these reservoirs will soon be empty and the probability of finding new fields like these in the North Sea and in shallow waters in the rest of the world in the future will become increasingly small.

The oil and gas industry will have to prepare itself for more and more fields in deeper waters. The likelihood of finding very big fields will also decrease. This means that the efforts have to be put into small deepwater fields.

In fields like these new platforms or FPSOs will often not be profitable. A possible solution will be subsea installations with tieback to already existing platforms, to shore or to other pipelines. This implies that a lot of pipelines might have to be installed in deep waters in the future.

## Stresses in pipeline during installation

Pipeline installation in deep waters is much more complicated than installation in shallow water, and makes greater demands on both the pipeline and the laying vessels.

As the water gets deeper the free spanning part of the pipeline from the T.D.P (touchdown point) to the stinger of the vessel gets longer. This will result in heavy weight of the free spanning pipeline, which means that the pipeline will be exposed to great stresses. In order to deal with these stresses and reduce the bending strains that will occur in the sagbend of the pipe, a large tension force has to be applied from the vessel. The deeper the water is, the larger tension force has to be applied to the pipe in order to secure a safe bending radius in the lower bend (the sagbend).
.
The heavy weight of the pipeline will therefore make great demands on the vessel's tension machines. A sudden failure or malfunction of the tension machine will hence be a nightmare scenario and can have damaging consequences for the pipe.

A number of theoretical formulas for calculation of stresses and required tension force exist. One of the purposes of this project is to verify these formulas by performing actual tests.

A study of how critical a malfunction in the tension system will be will also be carried out. It is of interest to investigate the effects of a malfunction in the tensioning system. It should be noted that a slip of the anchor system will have the same effect on the pipe as loss of tension.

# 2    Objectives

One of the purposes of this thesis is to study pipelines and installation of pipelines in general, and get to know the main challenges that may occur during pipeline installation. This will be done through:

- Finding the maximum stress/strain in overbend and sagbend as well as in the free spans on the seabed. A study will be carried out in order to investigate how these stresses change as the water gets deeper and the tension forces vary. It will be investigated whether loss of tension will lead to a plastic deformation, and if possible it will be determined how great the water depth has to be in order to get plastic deformation in sagbend if tension is lost.

- Measuring the span length of the pipe from the departure point of the stinger to the touchdown point. This will also be done for different tension forces. These lengths will be measured in order to get an understanding of how much the applied tension will affect the span length and how critical it will be if there should be a loss of tension.

- Investigating how the tension force will affect free spans on the seabed formed due to unevenness and whether a loss of tension force situation will result in plastic deformation in the free spanning pipeline on the seabed.

- Investigating the natural frequency of the free span from the touchdown point to the stinger. By doing this it is possible to figure out in which current velocities the pipeline can be installed without getting into resonance with vortexes shed by the current flow.

- Scale testing and back-calculation to investigate the correctness of theoretical analysis.

There are several ways of installing subsea pipelines, but the most important ones are
- S-lay
- J-lay
- Reeling
- Towing of pipelines

However, the main purpose of this report is to study S-laying of pipelines.

# 3 S-lay Method

## 3.1 Principle

S-lay is the most frequently used method of installing large diameter pipelines in shallow water and is feasible in water depths up to 700 meter. S-lay is performed either from a semi-submersible lay barge or from a ship. [5]

S-lay means that the pipeline takes the form of an S when it is lowered into the sea and an overbend and a sagbend are formed. In order to prevent the pipeline from taking the shortest path to the seabed, J-lay, a stinger is needed. The stinger, which is an arc-formed construction at the stern or at the side of the lay vessel is generally what makes the pipeline form into an S.

The overbend usually extends from the tensioners on the deck of the barge and continues over the ramp until the lift of point, which is the point where the pipeline leaves the stinger. The point at which the pipeline is straight is called the inflection point. At the inflection point the sagbend starts and lasts until T.D.P (the touchdown point), which is the point where the pipeline touches the seabed [3].  This is shown in Figure 1.
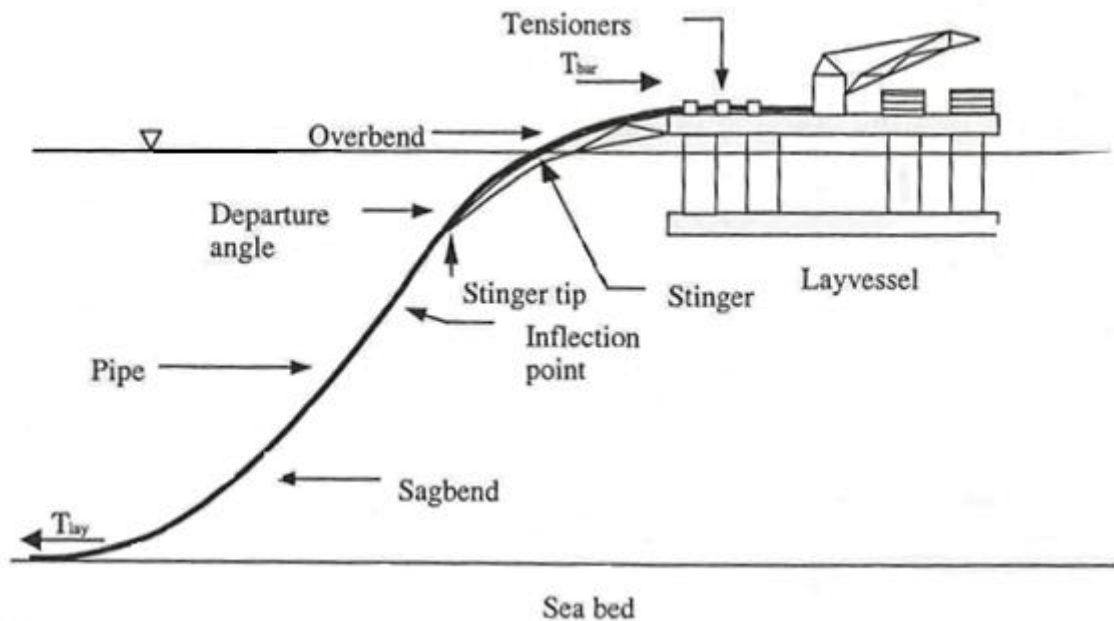


**Figure 1. S-lay configuration. [2]**

The pipeline is supported by the rollers on the deck of the vessel and the stinger. When the pipeline passes the stinger as the vessel moves forward it takes the form of a convex-

downward curve. This is called the overbend and is basically what distinguishes the s-lay method from the j-lay method. After the inflection point the pipeline takes the shape of a convex-upward curve. This is the sagbend [8].

# 4    The overbend

The radius of the stinger should be large enough so that the pipeline does not experience plastic deformations. In order to assure this, the bending stress should not exceed 85% of the SMYS (Specified  Minimum Yield Stress ) [3]. According to [3], the bending strain can be calculated with the following equation :

$$\varepsilon = \frac{D}{2R} \tag{4.1}$$

Where,
   $\varepsilon$ = Bending strain
   D = Outside pipe steel diameter
   R = Bending  radius of the pipeline in the overbend

Further, [3] states that the minimum over-bend radius is given by the equation:

$$R = \frac{E \cdot D}{2\sigma_0 \cdot DF} \tag{4.2}$$

Where,
   $\sigma_0$ = Minimum specified yield stress
   DF = Design factor, usually 0.85
   E = Elastic modulus of the pipeline
   D = Outside pipe steel diameter

As seen from Equation 4.1 large diameter pipelines need a larger stinger radius in order not to get plastic deformation.

DNV-OS-F101 states in section H 300 that when there is static loading, calculated strain shall satisfy criterion I in Table 1. Effects from bending, axial force and local roller loads shall be included in the calculated strain.

Further DNV says that for a combination of static and dynamic loading the calculated strain shall satisfy Criterion II in Table 1.

**Table 1. Criteria for strain in the overbend for pipes of different steel qualities [4].**

| Simplified criteria, overbend | | | | |
|---|---|---|---|---|
| Criterion | X70 | X65 | X60 | X52 |
| I | 0.270% | 0.250% | 0.230% | 0.205% |
| II | 0.325% | 0.305% | 0.290% | 0.260% |

## 4.1    The stinger

The main purpose of the stinger is to support the pipeline in the overbend and assure a secure bending radius in the overbend.

### 4.1.2  Different stinger types  [1]

Basically three different stinger configurations have been used in the North Sea. The main groups are:
1.  Rigid stinger firmly connected to the lay vessel
2.  Rigid stinger hinged to the lay vessel
3.  Articulated stinger

a. Rigid stinger firmly connected

b. Rigid stinger firmly connected to the side of the vessel

c. Hinged, rigid stinger

d. Articulated stinger

e. Articulated stinger
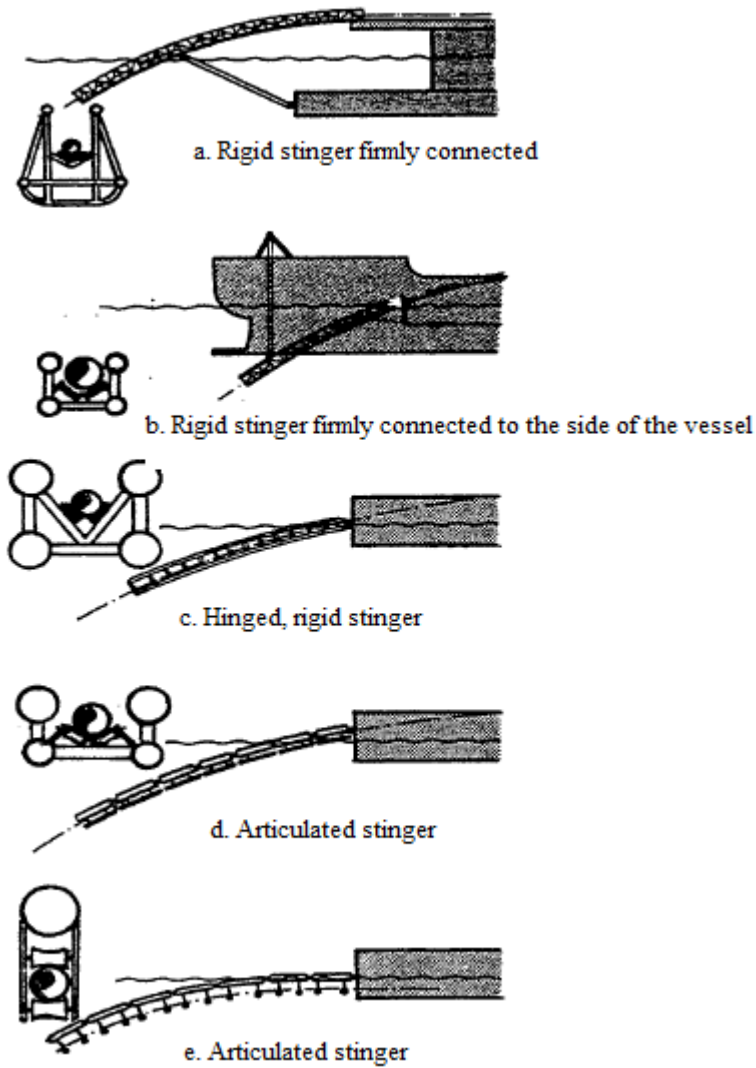
**Figure 2a-e. Different types of stingers [1].**

### 4.1.2.1      Rigid stinger firmly connected to the lay vessel  [1]

There are two different types of rigid stingers that are firmly connected. One is shown in Figure 2a. This type of stinger is firmly connected to the rear end of the vessel. It is constructed in a way that makes it possible to hoist the stinger from the water. Hence one is able to avoid that the greatest wave forces act on the stinger.

Figure 2b shows an example of a stinger firmly connected to the side of the vessel. This type of stinger is supported in both ends. The forces acting on the stinger are relatively small. Despite this, lack of horizontal support at the rear of the stinger may result in extensive forces on the narrow stinger connection point in the front end and on the pipeline in case of major departure sideways of the lay vessel or major directional departure in relation to the pipeline. Heave and pitch motions might cause huge dynamic loads on the stinger.

### 4.1.2.2        Rigid stinger hinged to the lay vessel  [1]

This type of stinger is shown in Figure 2c. The stinger can consist of several elements which are joined into a long, slim and arced construction. The relative motion between the stinger and the vessel will lead to significant movements in the hinge which connects the stinger to the vessel. This can result in great bending loads in the area of the pipeline close to the hinge. This means that the static curvature of the pipeline has to be less in this area than the maximum allowed curvature.

### 4.1.2.3        Articulated stinger hinged to the lay vessel  [1]

This type of stinger consists of several elements which are hinged together into a chain. Each element has a limited opportunity to rotate both in horizontal and vertical plane relative to the neighbour elements. Figures 2d and 2e show examples of this kind of stingers.

Each element has a net buoyancy equivalent to the loading from a curved pipeline segment on that specific element. Since the stinger has constant buoyancy per unit length, the overbend of the pipeline will take the shape of an inverted chain. The largest curvature will then be at the surface and decreases downwards.

It is desirable to maintain as large curvature at possible downwards the pipeline in order to be able to use a short stinger. In order to do this the buoyancy of the stinger has to increase as the gradient increases. The buoyancy can be calculated using the equation:

$$o = w_1 + \frac{K}{\cos\alpha} \qquad (4.3)$$

Where,
o   = The buoyancy of the stinger per unit length.
$w_1$ = The submerged weight of the pipeline per unit length.
α   = The horizontal angle of the stinger
K  = Factor proportional with the tension force and opposite proportional to the radius of
      curvature.

Because of the stinger's extensive flexibility, the static radius of curvature has to be larger than the allowed bending radius of the pipeline. In cases where the bending stresses on the stinger exceed the limited radius of curvature, e.g. due to large wave forces, the stinger will act as a rigid construction. However, large curvatures caused by large wave forces can damage the stinger.

### 4.1.3  Comparison and evaluation of the stingers [1]

There are many factors that need to be taken into consideration when choosing and designing a stinger. The most important ones are:

- Maximum stinger length
- Acceptable  wave conditions
- Additional dynamic loading on the pipeline
- Handling properties.

Rigid stingers firmly connected to the lay vessel have the greatest limitations when it comes to maximum stinger length. This is because of the large moments that occur as the length of the stinger increases. Hence, large stinger lengths make stricter demands on the stinger.

The articulated stingers are the ones that involve least problems as the stinger length gets large. The compressive force between the articulations will always be less than the tension force in the pipeline, because of this, no stability problem is caused.

When it comes to additional dynamic loading on the pipeline, the rigid, hinged stinger is the least favourable choice. This is because the whole relative motion between the stinger and the vessel is concentrated in the hinges between the stinger and the vessel. Because of this the pipeline has to be led over the hinges with a relatively small curvature.

The choice that gives the least additional dynamic loading is the rigid, firmly connected stinger.

Generally, the stinger shaped as a rigid framework and firmly connected, is the most favourable choice for large vessels which have small movements due to waves. This is also the best choice for vessels that have the production line high above the surface.

# 5 The sagbend

According to the Statoil Specification F-SD-101 the strains in the sagbend in a pipeline of steel quality X65 should not exceed 0.15 percent [2].

Further DNV-OS-F101 states in section H 300 that for a combination of static and dynamic loads the following equation shall be satisfied both in the sagbend and at the stinger tip:

$$\sigma_{eq} < 0.87 \cdot f_y \tag{5.1}$$

Where,

$f_y$ = Yield stress

$\sigma_{eq}$ = Equivalent stress, Von Mises

The material strength, $f_y$, can be calculated using the formula:

$$f_y = (SMYS - f_{y,temp}) \cdot \alpha_U \tag{5.2}$$

Where,

$f_{y,temp}$ = De-rating values due to the temperature of the yield stress and can be found in Figure 2 in DNV-OS-F101.

$\alpha_U$ = Material strength factor found in Table 5-5 in DNV-OS-F101.

The DNV-OS-F101 does not state any limit state criteria for pipeline bends. However, the DNV standard states on page 54 that the Allowable Stress Design (ASD) can be used given that:

- *"The pressure containment criterion listed in section D200 is fulfilled."*

- *"The applied moment and axial load can be considered displacement controlled."*

- *"The bend is exposed to internal over pressure or that the bend has no potential for collapse."*

- *"That the imposed shape distortion (e.g. ovalization) is acceptable."*

The ASD criteria are given by:

$$\sigma_{eq} \leq \eta \cdot f_y \tag{5.3}$$

$$\sigma_l \leq \eta \cdot f_y$$

$$\tag{5.4}$$

Where,

$\eta$ = Usage factor, see Table 5-13 in DNV-OS-F101

$\sigma_{eq}$ = Equivalent Von Mises stress

$\sigma_l$= Longitudinal/axial stress of the pipeline

The equivalent stress is calculated using the formula:

$$\sigma_{eq} \leq \sqrt{\sigma_h{}^2 + \sigma_l{}^2 - \sigma_h \cdot \sigma_l + 3 \cdot \tau_{hl}{}^2} \tag{5.5}$$

Where,

$\sigma_h$ = Hoop stress of the pipeline

$\tau_{hl}$ = Tangential shear stress

The hoop stress is calculated with the equation:

$$\sigma_l = (p_i - p_e) \cdot \frac{D - t_2}{2 \cdot t_2} \tag{5.6}$$

Where,

$p_i$ = Internal pressure of pipeline

$p_e$ = External pressure of pipeline

$t_2$ = Pipe wall thickness, see table 5-2 in DNV-OS-F101

Further, [4] states that the longitudinal stress is calculated using the equation:

$$\sigma_l = \frac{N}{\pi \cdot (D - t_2) \cdot t_2} + \frac{M}{\frac{\pi \cdot (D^4 - (D - 2 \cdot t_2)^4)}{32 \cdot D}} \tag{5.7}$$

Where,

N = Pipe wall force

M = Bending moment

# 6 Forces acting during installation

During all types of pipe laying axial tension, T, has to be applied by the tensioning system of the vessel. The main task of the applied tension force is to control the bending radius in the sagbend, S. In addition it must carry the weight, w, of the span which is the free hanging part of the pipeline. Even though the applied tension has some influence on the length that the pipe will follow the stinger, it will not have any major effect on the shape the pipeline will take in the overbend. However, a large tension force will make the pipeline leave the stinger a bit earlier [1].

The tension force is largest immediately after the tension machine and decreases all the way to the sea bed.

The tension force, T, required with S-laying is the same as what is needed for J-laying [1].

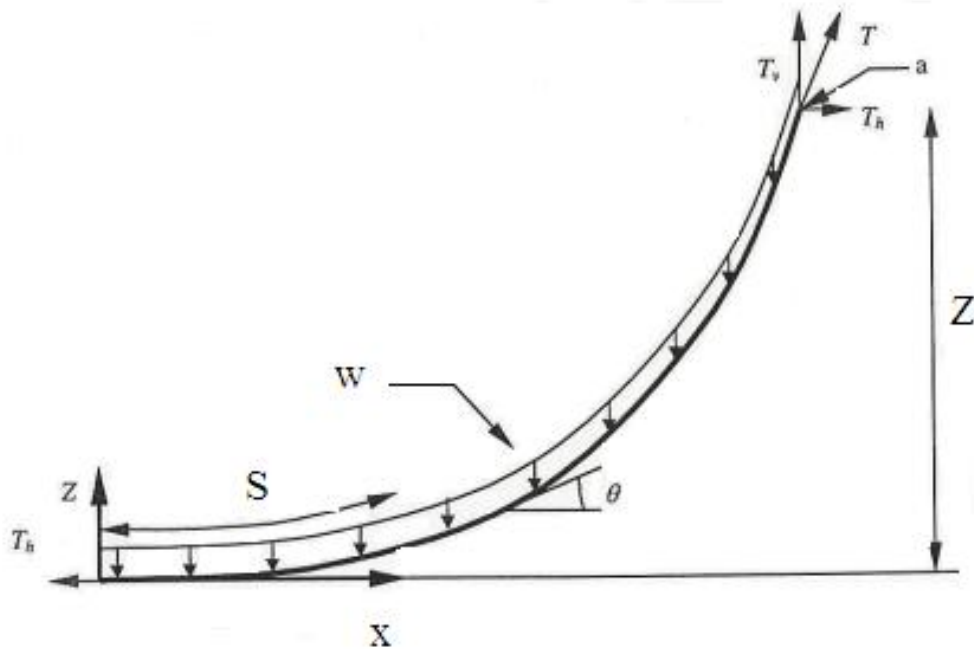Figure 3 shows the forces which are acting on the sagbend, S.



**Figure 3. Forces acting on the sagbend [2]**

It is worth noticing that the tension force applied by the tensioners is equal to the horizontal tension force at sea bottom if friction forces and the pipeline weight are neglected.

Hence the following equation can be made [3]:

$$T = T_h + w_1 \cdot Z_1 + w_2 \cdot Z_2 \tag{6.1}$$

Where,
T = Tension in pipeline
$T_h$ = The horizontal force in the pipeline at the bottom
$w_1$ = Submerged weight of pipeline per unit length
$w_2$ = Weight of pipeline per unit length in air
$Z_1$ = The pipeline's height from sea bed to surface
$Z_2$ = The pipeline's height above the surface

There are several different models for calculations of the behaviour of the pipe in free span between the stinger and the T.D.P. Some of these are described below.

## 6.1 Beam method [3]

For shallow water installations the beam method can be used. By using this method the deflections are assumed to be small and the following requirement is used:

$$\frac{dz}{dx} << 1 \tag{6.2}$$

Where,
x = Horizontal axis from T.D.P.

Rather than being looked upon as a chain the span in the sagbend is here being modelled as a segment of a beam. As opposed to the catenary model this method takes bending stiffness into consideration.

The bending equation for the beam method can then be expressed as follows:

$$-w_1 = EI \cdot \frac{d^4 z}{dx^4} - T_h \cdot \frac{d^2 z}{dx^2} \tag{6.3}$$

Where,
EI = Bending stiffness of the pipe

The following boundary conditions have to be fulfilled:

z (0) = 0 (which means that the x-axis has zero value at the seabed)  (6.4)

$$\frac{dz}{dx}(0) = \Theta \,(\text{slope of seabed}) \tag{6.5}$$

$$\frac{d^2z}{dx^2}(0) = 0 \tag{6.6}$$

z (L) = H, the water depth.  (6.7)

Where,

L = Horizontal length from T.D.P. to point of interest.

$$\text{EI}\,\frac{d^2z}{dx^2}(L) = M \quad (\text{M = 0 at inflection point}) \tag{6.8}$$

## 6.2   Nonlinear beam method  [3]

Another method that is applicable in all water depths is the nonlinear beam method. In this model the bending of the pipe span is described by considering the nonlinear-bending equation of a beam. This theory is valid for both small and large deflections, and is described by the following formula:

$$-w_1 = \text{EI}\,\frac{d}{ds}(\text{Sec}\theta\,\frac{d^2\theta}{ds^2}) - T_h\,\text{Sec}^2\theta\,\frac{d\theta}{ds} \tag{6.9}$$

Further we have

$$\text{Sin}\theta = \frac{dz}{ds} \tag{6.10}$$

Where,
s = distance along pipe span
θ = Angle at distance s

Due to the fact that the boundary conditions usually include the displacement at one of the two ends of the span the above differential equation can be described with y rather than θ. In order to get a more complex equation for z(s) than for θ(s), θ can be substituted in terms of z and s.

## 6.3    Natural catenary method

The vertical position of the pipe can be found using the following equation [1]:

$$z = \frac{T_h}{w_1}(\cosh\frac{x \cdot w_1}{T_h} - 1)$$

(6.11)

It is worth noticing that this is the equation that describes the shape of a chain. The boundary conditions are not satisfied so this theory is applicable only for parts of the pipelines which are away from the ends. For pipeline installations in deep water where the stiffness of the pipe is very small compared to the weight and the axial tension, the stiffness can be neglected. By doing this the pipeline will take the shape of a chain. By setting the stiffness of the pipelines to zero (EI = 0) in Equation 6.9, the following equation is obtained [3]:

$$w_1 = T_h \operatorname{Sec}^2\theta\frac{d\theta}{ds}$$

(6.12)

The fact that the actual pipe is stiffer than what is accounted for in the equation will lead to a larger radius of curvature than what is calculated using the chain equation, which means that this formula is conservative. This also applies to the calculated tension and stinger length needed.  In deep waters this equation will result in small errors and can therefore be used [3].

The curvature in the sagbend is largest at the T.D.P and can be calculated using the following equation [1]:

$$\frac{1}{R} = \frac{w_1}{T_h}$$

(6.13)

By using the bending radius found by Equation 4.2 and solving Equation 6.13 for the horizontal force, the horizontal tension force needed to avoid plastic deformation in the sagbend can be found.

According to [1], the following formula can be used in order to find the axial force acting at a specific point in the pipeline:

$$T = w_1 (z + \frac{r}{\varepsilon_0})$$ (6.14)

Where,

$\varepsilon_0$ = The accepted strain

r = Radius of the pipe

z = Height above seafloor where z = 0

Equation 6.14 can be rewritten in order to find a new equation for calculation of the required tension force in order to avoid plastic deformation in the sagbend [1]:

$$T = w_1 \left(D_1 + \frac{r}{\varepsilon_0}\right) + w_2 \cdot H$$ (6.15)

Where,

$D_1$ = Water depth

$w_2$ = Weight of pipeline in air

H = Distance from sea surface to top of pipeline

The length of the free span can also be calculated using the following equation [1]:

$$S = z \sqrt{1 + 2 \frac{T_h}{z \cdot w_1}}$$ (6.16)

Where,

S = length of the free spanning pipeline

## 6.4    Stiffened catenary method

Another way to perform calculations of the free span is to use the stiffened catenary method. What makes this method different from the catenary method is that it includes the bending stiffness of the pipe. In addition the boundary conditions are satisfied. Equation 6.9 is here solved asymptotically. One assumption that has to be made is that the non-dimensional term $\alpha^2$, which is a term depending on the stiffness of the pipe, has to be very small. This term is given by the following equation [3]:

$$\alpha^2 = \frac{E \cdot I}{w_1 \cdot S^3} \ll 1$$ (6.17)

As seen from Equation 6.17, if the water depth is not very large, the stiffness of the pipe has to be rather small and the weight of the pipe large. Because of the fact that the boundary

conditions are satisfied, this model provides accurate results for the whole pipeline including the regions near the ends [3].

## 6.5 Hydrostatic pressure

The deeper the water, the larger the external pressure on the pipeline will be, and therefore the external pressure is normally not critical in shallow water.

All pipelines will be exposed to external pressure during installation and a certain period after installation. During installation there is atmospheric pressure inside the pipeline and the external pressure acting on the pipe varies with the water depth. The main point of concern regarding external pressure is that it can lead to propagating buckling.

The external pressure is calculated using the equation:

$$p_e = \rho \cdot g \cdot h \tag{6.18}$$

Where,

$p_e$ = External pressure
$\rho$ = Density of seawater
$g$ = Acceleration of gravity
$h$ = Water depth

This means that for a constant seawater density, the external pressure is linear with the water depth. Figure 4 shows how the external pressure varies with different water depths when the density of seawater is chosen as 1026 kg/m$^3$. However, because of the compressibility of the seawater, the density of water will increase slightly as the water depth increases [6].
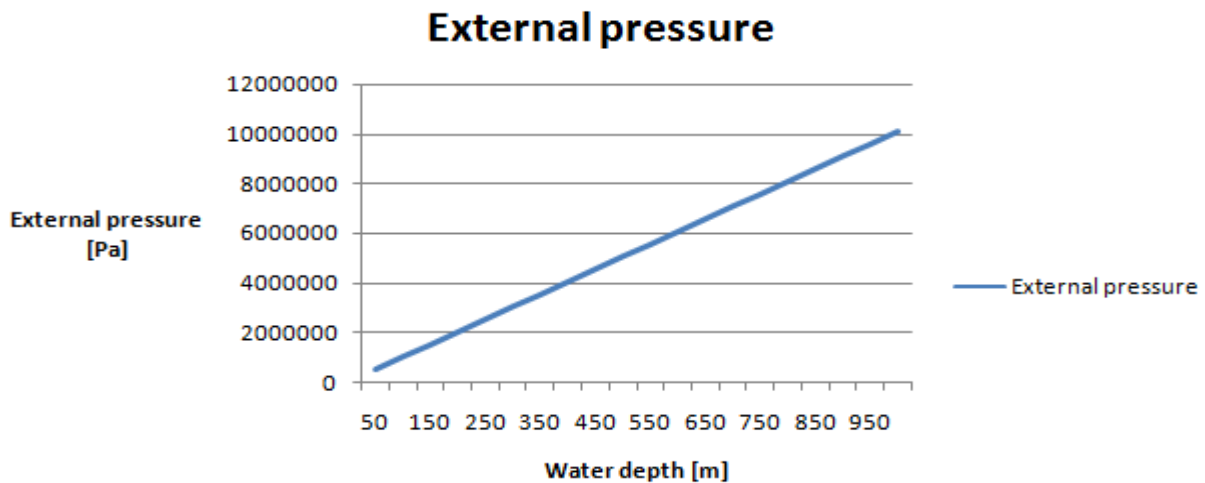


**Figure 4. The external pressure as a function of the water depth.**

DNV-OS-F101 states that the external pressure shall meet the following requirement listed in the equation below for any point of the pipeline. This is in order to avoid system collapse due to buckling.

$$p_e - p_{min} \leq \frac{p_c \cdot t_1}{\gamma_m \cdot \gamma_{SC}}$$

(6.19)

Where,

$p_e$ = External pressure

$p_{min}$ = Minimum internal pressure that can be sustained

$p_c$ = Characteristic collapse pressure

$t_1$ = Pipe wall thickness (see Table 5-2 DNV-OS-F101)

$\gamma_m$ = Material resistance factor (see Table 5-4 DNV-OS-F101)

$\gamma_{sc}$ = Safety class resistance factor (see Table 5-5 DNV-OS-F101)

This means that the larger internal pressure, the less critical the effect from external pressure will be.

During installation of pipelines $p_{min}$ is normally set as zero, hence the external pressure has to be considered carefully, especially for deep water installations.

# 7    Construction parameters [1]

There are several parameters which the contractor needs to consider before the laying process can start. The most important parameters which affect the burden on the pipe during installation are:

- Axial tension force
- Allowable variation of the tension force
- The radius of the stinger
- The length of the stinger
- The stinger type

As stated earlier, the applied tension force is absolutely crucial in order to secure a safe bending radius in the sagbend.

The tension force in the pipe will also affect the angle of departure at the stinger. A high tension force will make the pipeline leave the stinger earlier. It is worth noticing that a small tension force will not lead to a dangerous bending radius in the overbend. This is due to the stinger. The bending radius in the sagbend will, however, become too small.

The tension force also plays an important role when it comes to the stinger length. The higher the tension force is, the shorter stinger length needed.

The radius of the stinger will provide a safe bending curvature in the overbend. The average curvature of the pipeline in the overbend is in general about the same as the curvature of the stinger.

The laying system's sensitivity to the weather is also dependant on the stinger length.

Both the stinger length and the stinger radius depend on which type of stinger is used. Rigid stingers need a shorter length and a smaller curvature than what is needed for flexible stingers due to the fact that the flexible stingers often have a local dynamic variation of the stinger radius.

# 8    Criteria for dimensioning (selection) of laying parameters [1]

The stresses that the pipeline is exposed to during installation is a once-only phenomenon and the main consideration is to design the pipelines so that there will be no errors or malfunction in the pipeline that may prevent normal operation of the pipeline.

There are several parameters which will have an influence on the dimensioning of the pipelines, but the most important ones when dimensioning for loads during installation are:
- Residual curvature
- Residual ovalisation
- Possibility of exceeding the bending strength
- Damage to the concrete coating

Because of the fact that both the dynamic and static loading is different, the overbend and sagbend should be analysed individually.

## 8.1    The traditional criteria for dimensioning

For pipeline installation in the North Sea a limitation of bending strain from 80-85 % of the yield stress seems to be a basis for the choice of laying parameters [1].

## 8.2    The allowable strain of a pipeline

Previous experience has shown that a steel pipeline can be bent far beyond the yielding point without losing any capacity of tolerating internal pressure. During reeling, the curvature of the pipelines has in some cases been so large that the strains have reached 2-3%. The yielding point for pipelines is defined as the stresses at which the total strain is 0.5% [1]. The total strain is a combination of elastic and plastic strain. For 415 grade C-Mn steel, a total strain of 0.5% can consist of 0.2% elastic strain and 0.3% plastic strain [4]. This is shown in Figure 5.
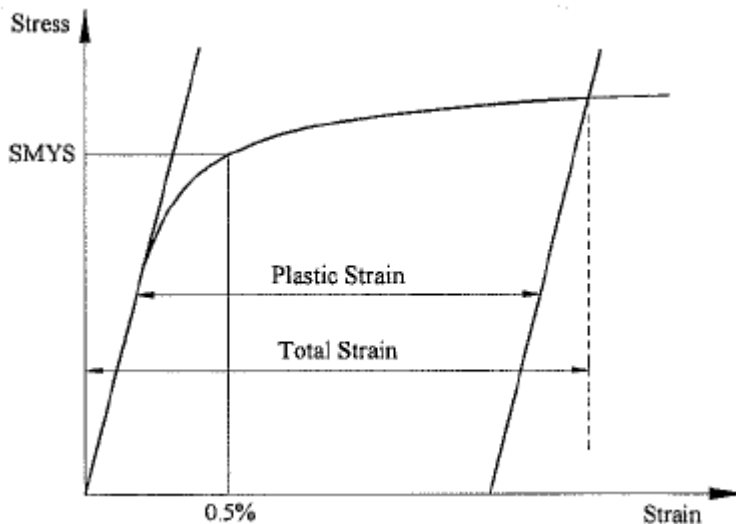


**Figure 5. Reference for plastic strain calculation [4].**

For pipelines the proportionality limit is normally 75% of the yield stress. Since it is normal to tolerate 85% of the yield stress, this means that the pipeline will experience plastic deformations even during normal laying conditions. Because of this it is common practice to base the criteria for dimensioning of laying parameters on accepted strains and not on stresses [1].

## 8.3    Special strength conditions during pipeline laying  [1]

As seen in Figure 6, the pipeline will not be in actual contact with the stinger but will rest on several rollers, which will reduce the friction force between the stinger and the pipeline. These rollers will cause an elevation in the pipeline's moment, which means that the bending moment will be highest over the rollers and will be at a minimum in the middle between two

rollers. This is also seen in Figure 6. The pipeline might experience plastic deformation if the curvature over a roll results in strains that exceed the proportionality limit.  .

When designing the stinger, the elevation of moment over the rolls as well as the reduced stiffness of the pipeline between the welds due to lack of concrete coating have to be considered carefully.

If the concrete coating increases the pipeline's stiffness by 15%, this will correspond to a 15% increase in strain above nominal strain based on average radius of curvature.
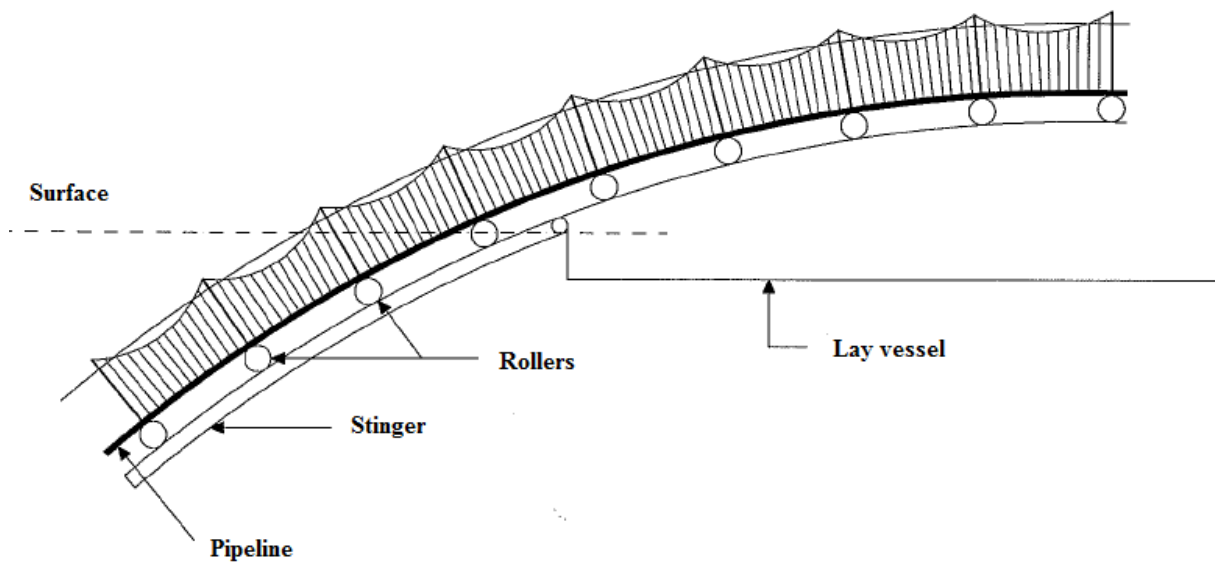


**Figure 6. Moments as the pipeline passes rollers on the stinger [1].**

## 8.4    Exceeding the bending strength

Pipelines which are installed in deep water need a large wall thickness due to the external pressure. These pipelines can usually be called thick walled pipelines, which mean that diameter/wall thickness ratio is less than 40-50. Figure 7 shows a typical moment – curvature diagram for thick walled pipelines [1].
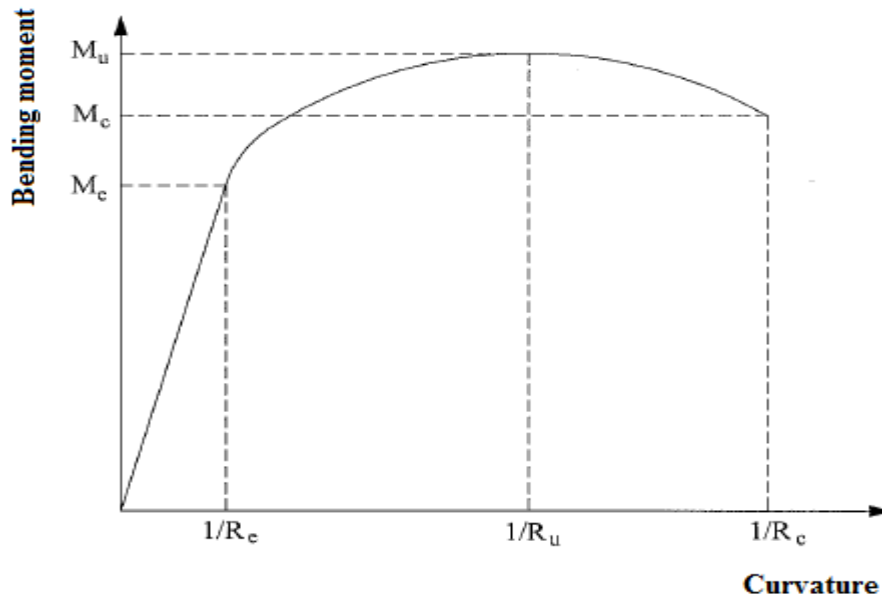
**Figure 7. Typical moment - bending curvature diagram [1].**

Here, $R_e$ is the bending radius where we will get plastic deformation. If the pipeline is bent even more, the cross section of the pipeline will experience an ovalisation. Eventually $M_u$ will be reached which is the maximum obtainable moment. The bending radius which corresponds to this moment is called $R_u$. If the bending radius is reduced even further, the pipeline's capacity of curvature is eventually reached. This radius is called $R_c$. When this degree of curvature is reached the pressure side of the pipeline will suffer from a local buckling. For pipelines with a very thin wall thickness, diameter/wall thickness larger than 250-300, the buckling will occur in the elastic area [1].

The curvature that corresponds to $R_c$ does not necessarily have to be larger than the curvature that corresponds to $R_u$. The smallest curvature of these two should be evaluated in order to ensure that local buckling will not occur [1].

It is important that the nominal bending radius in overbend and sagbend are large enough so that there is a significant safety against local buckling [1].


## 8.5    Residual curvature  [1]

Usually the pipeline will not lay perfectly straight on the seabed because of unevenness etc. this means that some residual curvature in the pipeline can be tolerated after installation.

The axial force in the pipeline, when resting on the seabed, is equal to the horizontal tension force during installation. This force will contribute to the straightening of the pipeline if there is residual curvature. However, the forces this will lead to, can cause serious problems during repairing of the pipeline.

Typically, residual curvatures with bending strains between 0.05-0.1 percent can be tolerated. For pipelines with diameters of 40 and 80 cm this corresponds to residual curvatures with bending radius of 200-400 meters and 400-800 meters, respectively.

Theoretically, the bending forces which the pipelines is exposed to in the sagbend could be used to straighten the pipeline if there would be a plastic deformation in the overbend. Figure 8 shows an example of a pipeline which is experiencing plastic deformations as it passes the stinger.
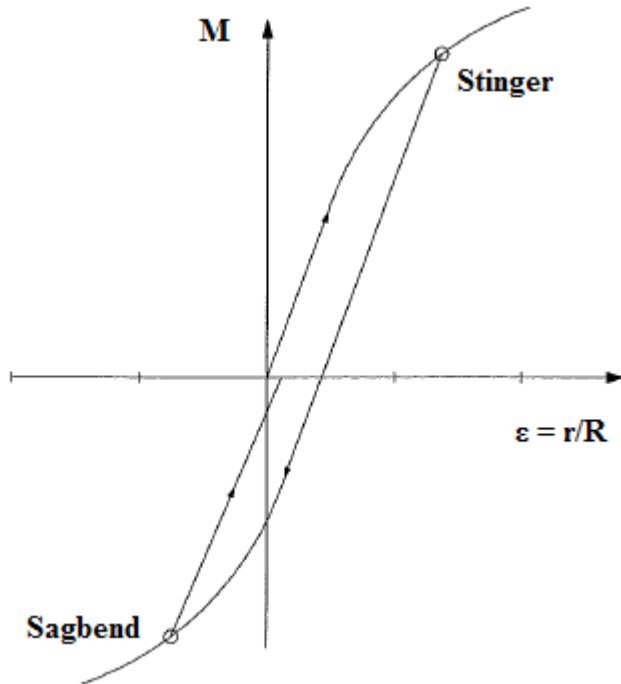


**Figure 8. Moments and strains in the pipeline from the stinger to the seabed [1].**

This means that there will be some residual curvature in the pipeline after the stinger. In the sagbend a greater moment than what it usually needed for a given curvature is added to the pipeline. This moment can straighten the pipeline and if the moment is very large, the pipeline can get residual curvature in the opposite direction.

## 8.6 Residual ovalisation

A pipeline which is bent will suffer from ovalisation. This mean that the pipe will not be a perfect circle but will be flattened by some degree. DN-OS-F101 states that the flattening of the pipe which is caused by bending and out-of-roundness tolerance from fabrication shall not exceed 3%. According to DNV-OS-F101, the ovality can be calculated using the equation:

$$f_0 = \frac{D_{max} - D_{min}}{D} \leq 0.03 \qquad (8.1)$$

Where,
$f_o$ = The ovality of the pipeline
$D_{max}$ = Largest measured inside or outside diameter of the pipeline.
$D_{min}$ = Smallest measured inside or outside diameter of the pipeline.

It should be noted that large ovalisation will lead to reduced structural capacity of the pipeline.

Point loads on the pipeline may arise at free span shoulders, artificial supports and support settlements. Further, the DNV code says that ovalisation shall be checked for such point loads at any part of the pipeline.

The thicker the wall thickness is, the less ovalisation will occur. The ovalisation will increase more than proportionally with the curvature of the pipe. If the curvatures result in plastic strains, some of the ovalisation will be plastic. This means that there will be some residual ovalisation even after the stresses are removed. If the strains are less than 0.5 percent, the maximal ovalisation for pipelines with a large wall thickness will be less than 0.5-1 percent. This means that the residual ovalisation after removal of stresses will be very small [1].

## 8.7    Concrete coating

During pipeline installation the concrete coating will experience the same strains as the pipeline. DNV–OS-F101 states that the mean compressive strains can be calculated by the formula:

$$\varepsilon_{mean} = -\frac{D}{2R} + \varepsilon_{axial}$$ (8.2)

Where,
D = Outer steel diameter
R = Stinger radius
$\varepsilon_{mean}$ = Calculated mean overbend strain
$\varepsilon_{axial}$ = Axial strain contribution

Further it is stated that $\varepsilon_{mean}$ shall satisfy Equation 8.3.

$$\gamma_{cc} \cdot \varepsilon_{mean} \geq \varepsilon_{cc}$$ (8.3)

Where,
$\gamma_{cc}$ = 1.05 safety factor for concrete crushing
$\varepsilon_{cc}$ = Limit mean strain causing crushing of the concrete

The diameter of the pipeline will have a direct influence on the cracking of the coating since studies have shown that the coating will tend to crack at intervals equal to the diameter of the pipeline [1].

Crushing of the coating will occur at the pressure side when the strains reach 0.15-3 percent. The larger the diameter of the pipeline, the larger strains can be tolerated before crushing occurs [1].

Even though the concrete does not fall off in the crushing zone in the overbend, there will be a risk that layers of the concrete may peel off in the sagbend when the crushed zones get into tension [1].

# 9    Laying vessel

Several types of laying vessels are available, but generally they can be divided into the classical lay barge and semi-submerged vessel.

Since the pipelines are welded together from 12.2 meter long joints there have to be several work stations on the vessel. A conventional pipe manufacturing vessel with 5-7 work stations requires a ship length of 100-120 meter and accommodation for 200-250 workers.

There are several parameters that govern the depth at which a conventional lay barge can operate and the most important ones are listed below [3].

- The capacity of the barge mooring system.
- Stinger size.
- Tensioner's capacity.
- Pipe diameter and wall thickness.
- Pipe weight coating.

# 10    Station keeping

It is important that the vessel's motions are as small as possible while laying pipelines. The vessel's movements can be divided into the categories shown in Figure 9 but the most important ones for pipe laying are roll, pitch and surge [18].
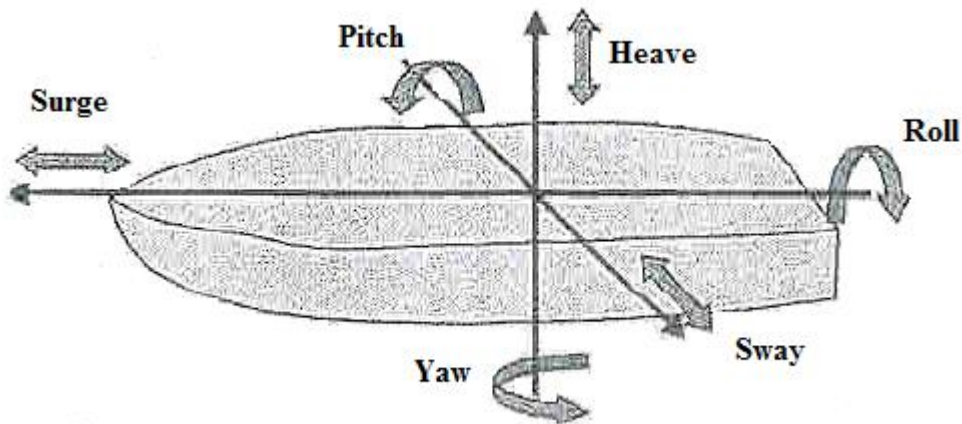
**Figur 9. The six degrees of freedom of a ship [7].**

The positioning forces acting on the vessel which come from wind, waves and currents depend on the size of the vessel. Forces from currents and wind are increasing proportionally with the size of the vessel while the forces from waves are decreasing as the size of the ship increases. In addition the shape of the hull plays an important role for the wave induced forces [1].

Whenever a pipeline installation is performed it is extremely important to keep the vessel in correct position compared to the route at which the pipeline is to be laid.  This is done by the vessel's positioning system. The other main task of the positioning system is to move the vessel forward as the laying takes place.

The positioning system has to counteract forces from waves, wind and currents and keep a tension force in the pipeline. In addition to handling this, the engines of the vessel have to have enough power to accelerate the vessel forward or carry out any position corrections if there should be any unwanted change of positioning [1].

This means that there have to be strict requirements when it comes to [1]:

- Positioning force
- Moveability
- Precision

The horizontal tension force acting at the bottom of the pipe, see Figure 3, will have a direct influence on the vessel's positioning system [1].

There are several types of ways to ensure that the position is kept and a few of them will be explained in this thesis.

## 10.1  Positioning by the conventional anchor systems  [1]

A conventional anchor system with 8-12 anchors and 900-1200 meters of anchor line have traditionally been used for station keeping.

Some of the most widely used anchor types are the Danforth and the Stockless anchor. These usually weigh between 10 and 20 tonnes and must have a good functionality on most types of sea beds.

A wire is attached to the anchor lying at the sea bottom. At the other end this wire is connected to a buoy floating at the surface. This wire is used for setting, pulling or repositioning the anchor. Usually 2-3 small tugboats take care of the movement of the anchors. This is done by slackening the anchor line which belongs to the anchor that is to be moved. When this is done the tugboat lifts the anchor by using the wire line located between the anchor and the buoy. Then the tugboat pulls the anchor forward parallel to the pipeline path at the same time as the anchor line is tightened.

If the distance between the anchors in front of the vessel and the vessel gets very small, the anchors have to be moved due to danger of being pulled up. The anchors astern of the vessel have to be moved when the available mooring line is used. The anchors can usually be moved by 300-500 metres.

When a new pipe joint is to be welded onto the pipeline the laying vessel has to be pulled forward by the length of the joint which is typically 12 meters. This is done by pulling 12 meters of the anchor lines which are placed in front of the vessel simultaneously with the anchor lines behind the vessel being slackened by 12 meters. Pulling the vessel forward by 12 meter normally takes between 30-60 seconds and is done every 10-15 minutes.

## 10.2  Position reference systems  [1]

A position reference system is necessary in order to situate the lay vessel such that the pipeline is installed along the correct pre-determined path. In addition, whenever an active position control system is used, position reference is needed in order to measure the vessel's movements compared to the desirable position.

The position reference systems can be divided into two main groups:

- Radio systems (electro magnetic systems)
- Hydro acoustic systems

There are also several other methods of station keeping. Some worth mentioning are Doppler sonar, visual observation, inertia systems and satellite systems. However none of these methods are sufficient as position reference system for lay vessels.

### 10.2.1 Radio navigation systems [1]

The radio based navigation systems come in many different varieties. The radio signals can have frequencies that vary within the range of 10 kHz and 10 GHz. The range and the precision of the navigation system depend on the frequency of the radio signals. The systems that have a low frequency have a large range and a low precision, while high frequency will give low range and high precision.

This kind of navigation system can be based on distance measuring and distance difference measuring. In addition, the radio signals can be either continuous or pulsating. These alternatives make 4 different main types of radio navigation systems.

The systems that are based on distance measurements require a minimum of two fixed stations which work as transmitters, while the systems based on distance difference measuring require at least three different transmitters. These transmitters can be used by many different users at the time. What is characteristic for the transmitters are that they must not move and their geographical position has to be known.

# 11    Loss of tension force

Basically there are two failure modes when it comes to loss of tension force. The first one is the situation where an error in the tension machines causes loss of tension force. In worst case scenarios this can lead to the entire pipeline being dropped down onto the seabed. This will in most cases damage the pipeline and can in some cases not be recovered at all.

There was an accident involving loss of tension force quite recently here in Norway.  A big oil company was installing a cable in Fensfjorden with only one tension machine on the vessel. When this tension machine failed, the entire cable fell down to the seabed. Luckily, the cable was recovered but parts of the pipeline had to be removed [10].

The second scenario is if there is a slip in the anchor system of the lay vessel. This may cause the vessel to move backwards. The result of this can be an extremely high curvature in the sagbend which can be damaging to the pipeline.

Several incidents have occurred due to a slip in the anchor system.
An investigation of 375 collision incidents from 1975 to 2001 in the United Kingdom showed that 11 of these incidents were due to anchor drag and an additional incident was caused by anchor drag due to bad weather. Further one incident was caused as an anchor line broke. This was not necessarily pipelaying vessels, however the same situation can occur for them [15].

If a digital positioning system is used, a blackout in the power supply can also make the vessel drift. 13 of the 375 incidents happened because the engines lost their power [15].


# 12    S-Lay in deep water [14]

Traditionally, J-lay has been the most feasible way of installing pipelines in deep water. This is partly due to the high stresses in the overbend. However, a number of improvements have been made when it comes to S-lay.


In the Gulf of Mexico s-lay is without doubt the most used method when it comes to deepwater pipeline installation. In 2005 75% of the length of pipelines installed in water depths more than 3000 feet was installed using the s-lay method.  One of the key elements needed in order to be able to use s-lay in very deep water is the departure angle from the stinger. A short stinger with a departure angle of typically 25-45 degrees would result in huge strains in the overbend if the water is very deep. One way to prevent this is to use a very long stinger so that the angle of departure becomes close to vertical. By doing this the pipeline will be supported by the stinger through the entire overbend.

The tension force in the pipeline while laying on the seabed will also become less when a stinger like this is used. A small tension force in the pipeline will result in fewer and smaller free spans on the seabed if the seabed is uneven.


# 13    Static calculation of free spans caused by an uneven seabed [13]

A tension force is often acting in long spanning pipelines and they do also often experience significant sag. This makes the span act partly as a suspended cable which means that the static capacity is much larger than for a beam. This means that calculation of free spans as a continuous beam is usually not correct.


When a pipeline is exposed to high temperature the steel will elongate. For an unconstrained pipe this means that the pipe will grow longitudinally. However, if the pipe is restrained the pipe cannot expand longitudinally and therefore a compressive effective axial force will act in the pipeline.
In order to get rid of this compressive force the pipeline will tend to slide towards the free span from both sides. This is because a span can be seen upon as a pipe with lack of restraint. The effective axial force is often used when calculating free spans, but it is important to notice that this is not the actual force acting in the pipe wall. The relationship between the effective axial force and the true axial force is given by the equation:

$$S = N - p_i \cdot A_i + p_e \cdot A_e \qquad\qquad (13.1)$$

Where,
S = Effective axial force
N = True axial force
$p_i$ = Internal pressure
$p_e$ = External pressure
$A_i$ = Internal cross-sectional area ($A_e$-A)
$A_e$ = External cross-sectional area
A = Cross sectional area of steel

Another important quantity for calculation of free span, when the pipeline is laid empty, is $S_0$, which can be found with the equation:

$$S_0 = H - p_i \cdot A_i \cdot (1 - 2v) - \alpha \cdot \Delta \cdot E \cdot A \qquad\qquad (13.2)$$

Where,
H= Horizontal pull
v = Poisson's ratio
$\alpha$ = Coefficient of thermal expansion
$\Delta$T= Temperature increase relative to the installation temperature
E = Young's Modulus

Due to insufficient restraint $S_0$ cannot always exist in the pipeline. In the case where only a force S can exist the strain in the pipe can be calculated with the equation:

$$\varepsilon = \frac{S - S_0}{E \cdot A} \qquad\qquad (13.3)$$

# 14    Vortex induced vibrations

There have been some serious accidents related to VIV (vortex induced vibrations) in the past. The most famous one is probably the collapse of the Tacoma Narrow Bridge.

When the water flows around a cylinder-formed pipeline, the water in contact with the pipeline will move slower than the water around the pipe (non slip condition), and form a boundary layer. Somewhere at the back of the pipeline this layer will separate from the pipe surface. At high flow velocities vortices will be shed downstream of the pipeline alternately at the top and bottom of the pipe. When a vortex is shed a small hydrodynamic force will act on

the pipeline which will cause the pipe to start oscillating. This is called vortex induced vibrations [8].

## 14.1 Natural frequency of the pipeline

Pipelines, like all other structures, will oscillate even though there is no external force acting on the pipeline. The frequency the pipeline will oscillate with is called the natural frequency of the pipeline.

[16] states in chapter 6.7.2 that the natural frequency of a pipeline can be calculated by using the equation:

$$F_0 = C_1 \cdot \sqrt{1 + CSF} \cdot \sqrt{\frac{EI}{m_e \cdot L_{eff}^4} \cdot \left(1 + \frac{S_{eff}}{P_{cr}} + C_3 \left(\frac{\delta}{D}\right)^2\right)} \qquad (14.1)$$

Where,

$C_1$-$C_3$ = Boundary conditions found in Table 6.1 in DNV-RP-F105

CSF = Concrete stiffness factor

EI= Bending stiffness of the pipeline

$m_e$ = Effective mass per unit length. See section 6.7.3 in DNV-RP-F105

$L_{eff}$ = Effective length of span. See section 6.7.9 in DNV-RP-F105

$S_{eff}$ = Effective axial force

$P_{cr}$ = Critical buckling load. See section 6.7.2 in DNV-RP-F105

$\delta$ = Pipe deflection

D = Outer diameter of the pipeline

## 14.2 Vortex shedding frequency

For a pipeline exposed to currents, vortices with a frequency of $F_s$ will be shed. The shedding frequency can according to [1] be calculated using the following equation:

$$F_s = S_t \cdot \frac{U}{D} \qquad (14.2)$$

Where,

$S_t$ = Strouhal Number, which usually can be set to 0.18-0.25 for pipelines

D = Outer diameter of the pipeline

U = current flow velocity

## 14.3  Resonance

When the shedding frequency of the vortices gets to be the same as or even close to the natural frequency of the pipeline, there can be trouble. The pipeline can then start to oscillate with very large amplitudes. This can be fatal to the pipeline and can also cause severe fatigue damage.

# 15    Experimental

The experiment was carried out in Professor Ove Tobias Gudmestad's barn in Nærbø. The reason for this is that the University did not have a laboratory that was big enough for these experiments. In order for the experiments to be executed, a 25 meter long and 6-7 meter tall laboratory facility was required, which made the barn perfect.

In this thesis, experiments were carried out in order to investigate the behaviour of the pipeline during S-lay.  The main objectives were to investigate how the span length of the pipeline from T.D.P. to the point where the pipeline leaves the stinger varies with different tension forces applied, as well as how this affects the pipeline. It was also of interest to see how the departure angle changes with different tension forces as well as how long stinger length is needed in order for the pipeline to be supported adequately. By doing this it is also possible to verify the correctness of different software used for pipelaying.

In order to investigate how the applied tension force will affect free spans on the seabed, an uneven seabed was created.

A situation was also simulated involving a slip of the anchor system of the laying vessel.

During the experiments the follow data were measured:
- The horizontal tension force at the end of the pipeline laying on the seabed.

- The horizontal span length from the T.D.P. to the departure point on the stinger.

- The actual length of the pipeline from the T.D.P. to the departure point on the stinger.

- The departure angle of the pipeline on the stinger.

- The length of the pipeline in contact with the stinger.

- The length of the pipeline in contact with the seabed.

- The strains in the pipeline when laying on the uneven seabed.

- Maximum strains in the sagbend and the overbend

- Natural frequency of the free span created from the departure point to the touchdown point.

Strain gauges were mounted on specific points of the pipeline, both in the spans on the seabed and from T.D.P. to the departure point in order to measure the strain in the pipeline.

## 15.1 The test rig

### 15.1.1 The lay vessel

The lay vessel consisted of a stinger mounted to a lift. The height from the seabed to the horizontal part at the top of the stinger was for this experiment 3.08 and 4.97 meters.

The radius of the stinger used was 3.36 meters. The length of the curvature of the stinger was 2.78 meters and the angle of the stinger tip was 49 degrees. The minimum radius in order to avoid plastic deformations of the pipeline in the overbend was calculated using Equation 4.2, see Appendix B.

An estimation of needed tension force in order not to get plastic deformations in the sagbend was obtained using Equation 6.15. See Appendix A. The smallest tension forces applied at any time were 2 kg for a laying height of 3.08 meters and 3 kg for 4.97 meters. Tension forces varying from 2 kg to 4.5 kg were used in the experiments. The lift with its stinger is seen in Figures 10a-10d.

**Figure 10a. The lift used for the experiments**



**Figure 10b. Pipeline laying on the stinger**

**Figure 10c. Pipeline laid from 3.08 meters height**



**Figure 10d. Pipeline laid from 4.97 meters height**

## 15.1.2  The pipeline

A great deal of time was spent finding the correct pipe. Testing showed that a copper pipe with an external diameter of 10 millimetres was to stiff. If this pipe was to be used, a much bigger laboratory would be needed for the tests. 10 millimetres copper pipe is the smallest diameter obtainable in Norway for stiff pipes. Therefore a visit to Randers, Denmark had to be made in order to get the pipe with the right stiffness. The smallest diameter pipe available

in Denmark, 8 millimetres, was then chosen. This pipe proved to bend a lot more easily than the 10 millimetres pipeline, hence the laboratory required could be of smaller dimensions.

Before the stinger could be made, the yield strength of the pipe had to be tested. This was done through tensile tests of the pipe.

In the experiments a copper pipe with the following properties was used:

| | |
|---|---|
| Outer diameter: | 8 mm |
| Wall thickness: | 1 mm |
| Young's modulus for copper: | $1.2 \cdot 10^5$ N/mm$^2$ |
| Yield strength: | 365 N/mm$^2$ |
| Weight: | 0.186 kg/m |

Each section of the pipe was 5 meters long and they were soldered together into a total length of 20 meters. A two centimetre long copper pipe with an outer diameter of 6 millimetres was placed inside the original copper pipe at the joints before the soldering in order to strengthen the joints. The joints can be seen in Figures 11 and 12.

**Figure 11. A piece of a smaller diameter pipeline was inserted into the main pipeline before soldering**



**Figure 12. Soldering of the joints**

### 15.1.3 The seabed

#### 15.1.3.1 One obstacle

Most of the measuring was done for different types of seabed. The first one was a flat seabed where the pipeline was laid straight onto the concrete floor.

The second one was to simulate an uneven seabed and an obstacle was placed under strain gauge number one. This is seen in Figure 13. This obstacle is referred to as obstacle number one.



**Figure 13. Pipeline laying on obstacle number one**

#### 15.1.3.2 Two obstacles

The last seabed scenario was made by placing two obstacles on the seabed. They were placed under strain gauges 1 and 4 and consisted of two parts of a pipeline made of plastic.

The horizontal distance from the fixed end of the pipeline to the first obstacle was 2.45 meters and 7.94 meters to the second one. A free span was now created between the two obstacles. The height of these obstacles was 16.2 centimetres. This scenario is shown in Figure 14.

Figure 14. A free span was created by placing two obstacles on the seabed

The obstacles used were made of solid plastic. In real situations the span shoulders are often made of sand, gravel or clay and the pipeline will often bury itself into the soil. Therefore, unless the free span is formed between big rocks, the obstacles used in these experiments are often not very realistic. However the seabed in arctic areas very often consists of solid clay. During the last ice age, ice bergs ploughed the seabed resulting in large grooves. Since there has been very little sedimentation the seabed is often very hard and uneven. Therefore, the obstacles used in the experiment become realistic for pipelines in these areas [10].

## 15.2   Execution of the experiment

### 15.2.1       Tension force applied to the pipeline

Tension force was applied to the pipeline through a wire connected to the pipeline. The wire was run over a pulley and accurate weights were attached to the wire. For the lowest laying height a rack was made for the pulley. The configuration for the tension force is seen in Figures15a and 15b.

**Figure 15a. Pulley for the wire which was used to apply tension force to the pipeline.**



**Figure 15b. The bucket that was attached to the wire. Calibrated weights were placed in the bucket.**

For the highest laying height the pulley was mounted to the ceiling.

The lifting of the pipeline onto the stinger before the tests could start was a critical operation. In order to make sure that the pipeline was not damaged, tension force had to be applied already at this stage. It was not enough to just fix the pipeline in one end and apply tension to the other end when lifting the pipeline since the force applied this way would only be enough to lift the pipe and not to give extra tension.

The way it was done was to connect a wire to the pipeline and run it over the pulley. By pulling this wire at the same time as someone was pulling in the opposite direction at the other end of the pipeline, a significant tension could be applied. The person at the other end moved closer to the stinger, applying tension force the whole time, while the pipeline was dragged onto the stinger in the air by the wire.

There were some uncertainties about how to apply the tension force. The friction in the model turned out to cause some problems. When the relevant tension force was applied, more tension force could be applied without anything happening to the pipeline. It was also possible to add more tension to the pipeline until it started sliding and then nothing happened when the extra applied tension force was removed again.

Therefore, before the measuring started, the bucket with the loading was heaved until it started to slide down again. By doing it this way, the same start criteria for every test were obtained. If the stinger had been frictionless, the tension force would probably have pulled the pipeline a bit further up on the stinger.

### 15.2.2 Measuring of tension force at the end of the pipeline on the seabed

A load cell was connected to the end of the pipe that was resting on the seabed. This was done in order to measure the horizontal tension force at the end of the pipeline. This configuration is seen in Figure 16.



**Figure 16. The load cell measuring the horizontal tension force at the end of the pipeline on the seabed**

### 15.2.3        Measuring of the required stinger length

In order for the pipeline to be fully supported in the overbend and to secure that the largest curvature in the overbend is in the part of the pipeline laying on the stinger, it is important to know how long the stinger needs to be. If the stinger is too short there is a risk of getting large bends in the overbend after the pipeline has left the stinger.

If the stinger length is too long the pipeline might slam up and down on the stinger tip. In real life situations the rollers on the stinger often work as supports, meaning that they can be adjusted to support the pipeline if the pipeline is not in contact with the stinger.

For simplicity, the stinger in this experiment did not have any rollers. So the way this length was found in the experiments was to measure the length from the start of the stinger to the departure point of the pipeline without taking any adjustable supports into consideration.

### 15.2.4        Measuring the departure angle of the pipeline

The departure angle relative to the horizontal plane was measured with an angle finder by placing it on top of the pipeline at the departure point. This instrument is shown in Figure 17.
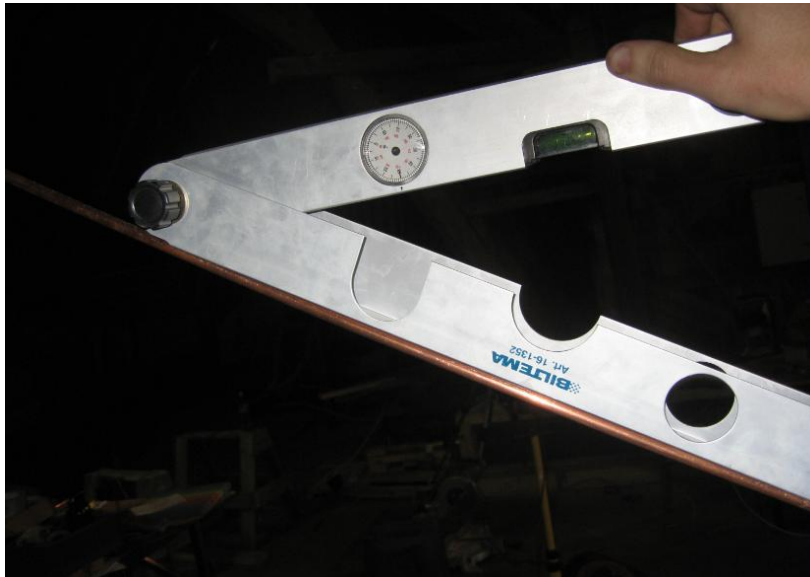


**Figure 17. Instrument used for measuring the departure angle**

### 15.2.5        Measuring the natural frequency of the pipeline

In order to get an understanding of how the applied tension force affects the natural frequency of the pipeline, the natural frequency of the span between the touchdown point and the departure point on the stinger was measured.

This was done by filming the oscillation of the pipeline after it had been exposed to an impact loading. The impact loading was caused by hitting the pipeline with a small hammer. An approximation of the natural period could be found by dividing the length of film with the number of oscillations in this period.

The natural frequency of the pipeline was very difficult to measure. The pipeline was only oscillating for a short period. This meant that the number of oscillations could only be counted for a short amount of time. For the lowest laying height the oscillations during a period of 10 seconds were counted, while for the highest laying height a period of 15 seconds was used.

When the natural period of the oscillations was found the natural frequency of the pipeline was calculated by using the equation:

$$f = \frac{1}{T}$$

(15.1)

Where,
f = Natural frequency of the pipeline
T = Natural period of the oscillations

This was done for both laying heights and for all the applied tension forces.


## 15.2.6 Friction coefficients

In order to get the analysis in OrcaFlex correct, the friction coefficients acting on the pipeline had to be measured. In this experiment there were two friction coefficients, one between the pipeline and the seabed and one between the pipeline and the stinger.

The friction coefficients from the seabed and the stinger were measured by pulling a one meter long section of the copper pipe along the concrete floor acting as the seabed as well on the stinger. The pipe was connected to a load cell. Force was applied to the load cell until the pipe started to slide. The highest force registered by the load cell just before the pipe started to slide was then chosen for further calculations since this was the force needed to overcome the friction force. This is shown in Figure 18.

**Figure 18. Measuring of the friction force on the seabed.**

This was done three times in order to eliminate errors.

The formula used to calculate the friction coefficients are:

$$F_f = \mu \cdot N \tag{15.2}$$

Where,
$F_f$ = Friction force
$\mu$ = Friction coefficient
$N$ = Weight of the pipeline

The friction coefficient is calculated in Appendix C.
It is seen from the graphs in the appendix that the force needed in order to make the pipeline slide on the seabed varied quite a bit from test to test. This is probably because of the unevenness of the concrete floor. The average value of the three tests was chosen.

## 15.2.7        Simulation of a slip in the anchor system

This was done by moving the lift slowly backwards. The pipeline was now fixed in both ends so that it could not slide, and this way the curvature of the pipeline would get larger. This is also a realistic scenario since the pipeline cannot slide very much forward on a vessel as the vessel moves backwards.

For practical reasons the laying height in this test was 3.40 meters.

## 15.3　　　　Strain gauges and data acquisition system

### 15.3.1　　　Strain gauges

The strain gauges used in this project are of the HBM K-LY41-3/120-3-3M type. They measure the strains in one direction in the pipeline. The strain gauges are placed as close as possible to the areas of the pipeline which will experience the largest stresses, typically in the sagbend and overbend as well as over the obstacles on the seabed. One of the strain gauges used can be seen in Figure 19.



**Figure 19. Strain gauge mounted on the pipeline**

It was important to be extremely accurate when attaching the strain gauges to the pipeline. If the gauges are out of angle they will not give the correct results. In addition, they have to sit precisely on the top and bottom of the pipeline. If this is not the case they will measure strains which are lower than the actual maximum strains. If this type of strain gauges is mounted with a five degree deviation in the angle, the measured strains will be 1% lower than the actual strains in the pipeline. This is if the pipeline is exposed to axial force only [9].
 If the angle of the strain gauge is correct but it is not placed exactly on the top of the pipeline, the errors will become big.

The strain gauges have to be scaled before the measuring can start. This can be done by selecting the correct gauge factor for the strain gauge. The gauge factor for these strain gauges is 2.02.

For each measuring point two strain gauges are needed. The first one, which is the one measuring the strains, is placed on the actual pipeline. Then a small piece of the pipeline has to be cut off and a new strain gauge is attached to it. This one is called a "dummy". The

dummy is not going to be exposed to any loads and the purpose of the dummy is to compensate for changes in the temperature. Each strain gauge has three different wires, one red and two grey ones. The wires from both the active gauge and the dummy are connected to a 15 pin port. The order in which these are soldered to the port is seen in Figure 20. The port is then inserted into the Spider8 which is the hardware used as a link between the strain gauges and the computer.
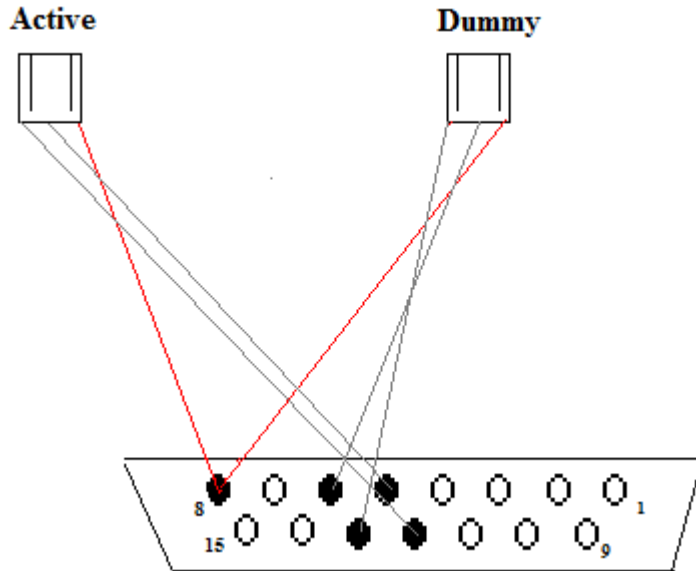


**Figure 20. The order in which the wires from the active and passive strain gauge is soldered.**

The Spider8 measures the results given by the strain gauges and is connected to a pc. The software used to calibrate, set up the measurements, read and display the results is called Catman 4.5 Professional. Catman shows the strains in the pipeline in µm/m and the tension force in kg. Figure 21 shows the Spider8.



**Figure 21. The Spider8.**

## 15.3.2 Load cell

The load cell used in order to measure the horizontal tension force in the pipeline was of the HBM U2A-200 type, where 200 means that the maximum measurable force is 200 kg. The output value of this load cell is mV\V and in order to convert this to kg, the load cell had to be scaled. This was done in Catman by measuring the mV/V factors for two different weights. The weights used in this calibration were 0 and 2 kg. The load cell is the same as described in chapter 15.2.2 and the cell can be seen in Figure 22.



**Figure 22. U2A-200 load cell [19].**

## 15.3.3 Positioning of the strain gauges

The strain gauges are placed as close as possible to the areas of the pipeline which will experience the largest stresses, typically in the sagbend and overbend as well as over the obstacles on the seabed.

On the part of the pipeline laying on the seabed, strain gauges were mounted just above the span shoulders as well as near the middle of the two shoulders in order to be able to measure the absolute maximum strain in the pipeline. The strain gauge in the middle of the two span shoulders was not completely in the middle of the span. This was due to the fact that tests showed that the maximum deflection would not be exactly in the middle. The reason for this might be that the soldered joints had some influence on the stiffness of the pipe.

Table 2 illustrates where the strain gauges are mounted to the pipe in order to measure the strains at the most critical places. The lengths are from the fixed end of the pipe resting on the seabed.

**Table 2. Longitudinal placement of the strain gauges along the pipeline**

|  | S.G. 1 | S.G 2 | S.G 3 | S.G 4 | S.G 5 | S.G 6 | S.G. 6,5 | S.G. 7 | S.G 8 | S.G. 9 |
|---|---|---|---|---|---|---|---|---|---|---|
| **Distance [meter]** | 2.47 | 5.215 | 6.685 | 7.95 | 9.2 | 10.41 | 12.32 | 16.41 | 17.54 | 18.54 |

The fact that there were not very many strain gauges available for our experiment made it difficult to hit the areas with maximum strains for every tension force and for both departure heights. This meant that the strain gauges had to be placed in areas so that there would be a few well-placed strain gauges for every scenario, while the ideal situation would have been to place several strain gauges in the areas which were expected to experience the largest strains in every attempt. This would assure that the largest strains would have been measured.
The length of the wires going from the strain gauges to the Spider8 was three meters. This meant that measuring from only six meters of the pipeline could be done at once. One option was to join the wires. However, this turned out to give very unstable measuring.

# 16    Analysis in OrcaFlex

OrcaFlex is a software which makes it possible to do modelling and analysis of marine systems like pipelines and risers, and is considered to be one of the leading software types in the world when it comes to both static and dynamic analysis. For more info about OrcaFlex see www.orcina.com

## 16.1   The modelling

The modelling in OrcaFlex was done by using two contact elements on the vessel. The first one was a cylinder placed at the back of the vessel with a radius equal to the radius of the stinger used in the laboratory experiments. This is the blue element seen in Figure 23. Since it is not possible to cut this shape into the wanted stinger length, the whole cylinder had to be used in the modelling. This will not have any large effects though, because the pipeline is supposed to leave the stinger before the maximum stinger length used in the experiments is reached.

The second contact element used was a block. This was placed at the same level as the deck of the vessel in order to be the contact element between the pipeline and the deck of the vessel. This is the green element shown in Figure 23.
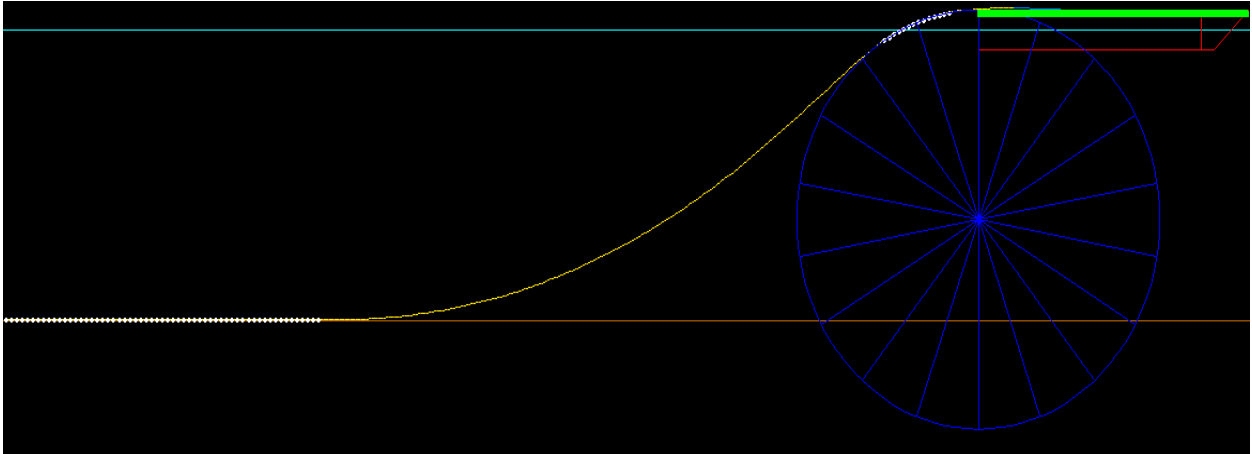
**Figure 23. An example of a laying simulation in OrcaFlex.**

The white dots shown in Figure 23 indicate that there is contact between the pipeline and the seabed or stinger/vessel.

As stated earlier the experiments were carried out by placing the start of the pipeline at a position on the stinger where the weight of the free span was equal to the tension force applied such that equilibrium was made and the pipeline did not slide in any direction. By doing it this way, further analysis in OrcaFlex showed that the results would not be the same as in OrcaFlex. However, since the starting point of the pipeline on the stinger was measured for every tension force applied, it was possible to make the geometry equal to the one in the experiments. Therefore, two different analyses are presented in this thesis.

### 16.1.1        Model with active tension force

This is the method that OrcaFlex uses when the tension force applied in the experience is used as input. The boundary condition of the starting point of the pipeline was here set to "free". A wire, which was to simulate the tension machine, was then attached to the pipeline. Hence, different tension forces could be applied. This model is referred to as the Long Span Model and this is the model automatically calculated by OrcaFlex. OrcaFlex does not take friction force on the stinger into consideration. Because of this the applied tension force causes the end of the pipeline to be pulled further up on the stinger than what was actually the case in the experiments. Because the stinger is frictionless in the Long Span Model, many of the results will not be the same as in the laboratory tests.

### 16.1.2        Model with fixed end conditions in both ends

Due to the fact that OrcaFlex does not account for the friction force from the stinger, only from the seabed, another model was made in OrcaFlex. This was done in order to obtain the same initial conditions as used in the experiments and described in chapter 15.2.1. This model is referred to as the Short Span Model.

The starting end of the pipeline on the stinger was here set to "fixed" at the same point that the actual pipeline started in the experiments. By doing this the model became equal to the one in the experiment but the tension force acting on the pipeline is lower than the tension force in the previous model. This model was not analysed for every scenario for the lowest laying height.

## 16.1.3 Calculation of the span length

In order to calculate the horizontal span lengths from the departure point on the stinger to the touchdown point in an accurate way, the graphs showing the contact forces between the pipeline and stinger/seabed had to be used. From these graphs one could see where the pipeline was in contact with the stinger and seabed.
By using these graphs the length of the pipeline in the span was found and not the horizontal length. In order to find this length a graph showing the horizontal coordinates as a function of the arc length of the pipeline was used. The calculation of the span lengths can be seen in Appendix D.

## 16.1.4 Strains in OrcaFlex

OrcaFlex defines maximum axial strain as the sum of the mean axial strain and the maximum bending strain [12].
The maximum strains in the pipeline as calculated by OrcaFlex can be seen in the attachments on the cd.

## 16.1.5 Stiffness in OrcaFlex

In order for OrcaFlex to do analyses, the bending stiffness and the axial stiffness of the pipeline are needed as input.

Since OrcaFlex considers the pipeline to consist of several beam segments, the bending and axial stiffness of a beam could be used, according to [11]. These were calculated using Equations 16.1 and 16.2

$$S_b = E \cdot I \tag{16.1}$$

Where,
I= Moment of inertia of the pipeline.

For the Axial stiffness Equation 16.2 was used.

$$S_a = E \cdot A \tag{16.2}$$

Where,

A = Cross-sectional area of the pipeline.

See Appendix G for calculations.

# 17    Results

The following are the results measured in the experiment and calculated in OrcaFlex.

## 17.1   Span lengths measured in the experiments and calculated in OrcaFlex

Figures 24- 29 show the measured as well as calculated horizontal span lengths in OrcaFlex from the departure point on the stinger to the T.D.P. as a function of applied tension force.
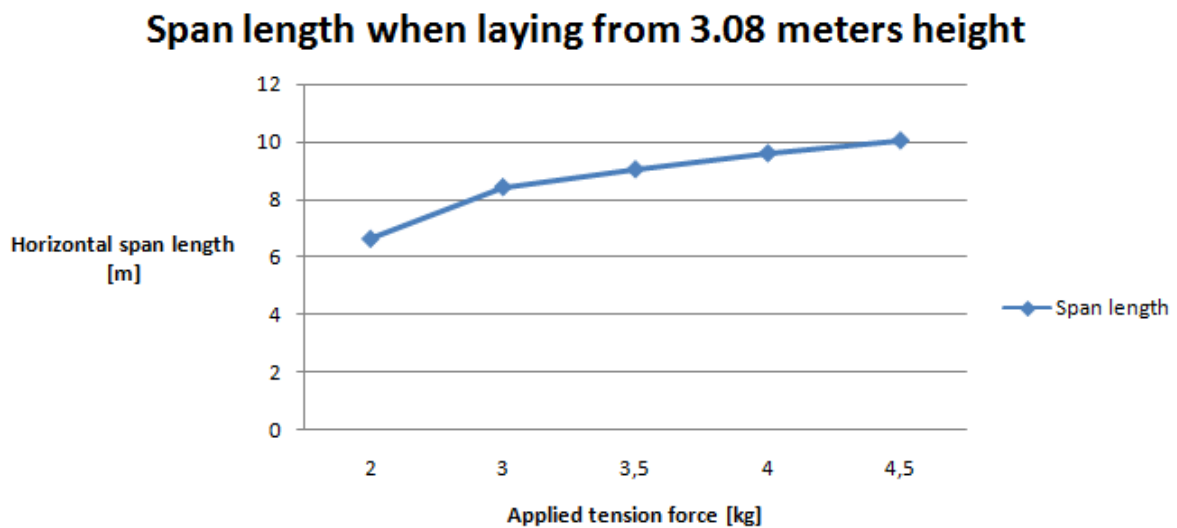
**Figure 24. Measured horizontal span lengths when the pipeline was laid from 3.08 meters above the seabed**

As expected, one can see from Figure 24 that the span length increases significantly as the applied tension force increases.
When the pipeline was laid from a height of 3.08 meters the horizontal span length varied from 6.65 meters for the lowest tension force to 10.03 meters for the highest force.
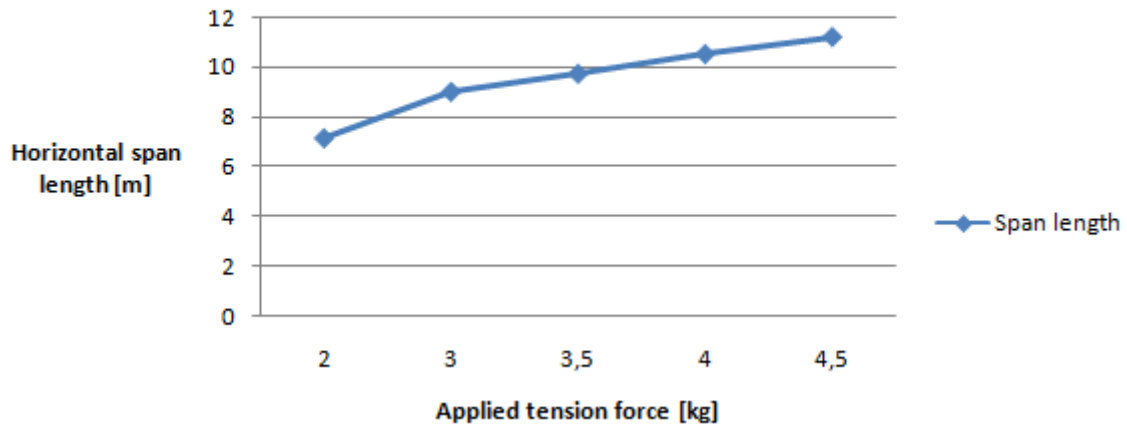
**Figure 25. Horizontal span lengths calculated from OrcaFlex when the pipeline was laid from 3.08 meters height and with an active tension force.**

It can be seen from Figure 25 that the span lengths obtained in OrcaFlex were much longer than the ones from the experiments. The shortest span length from OrcaFlex was for this scenario 7.16 meters while the longest was 11.18 meters. The reason why the span lengths from OrcaFlex are longer is probably that OrcaFlex does not account for the friction force on the stinger. This resulted in a larger tension force acting on the pipeline than what was acting on the pipeline in the real tests. The pipeline was pulled further up on the stinger in this model, hence the span lengths became longer.
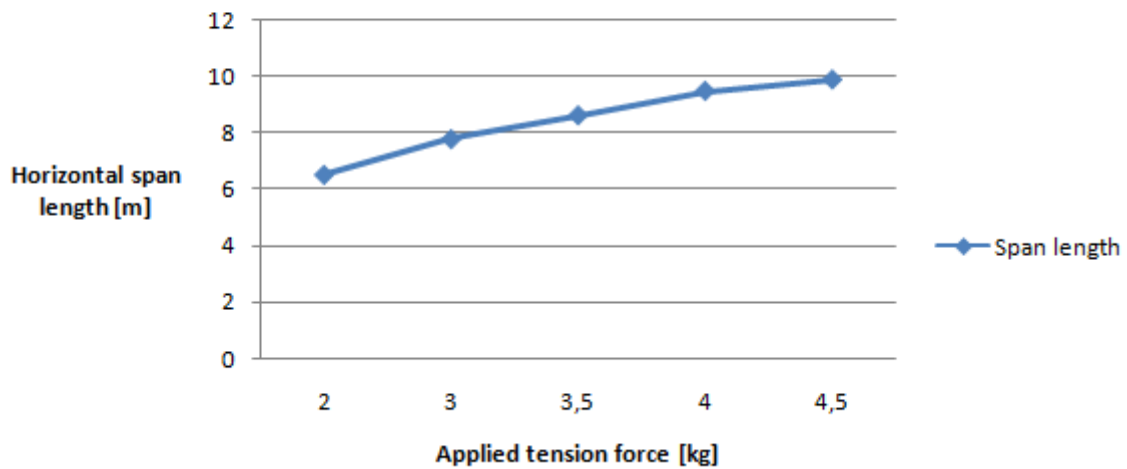


**Figure 26. Horizontal span lengths calculated from OrcaFlex when the pipeline was laid from 3.08 meters height and with fixed boundary conditions.**

When the pipeline ends were locked to the same positions as they were in the experiment the obtained span lengths from OrcaFlex were much more similar to the ones in the experiment. Figure 26 shows that the shortest span length is here 6.53 meters while the longest is 9.89 meters. These figures are differences of 0.12 and 0.14 meters from the practical tests.
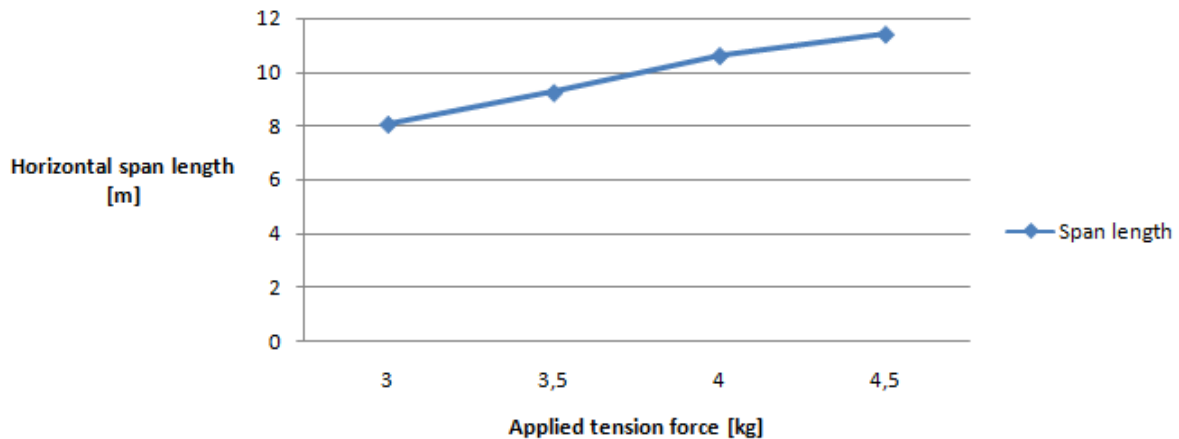


**Figure 27. Measured horizontal span lengths when the pipeline was laid from 4.97 meters above the seabed**

When the pipeline was laid from a height of 4.97 meters, the horizontal span length varied from 8.05 meters for the lowest tension force to 11.41 meters for the highest force. It can be seen from Figure 27 that the span lengths seem to follow a near linear curve as a function of applied tension.
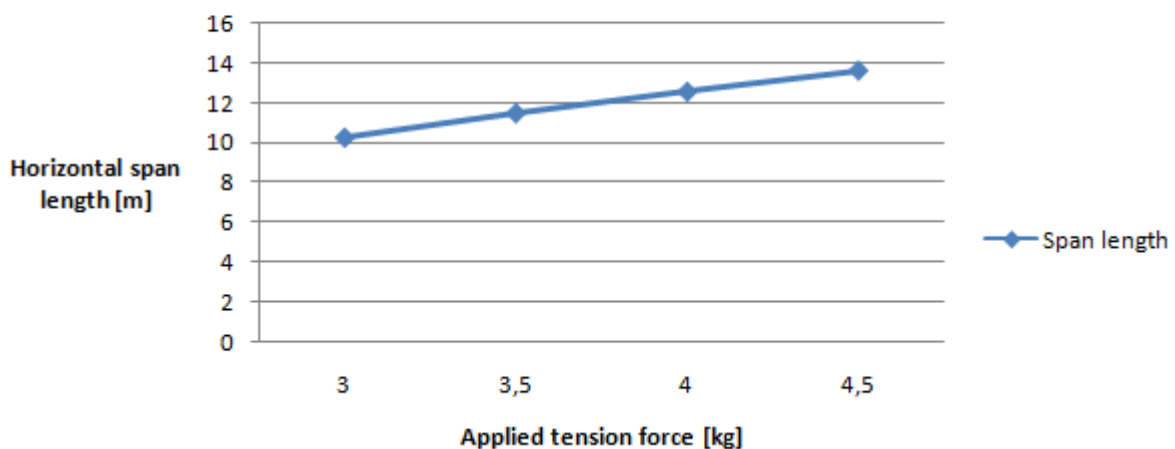


**Figure 28. Horizontal span lengths calculated from OrcaFlex when the pipeline was laid from 4.97 meters height and with an active tension force.**

It can be seen from Figure 28 that the lack of modelling of friction in OrcaFlex also affected the span lengths for this laying height as the span lengths obtained by OrcaFlex were much longer than in the practical experiments. The pipeline was here pulled much further up on the stinger by the tension force, which gave longer spans. The span length for the smallest tension force was here 10.29 meters and 13.59 meters for the highest force. These values represent differences of 2.24 and 2.18 meters from the experiments.
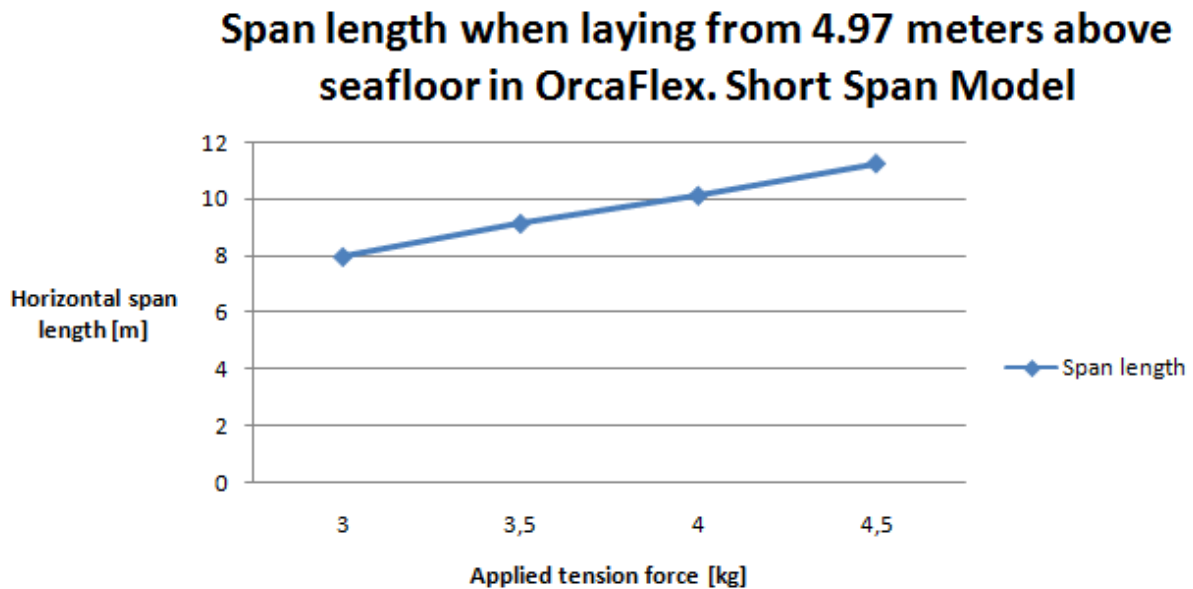


**Figure 29. Horizontal span lengths calculated from OrcaFlex when pipeline was laid from 4.97 meters height and with fixed boundary conditions.**

Figure 29 shows that the span lengths from OrcaFlex were much more similar to the ones in the experiments also for this laying height when the pipeline ends were fixed to the same coordinates as in the real test.

The span lengths now varied from 7.96 meters to 11.24 meters. These values give differences of only 0.09 and 0.17 meters, which is much closer to the real values than the ones in the last model.

It can be seen that both OrcaFlex models give us close to a linear span length curve.

## 17.2   Required stinger lengths

During the experiments the following lengths of the stinger before the departure point were measured:

From 3.08 meters height:

**Table 3. Required stinger lengths for pipeline laid from 3.08 meters height.**

| Tension Force [kg]: | Stinger Length [m]: |
|---|---|
| 2 | 2.15 |
| 3 | 1.73 |
| 3,5 | 1.57 |
| 4 | 1.39 |
| 4,5 | 1.23 |

Table 3 shows that the required stinger length almost doubled for the lowest tension force compared to the highest force. The required stinger length of 2.15 meters is quite high when considering that the laying height is only 3.08 meters.

For 4.97 meters height:

**Table 4. Required stinger lengths for pipeline laid from 4.97 meters height.**

| Tension Force [kg]: | Stinger Length [m]: |
|---|---|
| 3 | 2.55 |
| 3.5 | 2.3 |
| 4 | 2.03 |
| 4.5 | 1.98 |

Table 4 shows that the required stinger length is clearly dependent on the water depth as this table gives significantly higher values than table 3.
It is seen that when the tension force varied from 3 to 4.5 kg the decrease in required stinger length was 0.5 meters for the lowest laying height while the respective decrease in stinger lengths for the larger laying height was 0.57 meters. This means that the impact of a variation of applied tension force is approximately the same, with a slightly bigger impact for the largest height. This also means that for larger water depths significantly larger tension forces are needed in order to maintain the same stinger lengths as for shallower water depths

## 17.3  Departure angle from the stinger

The following departure angles were measured in the experiments:
The departure angles when pipeline is laid from 3.08 meters above the seabed are listed in
Table 5.

**Table 5. Departure angles when the pipeline was laid from 3.08 meters.**

| Tension Force [kg]: | Departure Angle [degrees]: |
|---|---|
| 2 | 30 |
| 3 | 23 |
| 3.5 | 21 |
| 4 | 18 |
| 4.5 | 16 |

The departure angles when laid from 4.97 meters are listed in Table 6.

**Table 6. Departure angles when the pipeline was laid from 4.97 meters.**

| Tension Force [kg]: | Departure Angle [degrees]: |
|---|---|
| 3 | 40 |
| 3.5 | 34 |
| 4 | 30 |
| 4.5 | 30 |

As seen from Table 5 and Table 6 the departure angle decreases as the applied tension force
increases. For a laying height of 3.08 meters the angle varied from 16 to 23 degrees, while
when laid from 4.97 meters height the angle varied from 30 to 40 degrees when the tension
force varied between 4.5 kg and 3 kg. A departure angle of 16 degrees is a bit low for the
lowest height. The main reason for this is that the tension forces used were a bit high
compared to the small weight of the pipeline and the small height. Another reason for this is
that the stiffness of the pipeline was rather large compared to the laying height.
It is stated in chapter 12 that if S-lay is to be used for very deep water depths, the departure
angle should be close to 90 degrees. By combining Tables 5 and 6 with Tables 3 and 4 one
can see that in order to obtain such a large departure angle a very long stinger would be
needed.

## 17.4   Measured and calculated strains in the pipeline

### 17.4.1        The overbend

The theoretical strain in the overbend is 0.119 percent. See Appendix H for calculations.

Figures 31-36 show the strains measured in the overbend as well as the strains calculated by OrcaFlex.

Figure 30 shows where the strain gauges in the overbend are placed. It is worth noticing that the strain gauges will move slightly as the pipe slides as more tension is applied.
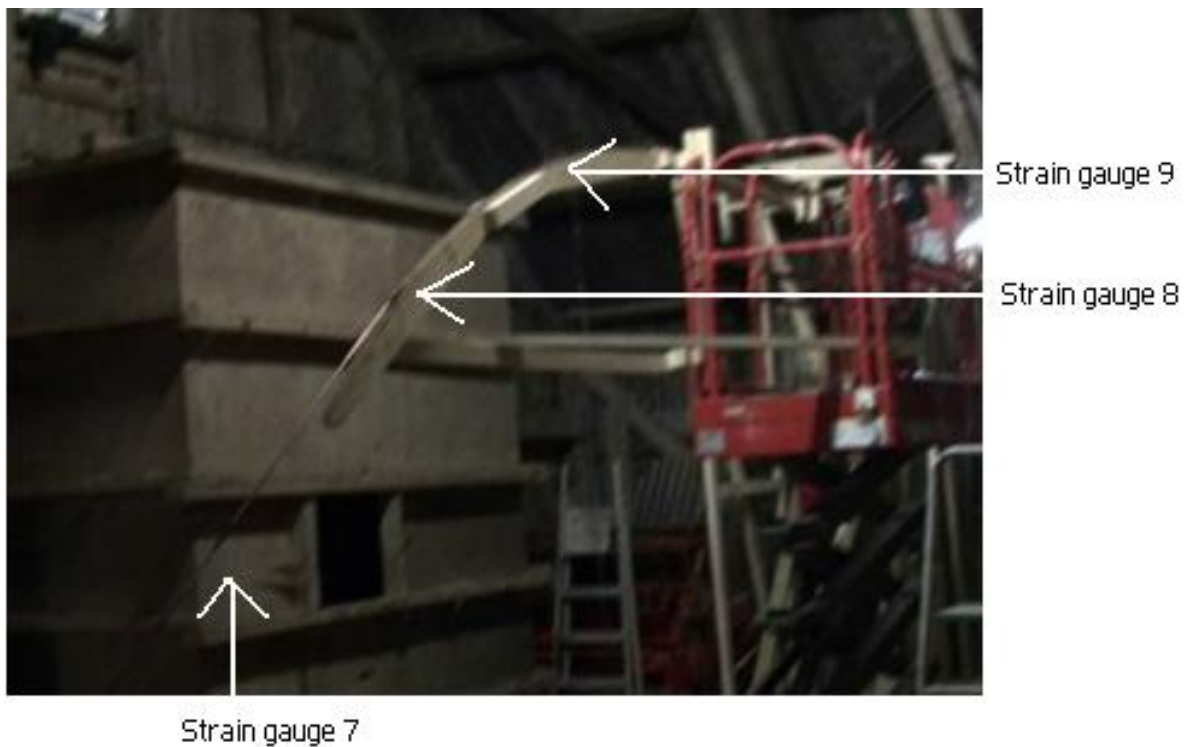


**Figure 30. Placement of the strain gauges in the overbend.**

### 17.4.1.1 Pipeline laid from 3.08 meters height:

Figure 31 shows the measured strains in the overbend of the pipeline when laid from 3.08 meters.
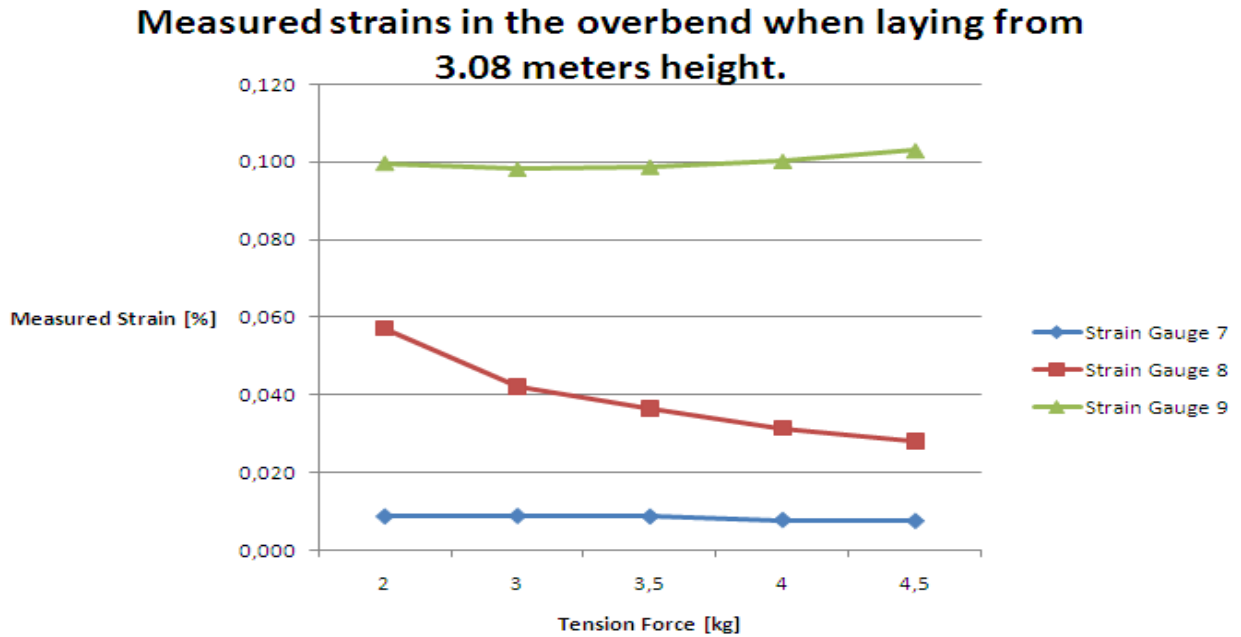


**Figure 31. Measured strains in the overbend of the pipeline when laid from 3.08 meters height.**

As can be seen from Figure 31, strain gauge numbers seven and eight show a decreasing trend as the curvature of the overbend gets smaller. The reason why strain gauge number seven decreases by such a small amount as a larger tension force was applied is that the strain gauge was mounted approximately 3.5 meters from the start of the pipe. This was below the departure point and close to the inflection point. Because of this the strains at this point were low and the change in tension force had little influence on the strains.

Strain gauge number nine shows the largest strains. Note that the largest strain was just above 0.1 percent. Table 1 states that for a pipeline of steel quality X65 a strain of 0.25 percent can be tolerated in the overbend. The maximum measured strain is somewhat smaller than the theoretical strain of 0.119 percent. This is probably because the strain gauge was mounted with a small deviation from the top of the pipeline, or that the strain gauge did not hit the area of maximum strain perfectly.

As seen from the figure the strains in gauge number nine decrease before they increase again with increased tension. One possible explanation of this is that the gauge was mounted close to the end of the pipeline and very high up on the stinger. At this point of the pipeline the effects from the earlier departure point as the tension force was increased, caused little influence on the strains. In addition, the fact that the tension force was increased might have contributed to increasing the strains in the pipeline at this specific point.
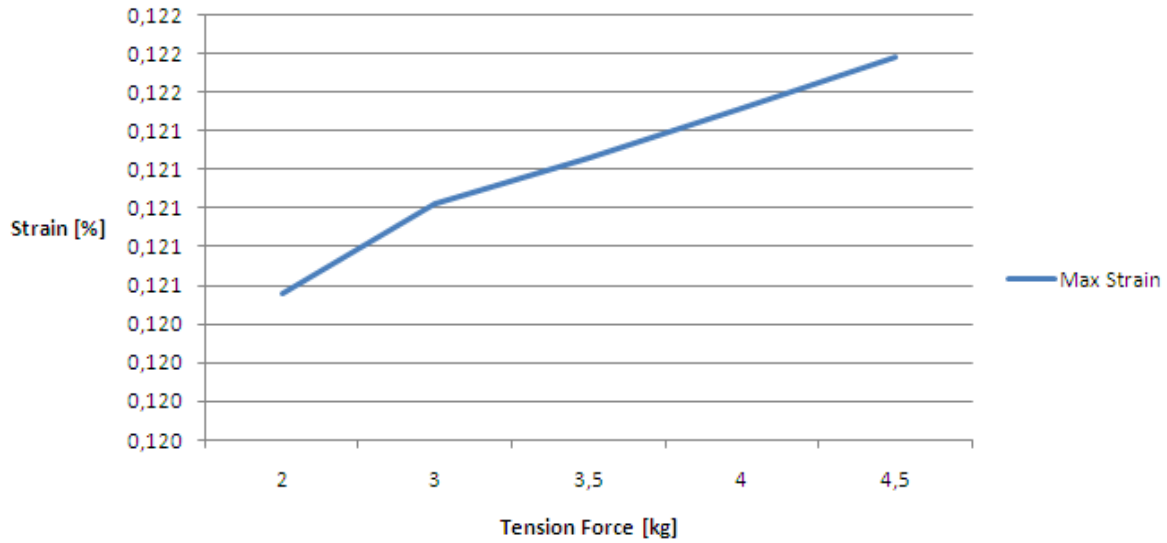
**Figure 32. Max strains obtained in OrcaFlex for the different tension forces when laid onto a flat seabed from 3.08 meters height. Long Span Model.**

Figure 32 shows that the strains in the overbend increase slightly for an increase in tension force also in OrcaFlex. This is probably due to the fact that the increase of axial strain as the tension force got larger had a greater effect than the effect of getting a larger bending radius as the pipeline was leaving the stinger earlier.

The curve seems to increase steeply. However, by looking at the values one can see that the increase in strain is marginal. The highest strain in this model was approximately 0.1218 percent.
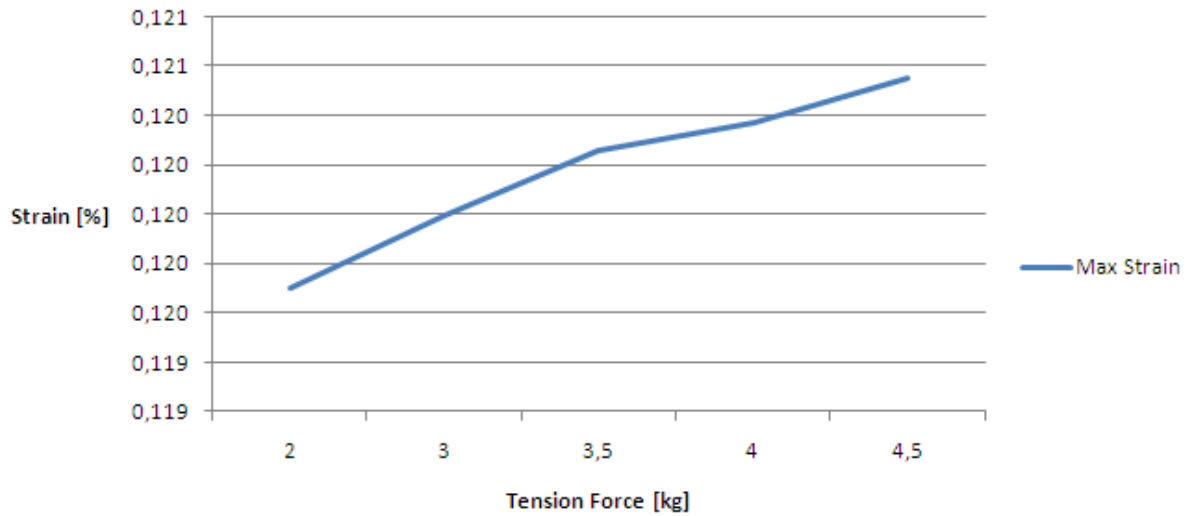
**Figure 33. Max strains obtained in OrcaFlex for the different tension forces when laid onto a flat seabed from 3.08 meters height. Short Span Model.**

As seen from Figure 33 this model also shows an increase in strains in the overbend as the tension force increases. These strains are a little smaller than the ones from the long span. This is probably because of the contribution of axial strain caused by the high "active" tension force in the previous model.

It can be seen from Figure 32 and Figure 33 that both the two OrcaFlex models gave larger strains in the overbend than the measured values in the experiment. There can be several reasons for this, but the most likely ones are that the strain gauges did not hit the point in the pipeline with that largest strain perfectly, or that the strain gauge was mounted at a small deviation from the top of the pipeline. Both these two OrcaFlex models give close to the theoretical strain of 0.119 percent in the overbend.

**17.4.1.2          Pipeline laid from 4.97 meters height:**



**Figure 34. Measured strains in the overbend when the pipeline was laid from 4.97 meters height onto a flat seabed.**

As seen from Figure 34 the values measured by the strain gauges seem to follow the same trends as in the overbend for the 3.08 meters laying height. However, in this case the largest strains were measured by strain gauge number eight and the maximum strain measured was just above 0.12 percent. As the tension force increases the strains measured by strain gauge number eight decrease as expected. This is very close to the theoretical strain of 0.119 percent.

Strain gauge number seven was mounted close to the inflection point, hence showing small strains that increase slightly as the tension force increases.

Strain gauge number nine also seems to follow the same pattern as for the lower laying height. Since it was mounted so high up on the stinger the reduced bending curvature of the pipeline as the tension force increased had little influence on the strain, and the increased tension force resulted in larger axial strain. However, the strains measured now were a bit smaller than last time for the 3.08 meters laying height for this gauge.
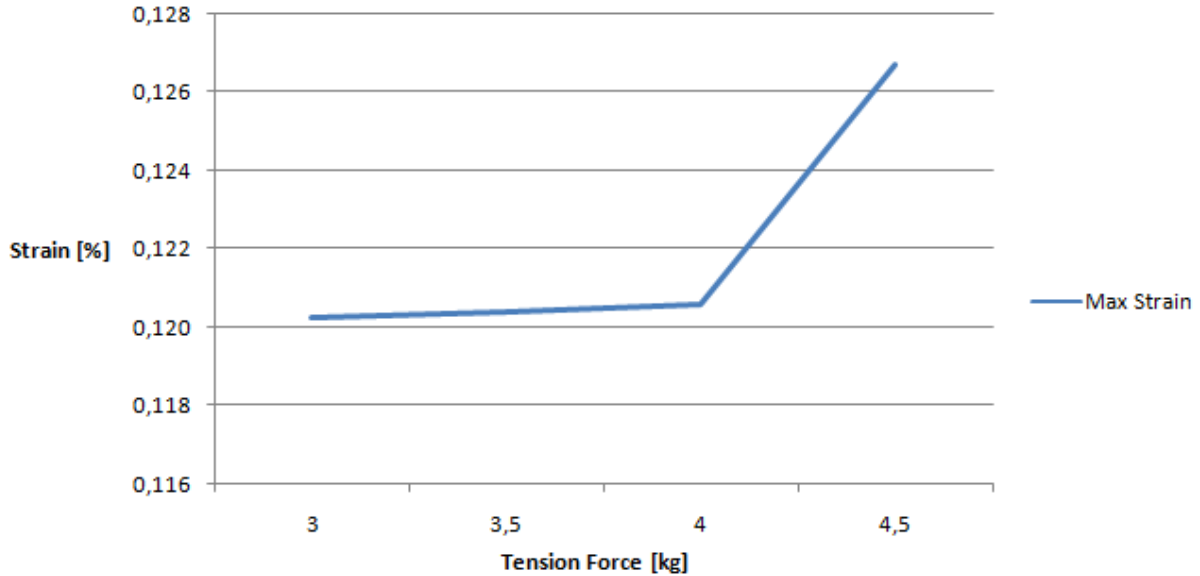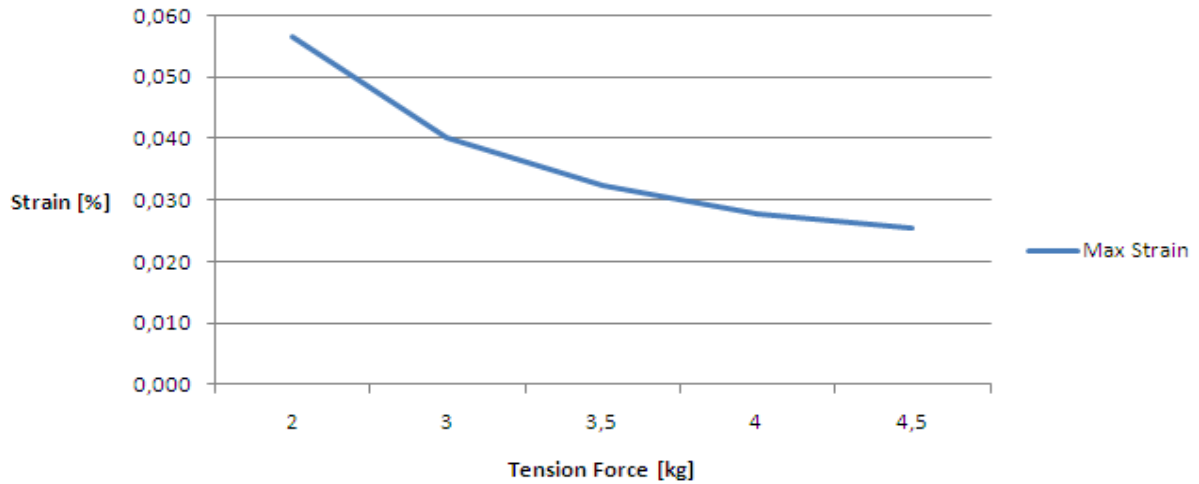
**Figure 35. Maximum strains in the overbend obtained from OrcaFlex when the pipeline was laid from 4.97 meters height onto a flat seabed. This is from the frictionless Long Span Model.**

Figure 35 shows that the maximum strain in the overbend as calculated from OrcaFlex was 0.127 percent. The maximum strain measured in the experiments was 0.123 percent so the difference between the test and the OrcaFlex model is quite small.
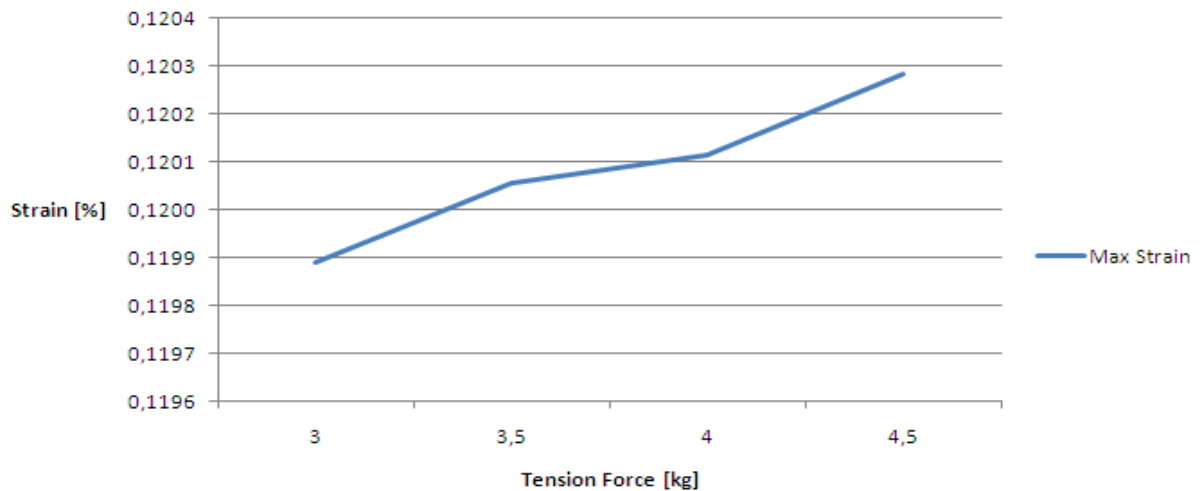


**Figure 36. Maximum strains in the overbend obtained by OrcaFlex when the pipeline was laid from 4.97 meters height onto a flat seabed. Short Span Model.**

It can be seen from Figure 36 that the strains obtained in OrcaFlex in this model are slightly smaller than the one from the previous model. The maximum strain from the Short Span Model is approximately 0.1203 percent. As seen from Figure 34, the maximum strain measured by the strain gauges was 0.123 percent. This means that the Short Span Model gave a bit smaller results than what was obtained in the experiment. The differences were very small. However, it is reasonable to believe that the maximum strains in the real tests might have been even larger due to imperfect placing of the strain gauges. This means that the difference between the strains in this model and the real test can be larger than what can be seen from the figures.

### 17.4.1.3        Test results vs. values found by OrcaFlex
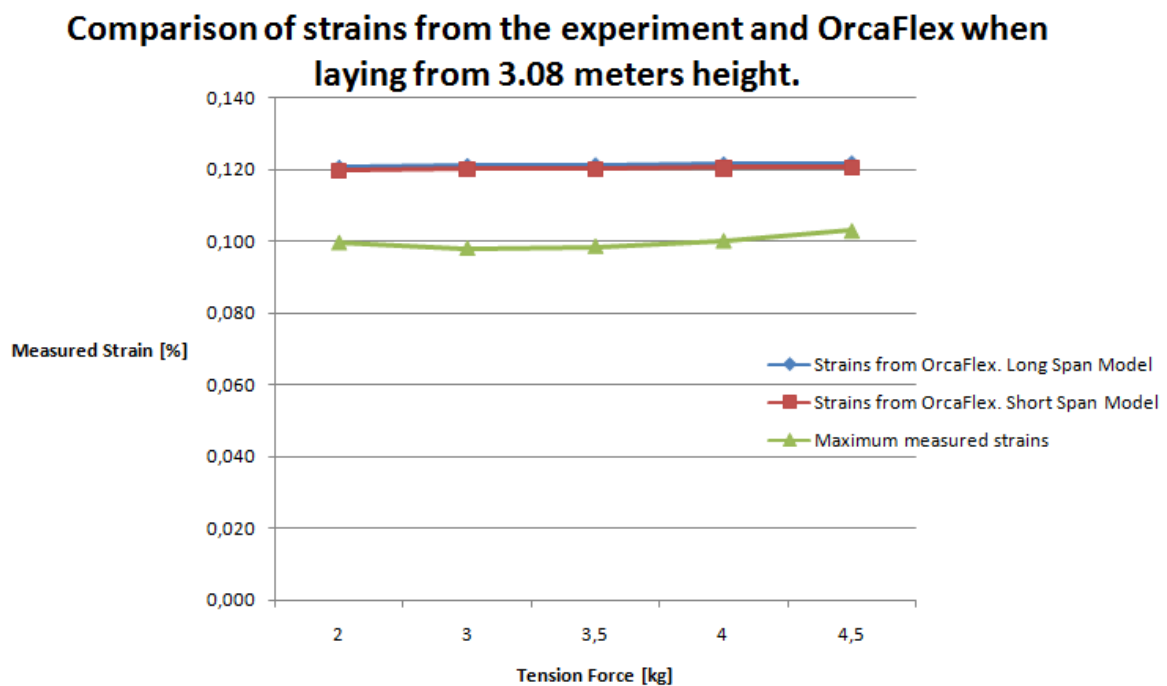


**Figure 37. Comparison of the strains obtained in the overbend  in the experiment and OrcaFlex when laid onto a flat seabed from 3.08 meters height.**

Figure 37 shows that the applied tension force seems to have little influence on the maximum strain in the overbend when the pipeline was laid from 3.08 meters height. Both the laboratory tests and the simulations done in OrcaFlex give a slight increase in maximum strain as the tension force is increased. However, this is marginal.

For the lowest laying height, the Long Span Model, which does not take friction on the stinger into consideration, gave slightly higher values than the Short Span Model which took friction into consideration by fixing the pipeline end at the same point on the stinger as in the experiment, but this was marginal.  Both OrcaFlex models gave slightly higher values than what was measured in the experiment. As stated earlier this probably has something to do with the placement or mounting of the strain gauges.

## Comparison of strains from the experiment and OrcaFlex when laying from 4.97 meters height
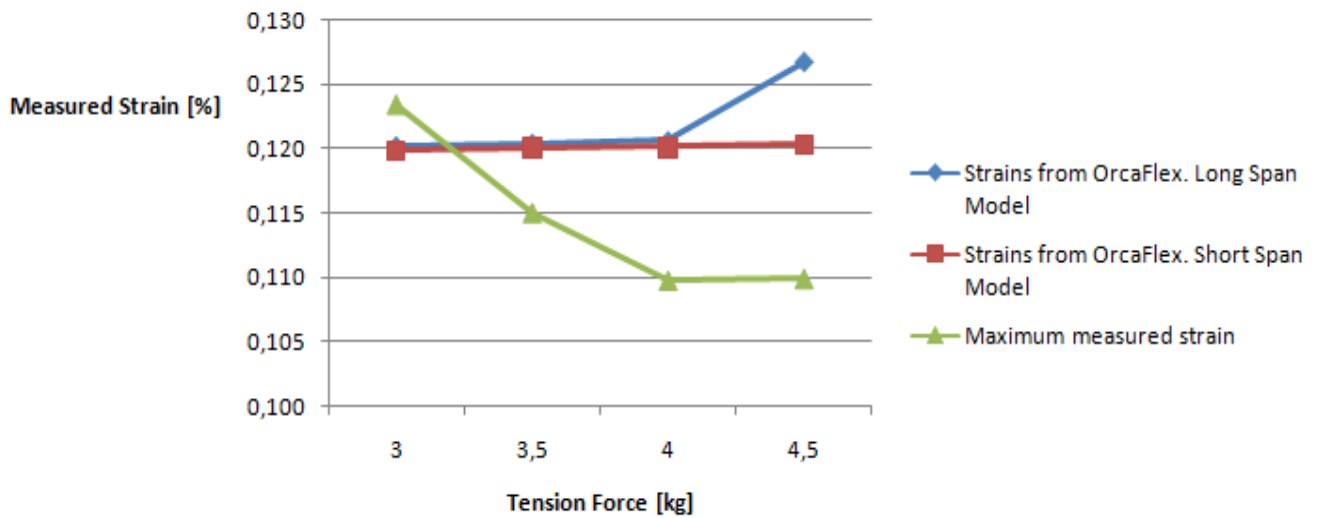


**Figure 38. Comparison of the strains obtained in the overbend in the experiment and OrcaFlex when laid onto a flat seabed from 3.08 meters height.**

As seen from Figure 38, when the pipeline was laid from 4.97 meters height the maximum strain measured in the experiments decreased as the tension force was increased. Both the frictionless Long Span Model and the Short Span Model gave increasing strains as the tension force was increased. However, the fact that in the frictionless model the end of the pipeline was pulled very far up on the deck of the vessel for the largest tension force, the increase in strain due to larger tension force affected the strains more than the increased bending radius over the stinger as the tension was applied. This resulted in a big increase in strain as the largest tension force was applied. This sudden increase in strain did not happen for neither the real test nor the OrcaFlex model which took friction into consideration, meaning the Short Span Model gave better results. However, one can see that the friction acting between the stinger and the pipeline did not affect the strain in the overbend very much except for when the highest tension force was applied. For most of the tension forces the OrcaFlex Models gave slightly higher strains than the experiments did.

## 17.4.2    The sagbend

Figures 39-44 show the measured strains in the sagbend as well as the strains from OrcaFlex when the pipeline was laid onto a flat seabed.

**17.4.2.1      Pipeline laid from 3.08 meters height:**

## Strains measured in the sagbend when laid from 3.08 meters height
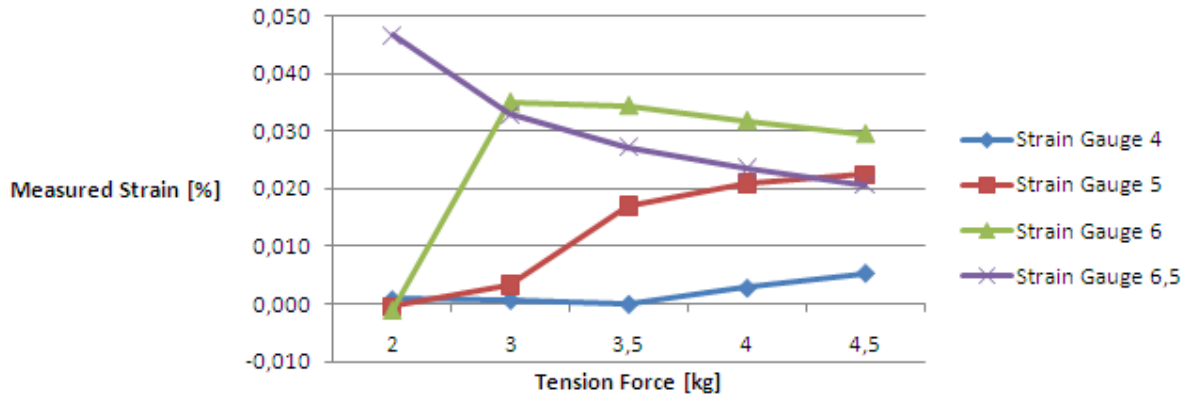


**Figure 39. Measured strains in the sagbend of the pipeline when laid from 3.08 meters height onto a flat seabed.**

As stated in previous chapters, the strains in the sagbend theoretically decrease as the tension force increases. As can be seen from Figure 39 strain gauge number 6.5 shows the most correct result according to the theory. This is because this gauge was mounted in an area of the pipeline that was above the seabed for all the different tension forces. The maximum strain measured was for a tension force of two kg and was 0.047 percent.

When it comes to strain gauge number six it shows close to zero strain when exposed to a tension force of 2 kg. This is due to the fact that this gauge was on a part of the pipeline resting on the seabed and which was lifted off the seabed as the free span got longer as a tension force of three kg was applied. Hence the strains increased dramatically before they decreased again when larger forces were applied after the strain gauge was already in the air. Strain gauges number 4 and 5 were also resting on the seabed when a tension force of 2 kg was applied. The reason the strains in gauge number five increase as the tension force increases is that the gauge was close to the touchdown point for all the tension forces. When a tension force of 3 kg was applied the strain gauge was barely lifted off the seabed and the pipeline was close to straight without much curvature at this point. As a higher tension force was applied, the strain gauge was lifted further from the seabed, hence experiencing larger strains. However, the strain gauge was still relatively close to the touchdown point.
Strain gauge number four had the same situation. It was resting on the seabed most of the time, resulting in small strains.
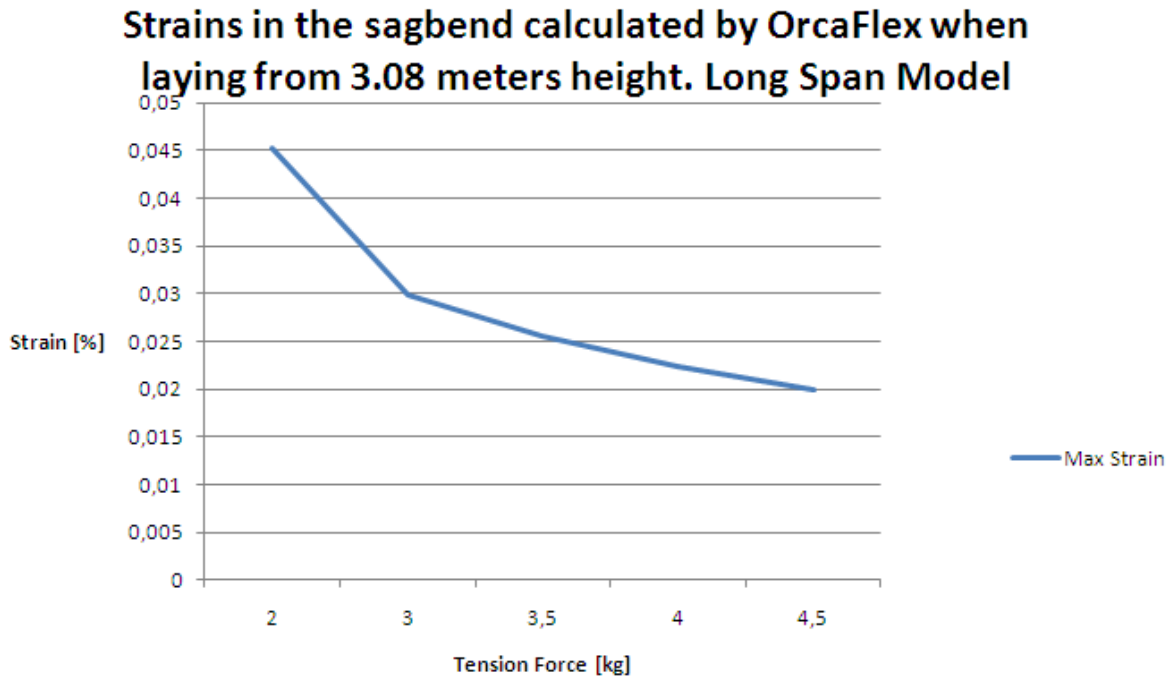
**Figure 40. Maximum strains in the sagbend obtained by OrcaFlex when the pipeline was laid from 3.08 meters height onto a flat seabed. This is from the frictionless Long Span Model.**

By studying Figure 40, one can see that the strains in the sagbend decrease rapidly as the tension force decreases. The smallest tension force resulted in a maximum strain of 0.045 percent while the largest force gave a strain of 0.02 percent. As can be seen from Figure 39 the respective strains from the experiment were 0.047 and 0.0295, which is larger than the ones from the OrcaFlex model. If the placing of the strain gauges was not perfect the differences would have become even bigger.

**Figure 41.** **Maximum strains in the sagbend obtained by OrcaFlex when the pipeline was laid from 3.08 meters height onto a flat seabed. Short Span Model.**

Figure 41 shows that the slope of the graph from this and the previous model is approximately the same. However the strains obtained by this model are larger than the ones from the model with the longer span. The maximum strain here is 0,056 for the smallest tension force and 0.025 for the smallest force. The highest strain here is somewhat larger than in the experiments. However, as stated earlier it is expected that the strains from the experiment might have been a little larger if the strain gauges had been mounted differently.

## 17.4.2.2    Pipeline laid from 4.97 meters height:
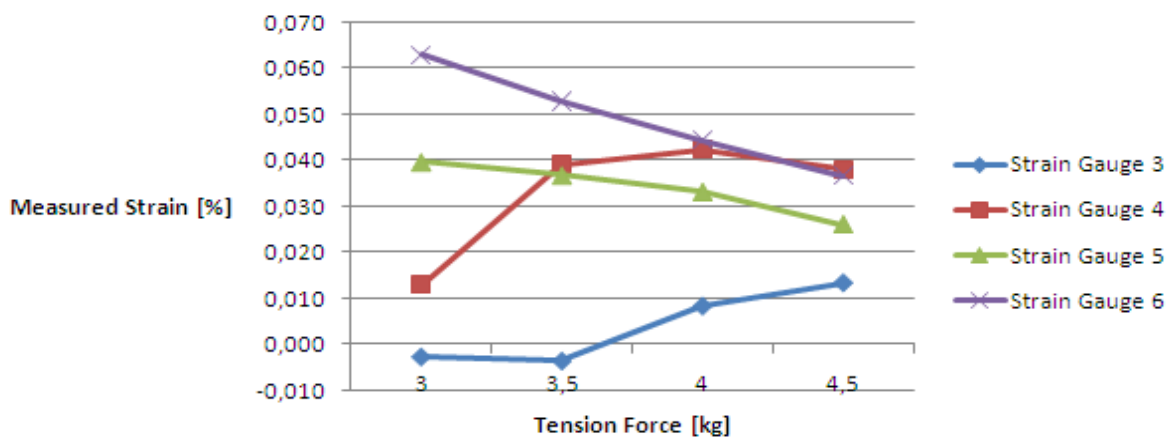


**Figure 42.** **Measured strains in the sagbend when the pipeline was laid from 4.97 meters height onto a flat seabed.**

As can be seen from Figure 42 the strain gauges seem to follow approximately the same pattern as for 3.08 meters. However the maximum strain measured here was 0.063 percent for a tension force of 3 kg. The same strain gauge also measured the highest strain for the lower laying height and the strain measured for the same tension force in the previous height was 0.033. This means that the strains almost doubled for this strain gauge when the laying height was increased from 3.08 to 4.97 meters and the same tension force was applied.

Strain gauge number five also follows the expected trend by decreasing as the tension force increases.

Strain gauge number four is experiencing larger strains than strain gauge six for the highest tension force.
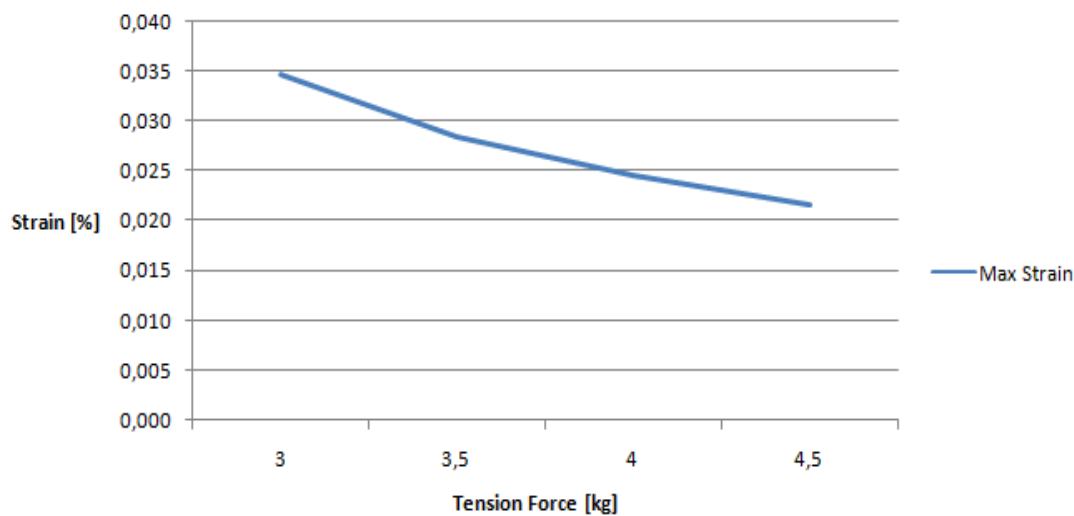


**Figure 43. Strains obtained in the sagbend by OrcaFlex when the pipeline was laid from 4.97 meters height onto a flat seabed. This is from the frictionless Long Span Model.**

Figure 43 shows that the strains in the sagbend decrease from 0.035 percent for the smallest tension force to 0.022 percent for the largest force. Figure 42 shows that the respective strains measured in the experiments were 0.063 percent and 0.038. This means that the strains from OrcaFlex are almost 50 percent less than the real ones, and perhaps even more if different mounting of the strain gauges would have resulted in larger strains.
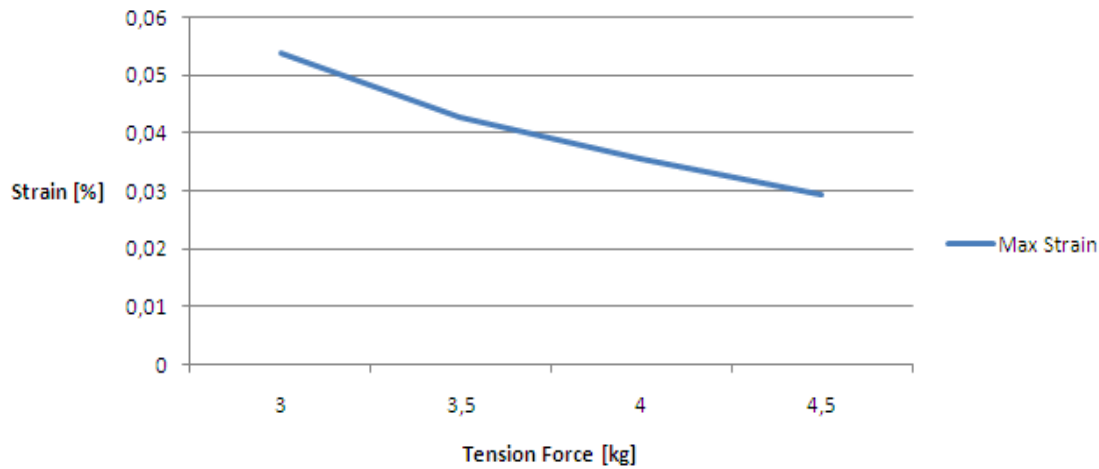
**Figure 44. Strains obtained in the sagbend by OrcaFlex when the pipeline was laid from 4.97 meters height onto a flat seabed. Short Span Model.**

Figure 44 shows that the highest strain obtained for a tension force of 3 kg when the Short Span Model was used was 0.054 percent and 0.03 for the largest tension force. Since the maximum strain obtained by the strain gauges was 0.063 percent, this model gives too low strains as well. However, the strains for this model were a lot closer than the ones obtained by the model with the long span.

### 17.4.3    The sagbend when the seabed was uneven

Figures 46-54 show the measured strains in the sagbend as well as the strains as calculated from OrcaFlex when the pipeline was laid on an uneven seabed with two obstacles as described in Chapter 15.1.3.2. For the strains in the sagbend, only the scenario involving two obstacles is included since in the one obstacle scenario, the obstacle was so far from the sagbend that the sagbend was not affected much.

Figure 45 shows the placements of some of the strain gauges used for measuring the strains in the sagbend when the seabed was uneven. Strain gauge number four is not included when measuring the strains in the sagbend. Strain gauge number 6.5 was placed approximately 1.9 meters in front of strain gauge number 6. It is worth noticing that the pipeline and the strain gauges moved a little bit as more tension was applied.
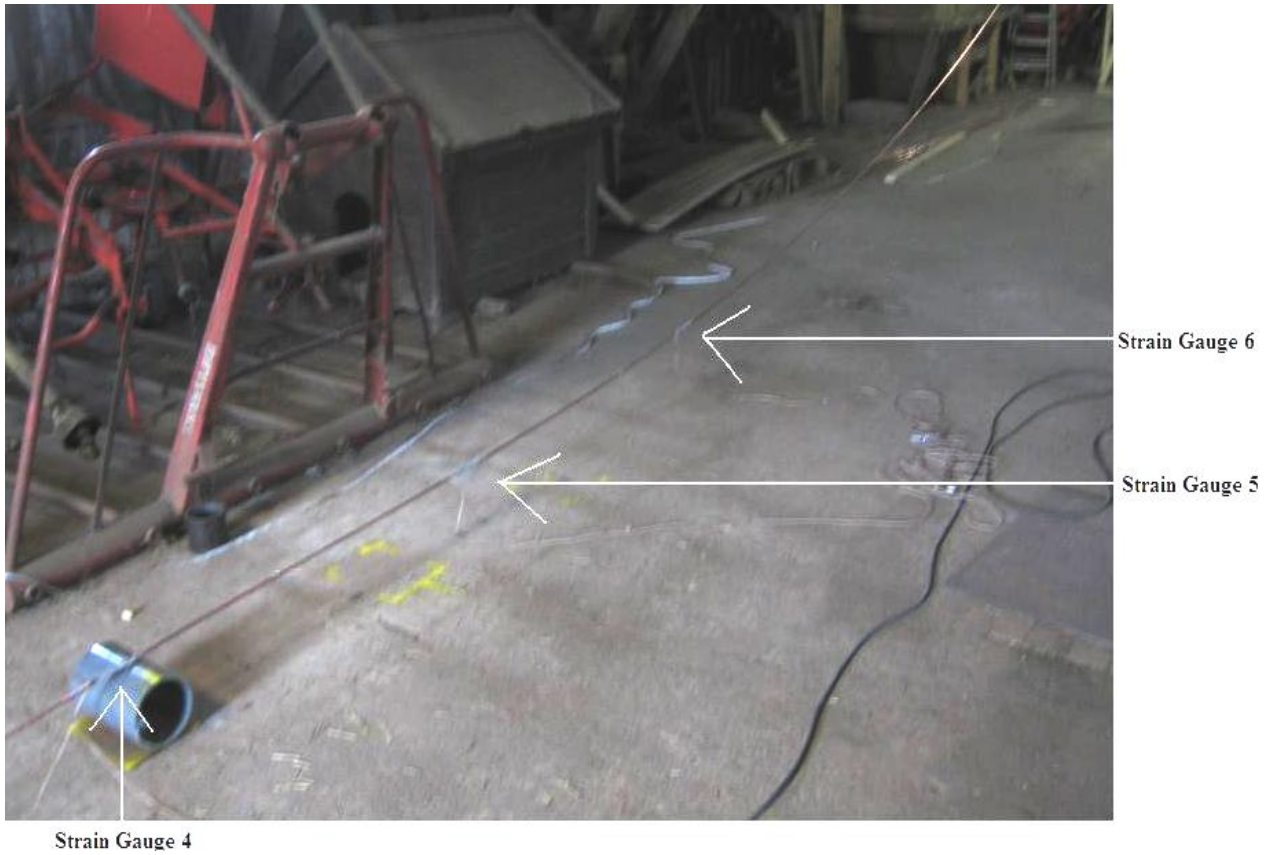
**Figure 45. The placement of some of the strain gauges used for measuring the strains in the sagbend.**

**17.4.3.1    Pipeline laid from 3.08 meters height:**

## Measured strains in the sagbend when laying from 3.08 meters onto two obstacles
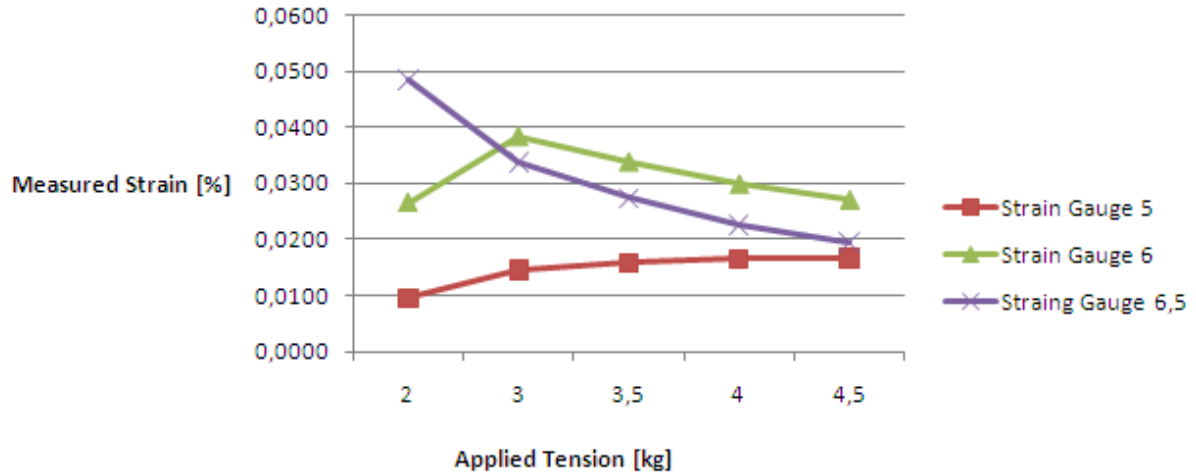


 Figure 46. Measured strains in the sagbend when the pipeline was laid from 3.08 meters height onto an uneven seabed with two obstacles.

It can be seen from Figure 46 that the highest strain measured when there was an uneven seabed was 0.048 percent. When comparing strain gauge number 6.5 for this scenario and for the one with a flat seabed it can be seen that the slope and the values of the graph are almost identical.

## Strains calculated in the sagbend by OrcaFlex when laying from 3.08 meters onto two obstacles. Long Span Model
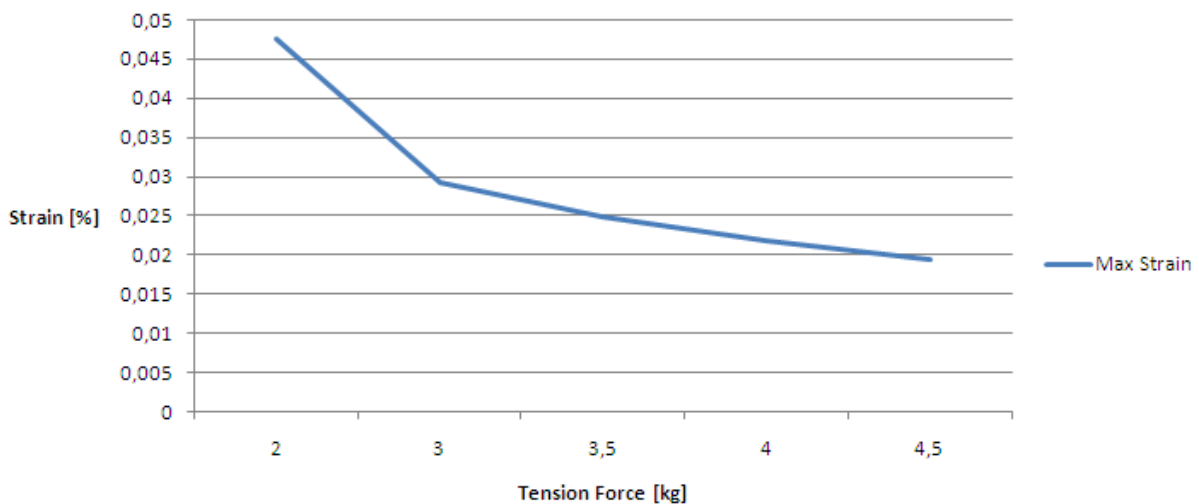


Figure 47.  Maximum strains obtained in OrcaFlex when the pipeline was laid from a height of 3.08 meters over two obstacles on the seabed.

71

Figure 47 shows that for the largest tension force a maximum strain of approximately 0.047 percent was obtained. The highest tension force resulted in a strain of 0.019 percent. The highest strain is almost similar to the one obtained in the experiment, as seen from Figure 46. However, the strain from the experiment is larger for the largest tension force.

It should be noted that since this was one of the last tests carried out, it was not tested in advance where the strain gauges should be mounted. Therefore, the strains might have been somewhat larger than what was measured in the experiment. The simulation can be seen in Appendix E.

**17.4.3.2      Pipeline laid from 4.97 meters height:**



**Figure 48.  Measured strains in the sagbend when the pipeline was laid from 4.97 meters height onto an uneven seabed with two obstacles.**

Figure 48 shows that the maximum strain measured when the pipeline was laid on an uneven seabed from a height of 4.97 meters was 0.062 percent. This is approximately the same value as for the flat seabed. A further comparison of flat and uneven seabeds shows that the strains are almost the same for all the different tension forces. The reason for this is probably that the pipeline was barely resting on the last obstacle and for the highest tension force the pipeline was lifted so there was no contact between the pipeline and the last obstacle at all. This means that the uneven seabed had little influence on strain gauge number six.

Strain gauge number five was closer to the last obstacle. Since the pipeline was barely resting on this obstacle before it went up to the stinger the area where strain gauge number five was mounted was not exposed to a large curvature and hence the variation in strains was small.
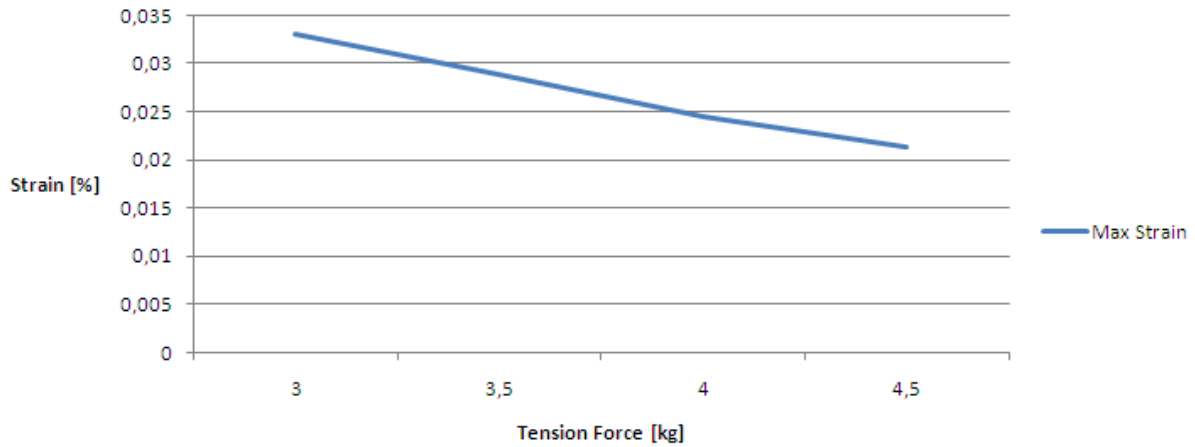
**Figure 49. Maximum strains obtained by OrcaFlex when the pipeline was laid from a height of 4.97 meters onto a seabed with two obstacles. Long Span Model**

Figure 49 shows that the maximum strains in OrcaFlex for the Long Span Model was approximately 0.033 percent when a tension force of 3 kg was applied. When a force of 4.5 kg was applied OrcaFlex calculated the maximum strain to be 0.021 percent. These strains are almost 50 percent less than the ones from Figure 48 which were measured in the experiment.



**Figure 50. Maximum strains obtained by OrcaFlex when the pipeline was laid from a height o 4.97 meters onto a seabed with two obstacles. Short Span Model.**

It can be seen from Figure 50 that when the Short Span Model was modelled in OrcaFlex, the lowest tension force resulted in a maximum strain of 0.06 percent, while the smallest force gave a strain of approximately 0.044 percent. This was a difference of only 0.002 percent for the smallest force compared to what was measured by the strain gauges. For the largest tension force the maximum strain from this model was actually slightly bigger than the one from the real test. This is probably because of the fact that the placement of the strain gauge did not hit the area of maximum strain very well.

It is also worth noticing that the maximum strain from this model increased when the tension force was increased from 4 kg to 4.5 kg. The simulation can be seen in Appendix E.

### 17.4.3.3        Test results vs. values found by OrcaFlex
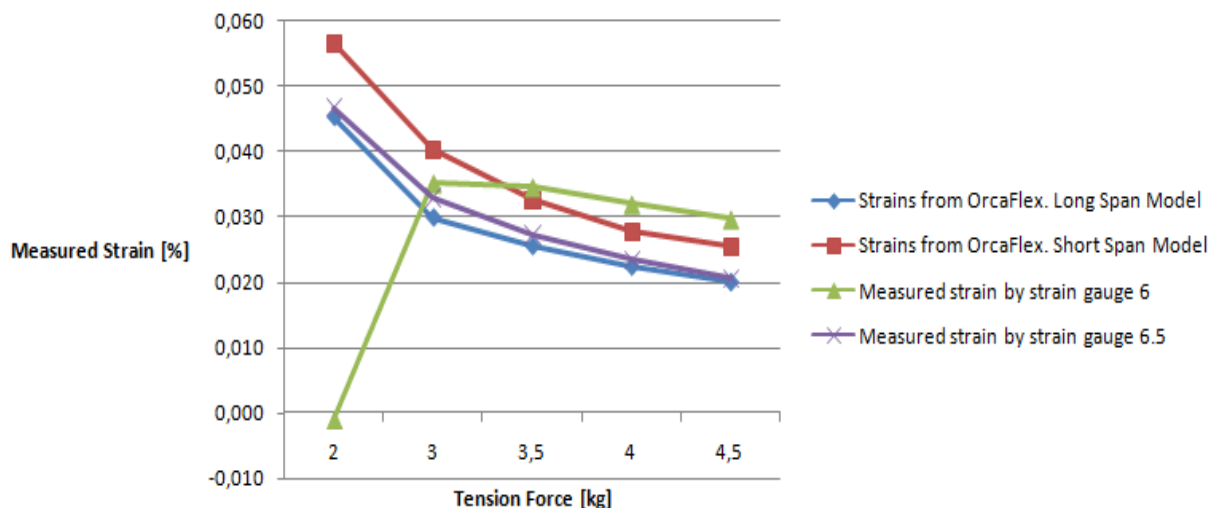


**Figure 51. Comparison of the strains obtained in the sagbend from the experiment and OrcaFlex when laying onto a flat seabed from 3.08 meters height.**

As seen from Figure 51 when the pipeline was laid from 3.08 meters, the Long Span Model was closer to the real results than the Short Span Model, especially for the small tension forces. The Short Span Model gave slightly higher values than the experiment for the smallest tension forces. The differences between the experiment and the frictionless Long Span Method became bigger as the tension force increased. However, as stated earlier, the strains from the tests also might have been higher if the strain gauges had been placed differently.
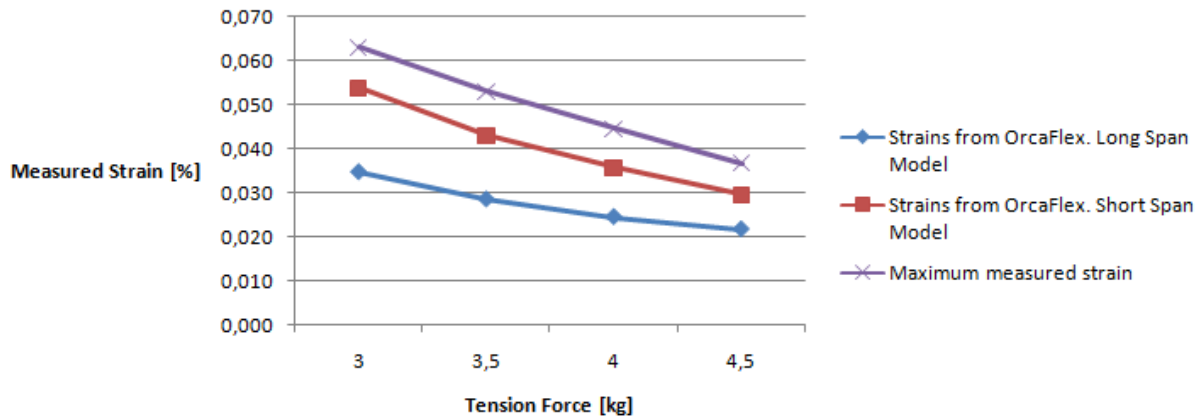
**Figure 52. Comparison of the strains obtained in the sagbend from the experiment and OrcaFlex when laying onto a flat seabed from 4.97 meters height.**

Since the measuring from 4.97 meters height was done first, the strain gauges in the sagbend were positioned more favourably than for the lowest laying height. This resulted in large strains compared to the ones from OrcaFlex.

Figure 52 shows that the test results when laying from 4.97 meters height onto a flat seabed gave significantly higher strains than what was calculated by OrcaFlex, especially for the Long Span Model where the friction force on the stinger was not taken into consideration. The lack of friction force led to the pipeline end laying further up on the deck of the vessel than what it did in the real tests. This means that a higher tension force was acting on the pipeline in the OrcaFlex model than what was acting on the real pipeline. This led to a longer span in the OrcaFlex model which resulted in smaller strain in the sagbend.

Since the Short Span Model was adjusted for the friction force on the stinger, the tension force acting in the pipeline in this model was much lower than for the Long Span Model, resulting in larger strains. Even though the Short Span Model also gave smaller strains than what was measured in the tests, they were a lot closer.

## Comparison of strains from the experiment and OrcaFlex when laying from 3.08 meters height onto two obstacles
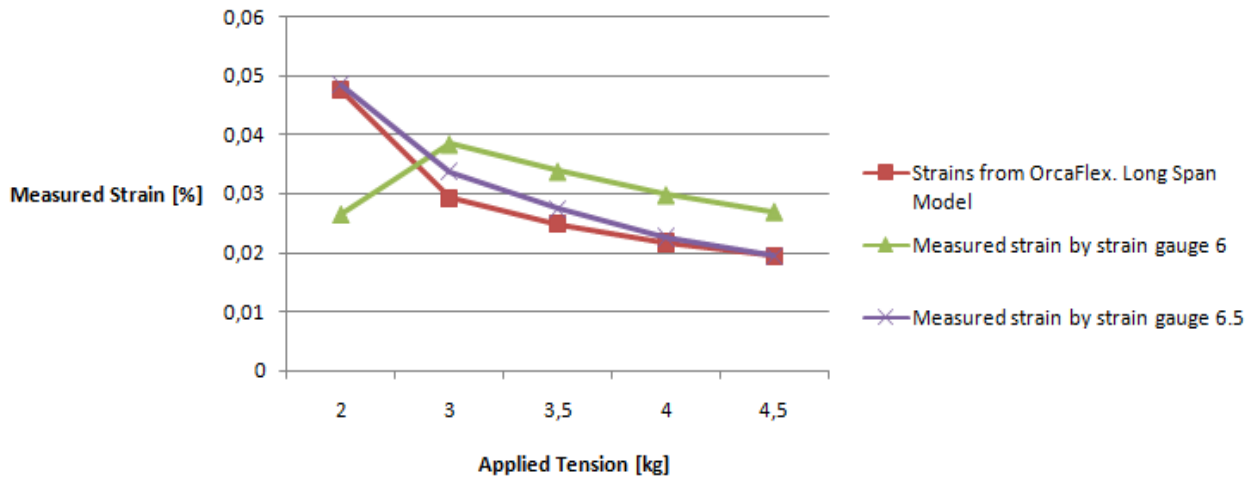


**Figure 53. Comparison of the strains obtained in the sagbend from the experiment and OrcaFlex when laying onto two obstacles from 3.08 meters height.**

## Comparison of strains from the experiment and OrcaFlex when laying from 4.97 meters height onto two obstacles
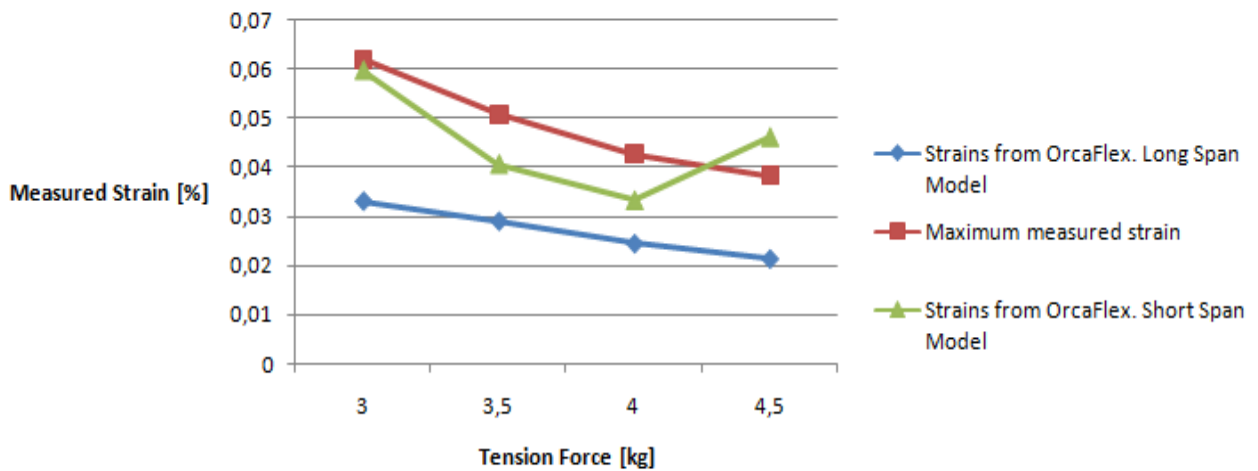


**Figure 54. Comparison of the strains obtained in the sagbend from the experiment and OrcaFlex when laying onto two obstacles from 4.97 meters height.**

As seen from Figures 53 and 54, when there were two obstacles on the seabed, the test results gave larger strains than OrcaFlex for both laying heights. However, for the largest laying height, the Short Span Model, which was adjusted for friction, was again very much closer to the real test results; it actually gave a bit larger strains for the highest laying height when the largest tension force was applied.

### 17.4.4 Strains acting in the pipeline laying on the seabed

Figures 56-69 show how the strains in the part of the pipeline laying on the uneven seafloor vary with the applied tension force. Figure 55 shows where the strains are measured.



**Figure 55. The placement of the strain gauges on the part of the pipeline laying on the seabed.**
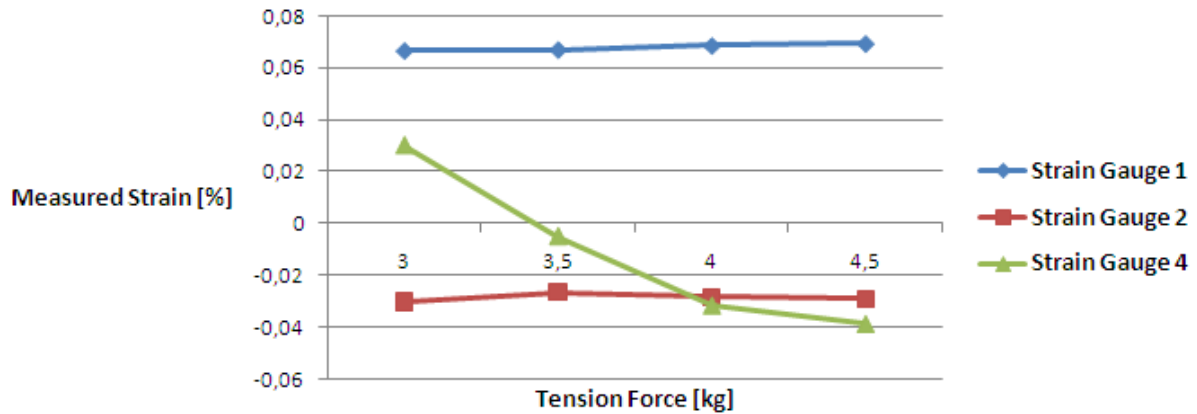
### 17.4.4.1 Pipeline laid from 3.08 meters height:
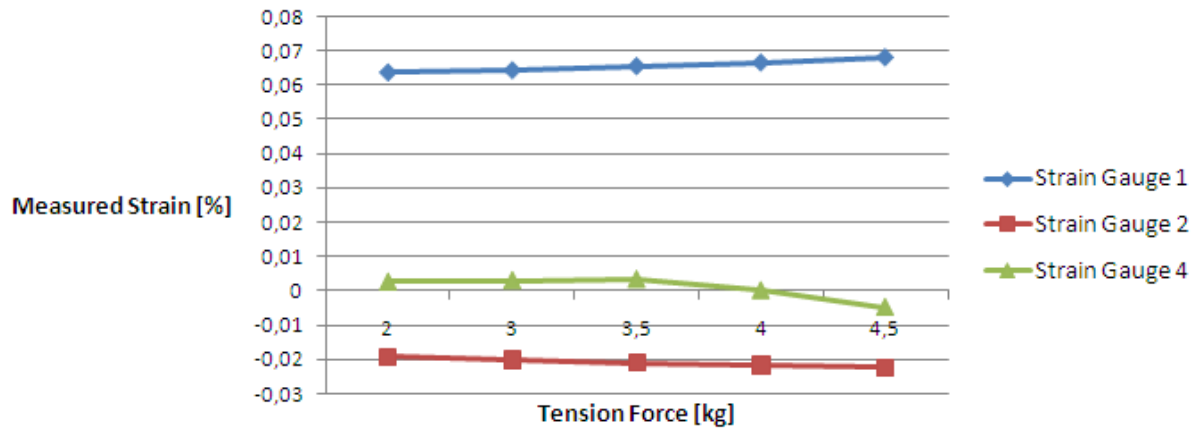


**Figure 56. Strains acting in the pipeline laying over one obstacle on the seabed when laid from 3.08 meters height.**

Figure 56 shows that strain gauge number one which was placed right on top of the obstacle experienced quite high strains. For this scenario the pipeline was resting on the seabed in front of the obstacle for every tension force. The curvature of the pipeline as it went over the obstacle remained more or less the same as more tension was applied. Therefore the strains caused by the larger tension force gave larger effects than the reduction in strains due to an increasing bending radius. This resulted in slightly increasing strains as the tension was increased.
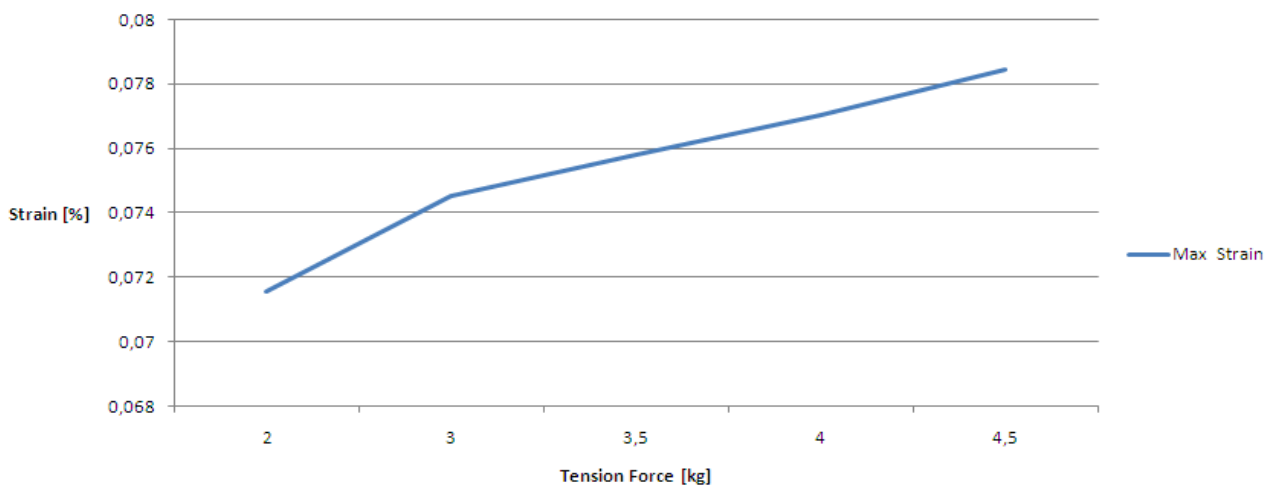


**Figure 57. Maximum strains obtained by OrcaFlex in the pipeline laying on the seabed when laid onto one obstacle from 3.08 meters height. This is the frictionless Long Span Model from OrcaFlex.**

Figure 57 shows the strains from OrcaFlex in the pipeline on top of obstacle number one since this was the point of the pipeline with the highest strain. As seen, the strain varies from 0.0715 percent for the smallest tension force and 0.0785 for the largest force.  These strains were a bit higher than the ones measured in the experiment which can be seen in Figure 56. The respective strains for the laboratory tests were 0.065 percent and 0.069 percent.

The reason for obtaining higher strains in the OrcaFlex model is probably the placement and mounting of the strain gauges. However, the differences were not very big. The simulation can be seen in Appendix E.

**17.4.4.2      Pipeline laid from 4.97 meters height:**
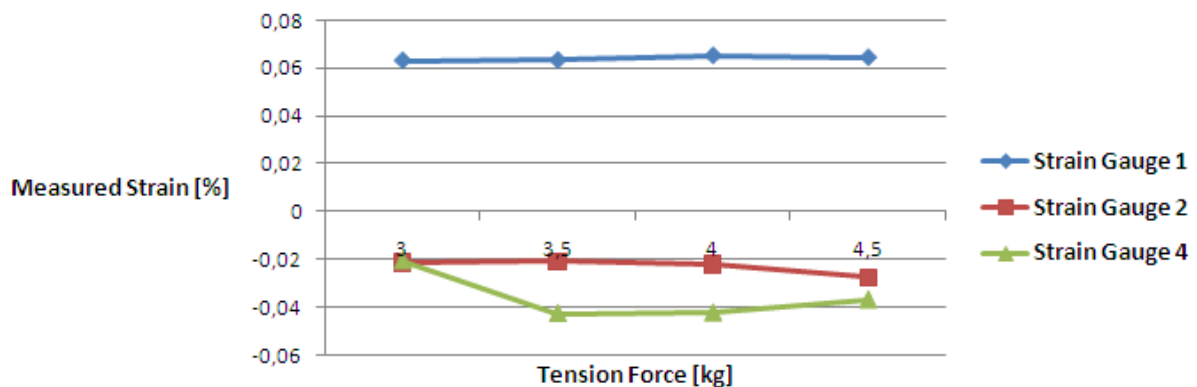


**Figure 58. Strains acting in the pipeline over one obstacle on the seabed when laid from 4.97 meters height.**

Figure 58 shows that the strains on top of the obstacle remained more or less the same for the different tension forces. However one can see that there is a small increase as the tension force increases also here.

By combining Figure 56 and Figure 58 one can see that a larger departure height does not make a big difference when it comes to the strain on top of the obstacle.

Strain gauge number two was resting on the seabed but was pretty close to the obstacle, hence it experienced some strains.

Strain gauge number four was affected by the strains from the sagbend.
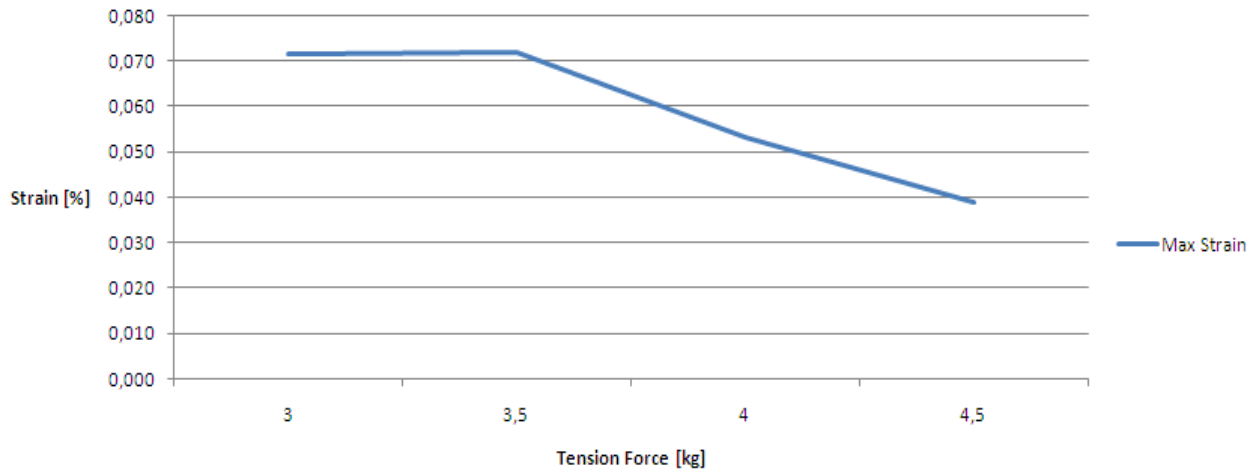
**Figure 59. Maximum strains in the part of the pipeline laying on the seabed when laid onto one obstacle from 4.97 meters height. This is the frictionless Long Span Model from OrcaFlex.**

Figure 59 shows the strains from OrcaFlex in the pipeline on top of obstacle number one. One can see from the figure that for the smallest tension, the strain remains constant at approximately 0.071 percent, which is a bit higher than for the real experiments. This is probably also due to the mounting of the strain gauges. However, in the OrcaFlex model the pipeline was lifted off the seabed in front of the obstacle for a tension force of 4 kg. This resulted in a significant drop in strain.

In the real test model, the pipeline was not lifted off the seabed for any of the tension forces. The reason it was lifted off in the OrcaFlex model is probably because it does not account for friction force on the stinger, resulting in a longer span. The simulation can be seen in Appendix E.
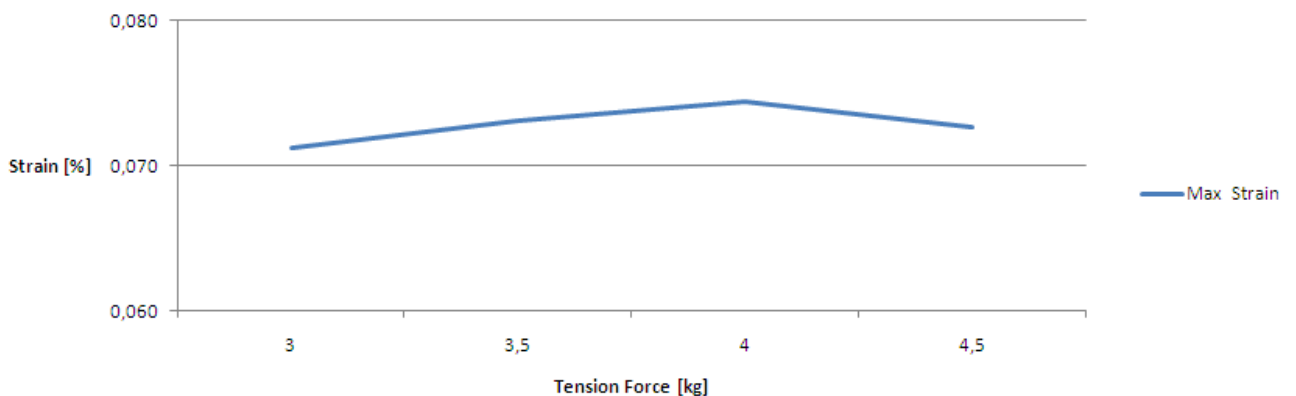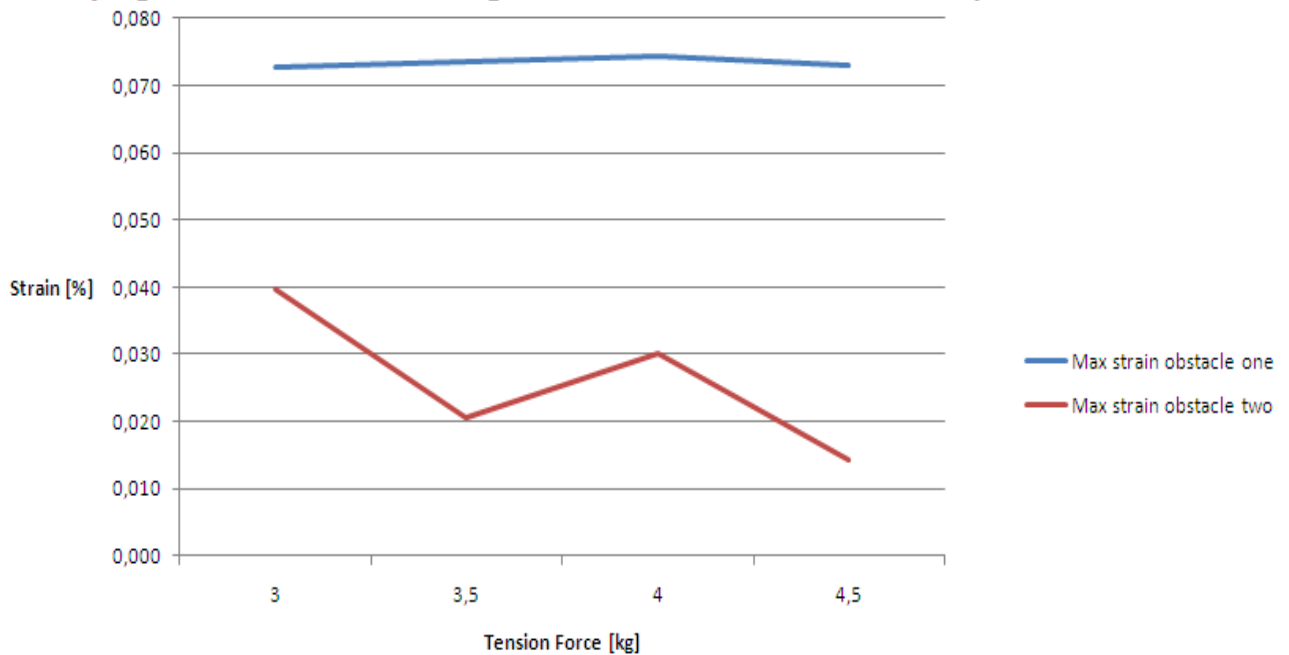


**Figure 60. Maximum strains in the pipeline laying on the seabed when laid onto one obstacle from 4.97 meters height. Short Span Model from OrcaFlex.**

80

As seen from Figure 60 the maximum strain over obstacle number one is varying from approximately 0.072 percent to 0.075 percent. Also for this model the strains from OrcaFlex are slightly higher than the ones from the experiments. But for this model the pipeline was not lifted off the seabed in front of the obstacle which gave a curvature much more like the one in the experiments. The strain did not drop significantly for the largest tension forces, which means that this model gives a much more reliable result. The simulation can be seen in Appendix E.

**17.4.4.3      Pipeline laid from 3.08 meters height:**
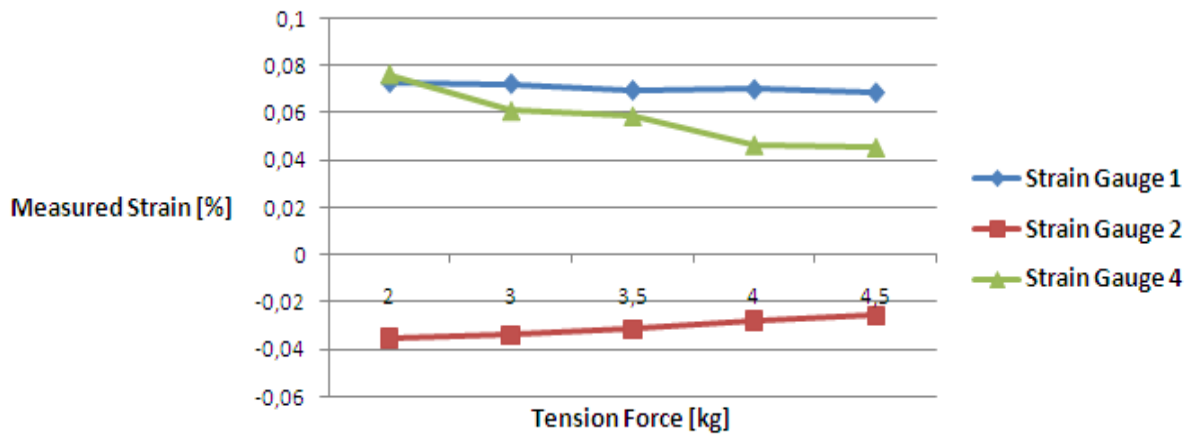


**Figure 61. Strains acting in the pipeline over two obstacles on the seabed when laid from 3.08 meters height.**

When the pipeline was laid over two obstacles Figure 61 shows that the strains on top of obstacle number one was slightly higher than when laid over only one obstacle. The strain in this area of the pipeline seems to decrease marginally as the tension force increases.
For the smallest tension force the strain on top of obstacle number two was the same as for obstacle number one. This is because the pipeline was resting on the seabed at both sides of the obstacle; hence the curvature over the two obstacles became the same. However, as more tension was applied the pipeline was lifted off the seabed in front of obstacle number two which resulted in a decrease in strain as seen from the figure.

Strain gauge number two which was placed in the middle of the two obstacles was also lifted higher from the seabed as the applied tension force increased. This resulted in lower strain as the force increased.
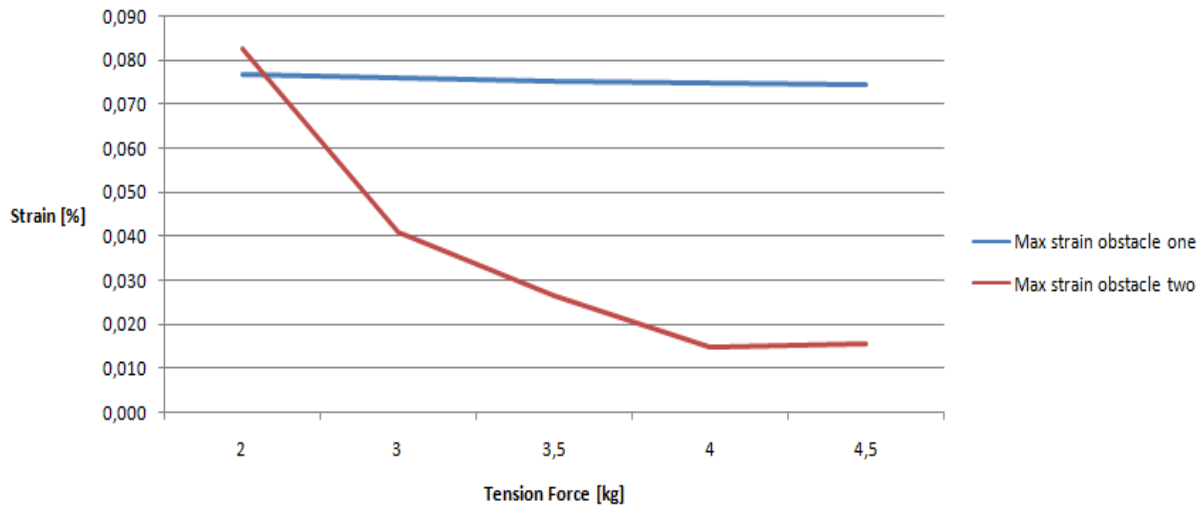
**Figure 62. Maximum strains in the part of the pipeline laying on the seabed when laid onto two obstacles from 3.08 meters height. Long Span Model from OrcaFlex.**

One can see from Figure 62 that the strains on top of obstacle one did not vary very much. As for the other scenarios these strains were also slightly higher when calculated in OrcaFlex than for the laboratory experiments.
The strain on top of obstacle number two was here 0.083 percent for the smallest tension force and dropped down to approximately 0.015 as the tension was increased.

The respective strains measured in the real results were 0.075 and 0.045. This means that for the largest tension force the strains from the experiments were much larger than what was calculated in OrcaFlex. The simulation can be seen in Appendix E.

**17.4.4.4        Pipeline laid from 4.97 meters height:**

# Measured strains in the pipeline on the seabed when laying onto two obstacles from 4.97 meters height



**Figure 63. Strains acting in the pipeline laying over two obstacles on the seabed when laid from 4.97 meters height.**

One can see from Figure 63 that the strain on top of obstacle number one increased marginally as the tension was increased. However, the strain seems to be approximately the same as for all the other scenarios for one and two obstacles.
This time the pipeline did not touch the seabed in front of obstacle number two for any of the tension forces. Therefore the strain in the pipeline on top of the obstacle was much smaller than when laid from a lower height. The figures show that the tension in strain gauge number four decreases drastically as the tension decreases until the strains become compressive when the curvature of the pipeline changes direction as the strain gauge enters the sagbend.
The figure also shows that for this laying height the variation in tension force had little influence on the strains measured in the sagbend created between the two obstacles (strain gauge number two).

## Strains calculated in the pipeline on the seabed when laying onto two obstacles from 4.97 meters height. Long Span Model
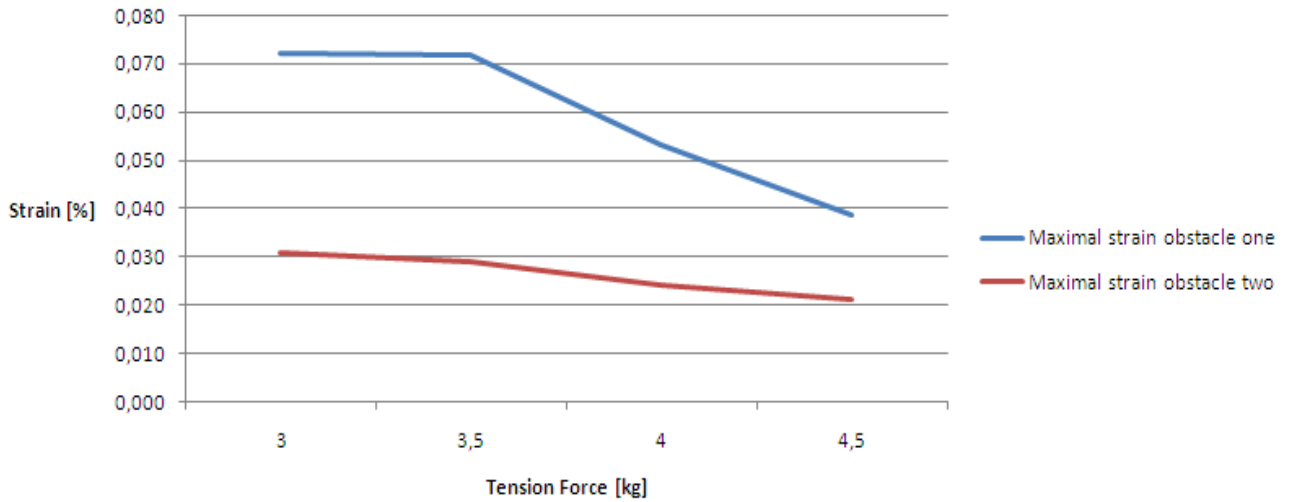


**Figure 64. Maximum strains in the pipeline laying on the seabed when laid onto two obstacles from 4.97 meters height. Long Span Model from OrcaFlex.**

One can see from Figure 64 that the strain on top of obstacle number one is nearly equal to the strains from the same model in OrcaFlex when there was only one obstacle. The strains drop significantly when the pipeline is lifted from the seabed in front of the obstacle when a tension force of 4 kg is applied.

The strain over obstacle number two is about 0.03 percent for the lowest tension force which is approximately the same as what was measured in the experiments, see Figure 63. The strain drops as more tension is applied. The strain for the largest tension force however is 0.02 in the OrcaFlex model and 0.04 in the real model. This is because the real model gives a shorter span length than the Long Span Model in OrcaFlex. The simulation can be seen in Appendix E.

**Figure 65. Maximum strains in the pipeline laying on the seabed when laid onto two obstacles from 4.97 meters height. Short Span Model from OrcaFlex.**

As can be seen from Figure 65 the strains on top of obstacle number one do not decrease as the tension force is increased like they do for the Long Span Model in OrcaFlex. They remain more or less constant as they do for the real experiments, only slightly larger.

When it comes to obstacle number two, the strain from this OrcaFlex model is 0.04 percent for the smallest tension force, compared to 0.03 for the real model. This is probably due to the fact that this strain gauge was not mounted in an absolute correct position. It is also worth noticing that the pipeline, including the strain gauges, was moved a bit towards the stinger as more tension force was applied. Since the strains in the pipeline from OrcaFlex are precisely from the top of the obstacles, the strains might have been taken from slightly different positions in the laboratory tests and in OrcaFlex. However, this is not much. One can also see that the strains over obstacle two increase for the two largest tension forces. This is because the strains go from tension to compressive strains on the top of the pipeline as the part of the pipeline in front of the obstacle lifts higher from the seabed. The simulation can be seen in Appendix E.

### 17.4.4.5 Test results vs. values found by OrcaFlex
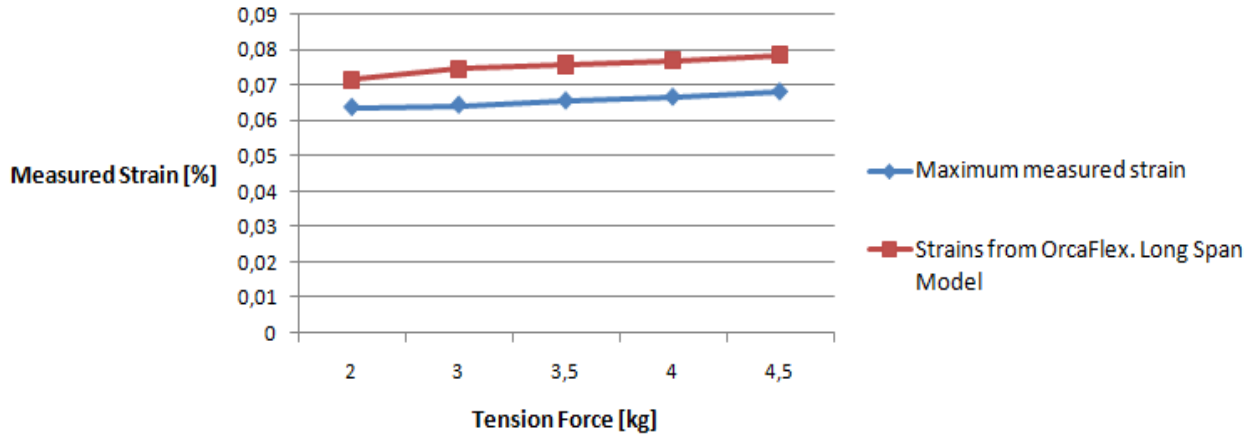


**Figure 66. Comparison of the strains acting in the part of the pipeline laying on the seabed when laid from 3.08 meters height onto one obstacle.**
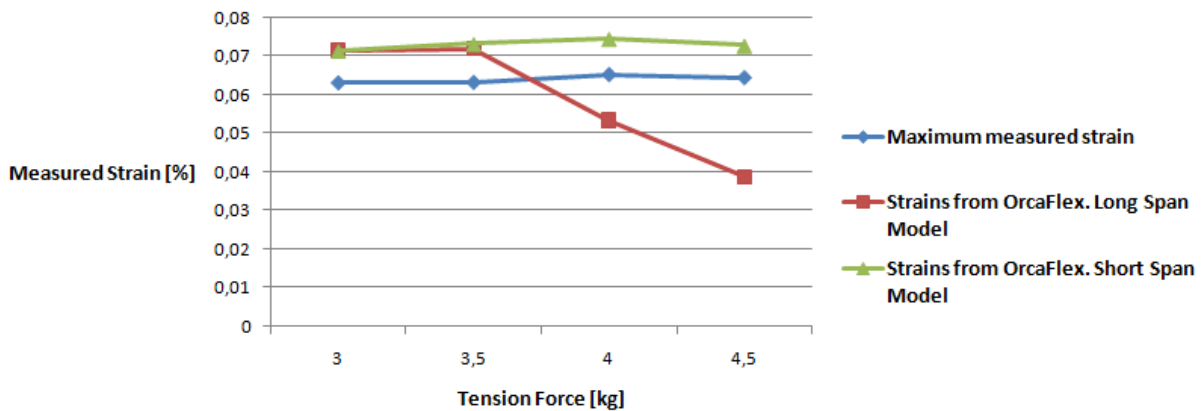


**Figure 67. Comparison of the strains acting in the part of the pipeline laying on the seabed when laid from 4.97 meters height onto one obstacle.**

The measured test results shown in Figures 66 and 67 show that the strains in a pipeline laying over one obstacle far away from the touchdown point are not affected very much by an increase in tension force. For the lowest laying height, the strains calculated by the frictionless OrcaFlex model were slightly higher than the ones measured in the test result. When the touchdown point is close to the obstacle, like it was for the largest laying height, the strains calculated by OrcaFlex become more unreliable because the touchdown point in OrcaFlex was on the top of the obstacle for the largest tension forces. This resulted in much too small strains for the highest tension forces. The reason for this is that the span length was much larger for this model than it was in the experiment

When the strains were calculated in the Short Span Model in OrcaFlex, the strains were a bit higher than the test results, but they did not drop to values far lower than the test results as they did in the frictionless Long Span Model. This means that The Short Span Model, which is adjusted in order to take friction force into consideration, in OrcaFlex is much more reliable for scenarios like this.
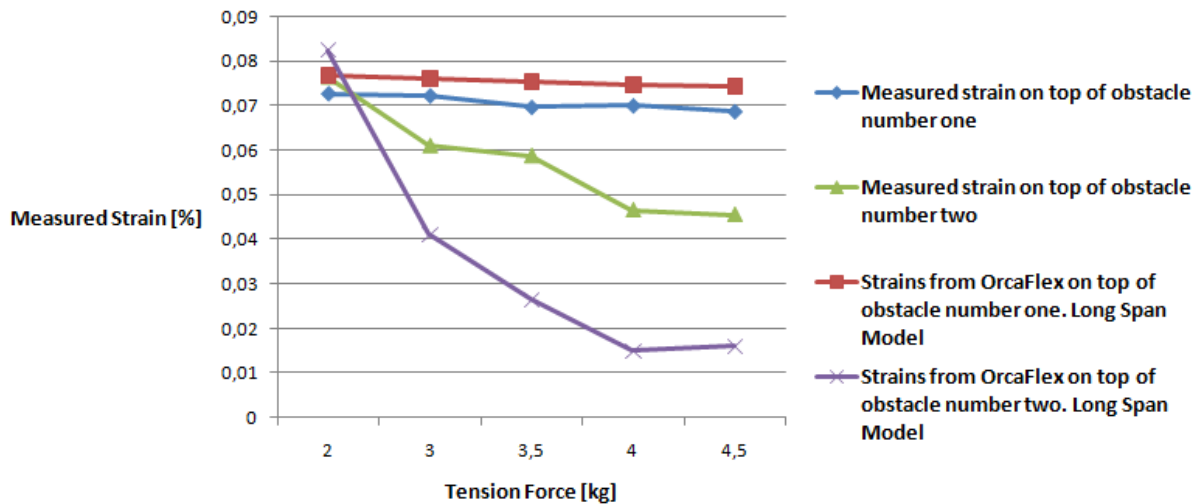


**Figure 68. Comparison of the strains acting in the part of the pipeline laying on the seabed when laid from 3.08 meters height onto two obstacles.**
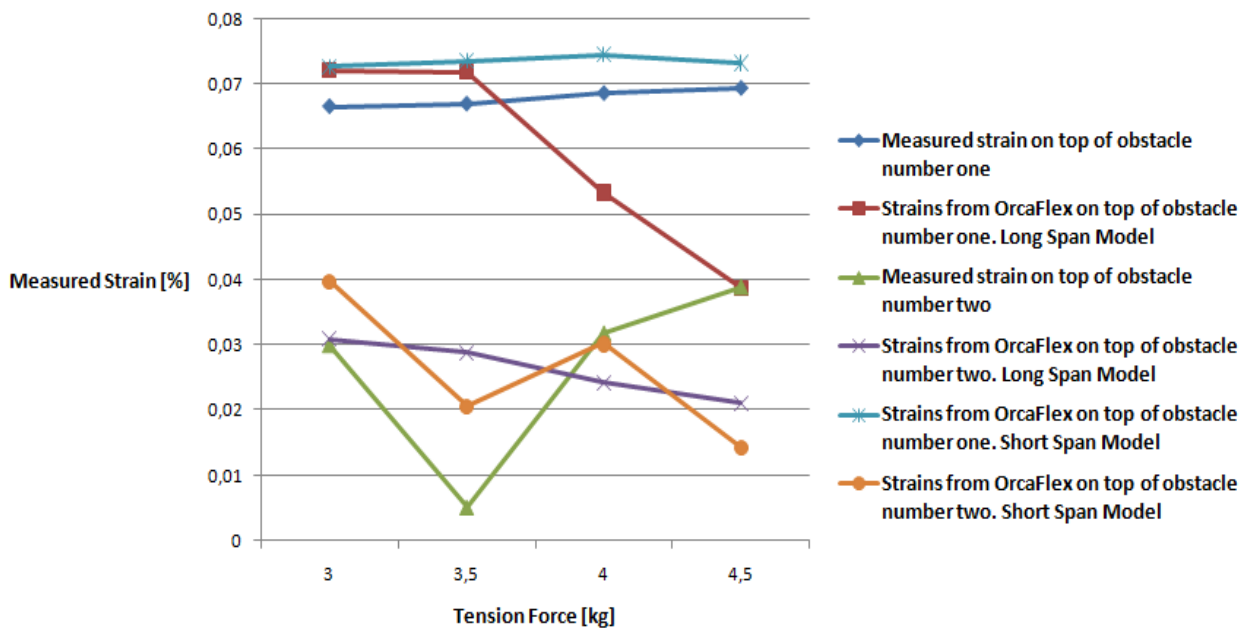


**Figure 69. Comparison of the strains acting in the part of the pipeline laying on the seabed when laid from 4.97 meters height onto two obstacles.**

One can see from Figures 68 and 69 that the increase in tension force had little influence on the strains on top of obstacle number one also when the pipeline was laid on top of two obstacles. The frictionless Long Span Model gave rapidly decreasing strain as the tension force was increased and the sagbend between the two obstacles was lifted off the seabed. The sagbend between the two obstacles did not lift from the seabed for any of the tension forces neither in the experiment nor in the Short Span Model. Therefore, by including the friction on the stinger, the Short Span Model in OrcaFlex gives significantly better results.

The curve for the measured strain on top of obstacle number two, seen in Figure 69 is showing only positive values this time because OrcaFlex only shows positive values. From the strains on top of obstacle number two it can be seen that when the obstacle is close to the touchdown point of the pipeline the strains will decrease rapidly as more tension is applied.

## 17.5 Slip of the anchor system scenario

Figure 70 shows the strains measured in the sagbend as the lift was moved backwards.

As seen from Figure 70, the strains measured were not very large. The areas of maximum curvature in the sagbend moved as the lift moved. This meant that when the really large curvatures occurred they occurred in areas where there was no active strain gauge.
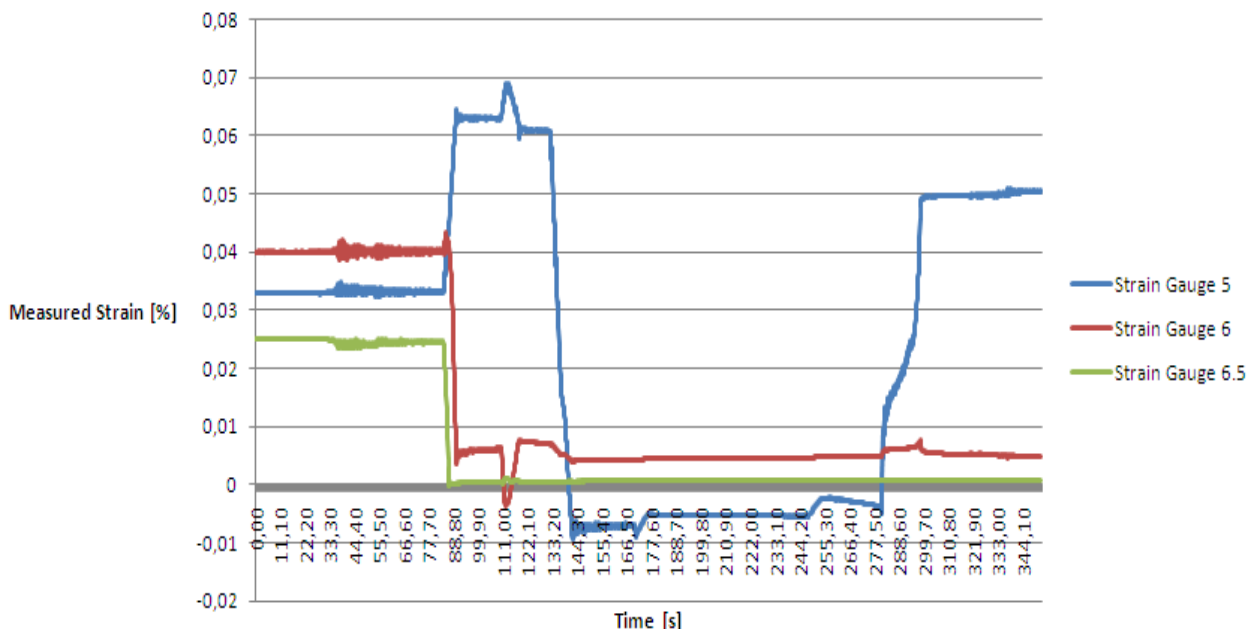


**Figure 70. Measured strain as a function of time when the lift was moved backwards.**

Figure 70 shows that the largest strain measured in the sagbend as the lift moved was approximately 0.069 percent which was much lower than the actual strain in the pipeline.

As seen from Figures 71-75 the curvature of the pipeline increased significantly as the lift was moved. What was worth noticing was that not only did the curvature in the sagbend get big, but the pipeline in the overbend was also exposed to very large bends.



**Figure 71. The sagbend before the lift started to move.**
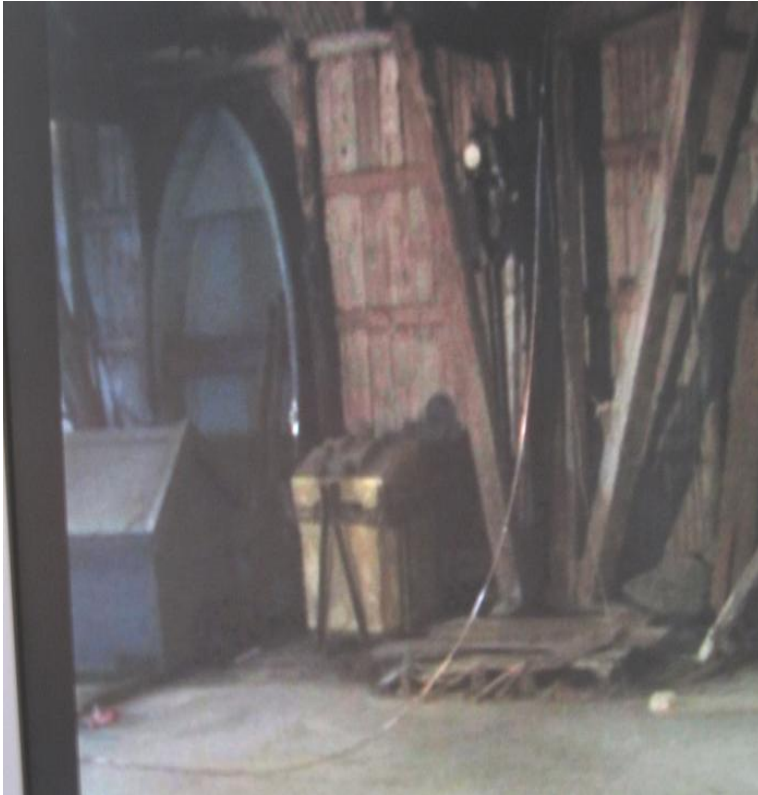


**Figure 72. The curvature of the sagbend as the lift was moved.**

**Figure 73. The curvature of the sagbend as the lift was moved.**



**Figure 74. The stinger as the lift was moved.**

**Figure 75. The stinger as the lift was moved**

One can see from Figures 74 and 75 that as the lift was moved backwards, the pipeline was lifted from the stinger and was only in contact with the stinger tip. From the figures it seems that the stinger tip is exposed to larger loads the further the lift was moved. This means that the stinger needs to be very solid in order to withstand a situation like this.

The pipeline was pushed down onto the seabed as the lift moved. This means that the touchdown point moved closer to the lift, in addition to the reduced span length caused by the lift moving closer to the touchdown point. This resulted in the lift not having to move very far before the stinger tip was very close to the touchdown point, giving a closer to vertical S-shape of the pipeline.

When the lift was moved 1.67 meters the lift was stopped for a little while to allow for an inspection of the situation. When the lift stood still one of the joints broke. This was probably due to escalation of stresses which finally made the pipe break. This can be seen in Figure 76.

**Figure76. One of the solders broke during the testing.**

It can be argued that the lift was moved a very large distance compared to the laying height. The lift had to be moved approximately one half of the water depth before the soldering broke. However, by looking at the curvature of the pipeline there is reason to believe that the pipeline will experience plastic deformations long before the lift had been moved 1.67 meters.

How far a vessel would move if the anchors slipped depends on many factors, where the seabed is one of the most important ones. If the anchor gets a new hold, the vessel does not necessarily move very far.

Figure 77 shows one of the pipe segments after the test had been done and it can be seen that the pipeline has experienced severe plastic deformations.



**Figure 77. One of the pipe segments after the test was done.**

It was not possible to perform this simulation in OrcaFlex. The big stinger seen in Figure 23 would have prevented the pipeline from bending very much. If this test was to have been modelled in OrcaFlex the water depth would have to be much larger or the stinger radius would have to be much smaller.

## 17.6 Natural frequency of the pipeline

The following natural frequencies of the pipeline were measured in the laboratory tests.

For 3.08 meters height:

Table 7. Natural frequency of the pipeline when laid from 3.08 meters height.

| Tension Force [kg] | Number of oscillations | Natural period [s] | Natural Frequency [Hz] |
|---|---|---|---|
| 2 | 8 | 1,25 | 0,8 |
| 3 | 8 | 1,25 | 0,8 |
| 3,5 | 8 | 1,25 | 0,8 |
| 4 | 7 | 1,43 | 0,7 |
| 4,5 | 7 | 1,43 | 0,7 |

For 4.97 meters height:

Table 8. Natural frequency of the pipeline when laid from 4.97 meters height.

| Tension Force [kg] | Number of oscillations | Natural period [s] | Natural Frequency [Hz] |
|---|---|---|---|
| 3 | 9 | 1,67 | 0,6 |
| 3,5 | 9 | 1,67 | 0,6 |
| 4 | 9 | 1,67 | 0,6 |
| 4,5 | 9 | 1,67 | 0,6 |

The number of oscillations includes whole oscillations, half oscillations were not included. If the pipeline had oscillated for a longer period of time, there probably would have been bigger variations in oscillations for the different forces. However, one can see from Tables 7 and 8 that the natural frequency when laid from 4.97 meters is lower than when laid from 3.08 meters. This means that a longer span gives smaller frequency.  This is also theoretically correct according to Equation 14.1. However, Equation 14.1 states that the larger the tension force, the larger frequency. This means that in this experiment the effect of the span getting longer was larger than the effect of increasing tension force.

# 18       Scaling of the model used in the experiment [1]

Scaling of the model into real sizes used in the industry can be very complex. However, scaling for stresses caused by wind and hydro-static/dynamic forces is the most critical.

If hydrostastic stress is what is being studied, this can be done with small scale models both in water and air. However, the condition for similarity when it comes to deflection states that Equation 17.1 is similar for both the test model and the real size model.

$$\frac{w \cdot L^3}{E \cdot t \cdot d^3} \tag{18.1}$$

Where,
w = Submerged weight of pipeline per unit length
L = Characteristic length of the pipeline
E = Young's modulus of the pipeline
t = Wall thickness of the pipeline
d = Outer diameter of the pipeline

When it comes to hydrodynamic stresses on the pipeline and the stinger there has to be similarity of geometry, gravity, inertial force, viscous forces and the stiffness of both the pipeline and stinger. It is worth noticing that this only applies to the extent possible as full similarity between the model and real situations is not possible.

If stresses from waves are being studied, the gravity and inertial forces are dominant.

A Froude's model can be used for similarity as regards the viscous friction forces between the test model and the real size situation. If this is done, additional terms for mass and stiffness of the material have to be added to the Froude model. However, this model will give some errors due to the similarity not being perfect.

If the yield strength is not taken into account the scaling can be done purely geometrically [17]. By simulating laying of a pipeline with an external diameter of 36 inches the scaling between our test model and the real size model would be 1:114. The length of the pipeline would then be 2280 meters and the water depths would become approximately 350 and 570 meters. The height from the deck of a potential lay vessel to the sea surface is not accounted for here.

In order for the condition stated earlier in this chapter to be satisfied, a steel pipeline with an outer diameter of 36 inches would need a wall thickness of 31 millimetres. However, it is worth noticing that the equation is very sensitive and even for a small deviation of the calculated wall thickness the condition will not be satisfied.

For a steel pipeline with an outer diameter of 20 inches the scaling ratio would be 1:63.5 purely geometrically. This would correspond to a water depth of 200 meters and 315 meters. The necessary wall thickness of this pipe in order for the condition to be satisfied is approximately 17.7 millimetres.

For calculations, see Appendix F.

# 19    Conclusion and recommendations for further work

During this thesis several issues and parameters related to S-laying of pipelines have been investigated. The investigations have been carried out though laboratory experiments and numerical analyses in the software OrcaFlex.

 The main objectives have been to investigate the strains in the pipeline during installation and to investigate how the span length of the pipeline from the vessel to the seafloor is affected by water depth and applied tension force. The strains have been measured in this free span as well as in the pipeline laying on an uneven seabed. In addition an investigation of the departure angle of the pipeline from the stinger and the required stinger length was performed. All these investigations were done from two different laying heights and for a number of different applied tension forces.

During this project very much time was spent on constructing and testing. The actual tests also proved to take a lot more time than expected.  Therefore, some of the planned tests had to be excluded from the experience.

The results show that the calculation done by OrcaFlex can be quite different from the measurements obtained in the laboratory tests. Some of the differences may be due to some of the strain gauges not being mounted perfectly. However, the main contribution to the differences between the test results and OrcaFlex results is probably the fact that the friction force on the stinger is not taken into consideration by OrcaFlex. This means that a larger tension force is applied to the pipeline in OrcaFlex than what is actually acting on the pipeline. This will in turn lead to a much longer span in OrcaFlex, resulting in a much smaller curvature in the sagbend than what is actually acting on the real pipeline.  For the worst cases this resulted in 50 percent larger strains than what was calculated by OrcaFlex.

One might argue that on real vessels there will be rollers on the stinger to reduce the friction forces; hence the differences between OrcaFlex and real-life situations will not be this substantial. However, certain friction force will still be acting, resulting in smaller strains in OrcaFlex. This means that OrcaFlex simulations do not necessarily have to be conservative.

The lack of friction on the stinger in OrcaFlex did not affect the strains in the overbend very much since the bending radius here is the same as the radius of the stinger for the majority of the overbend.

For the situation where the tension force did not affect the strains very much, like on top of an obstacle laying far away from the touchdown point or in the overbend, the strains as calculated by OrcaFlex were pretty similar to the ones measured in the tests. This means that the lack of friction force in OrcaFlex probably is the reason for the big differences in the sagbend stresses between those calculated by OrcaFlex and the test results. Another reason for assuming that the lack of friction force is the main reason for the big differences is that when an OrcaFlex model adjusted to take the friction force into consideration was used, most of the results became much closer to the results obtained from the experiments.

This means that the greater impact the tension force has, the bigger the differences between OrcaFlex and real situations will be. Furthermore, this means that for very large water depths, where an extensive tension force is needed in order to control the curvature of the sagbend, the differences between the strains as calculated by OrcaFlex and real situations will possibly be huge.

The strains measured in the pipeline laying on an uneven seabed show that in order for a small tension force or a loss of tension force scenario to result in plastic deformations of the pipeline the unevenness has to be very significant. The obstacles used in this thesis had a diameter which was approximately 20 times larger than the diameter of the pipeline, and the pipeline on the seabed was never close to experiencing plastic deformations.

A scenario simulating a potential loss or slip of the anchor system was also investigated. The results show that this can be very damaging to the pipeline. In the test done in this thesis, one of the solders broke, and the pipeline experienced some serious plastic deformations.

In this thesis it was not possible to get the pipeline to experience plastic deformations only by loosening up the tension force. It would therefore be interesting to perform a study equal to this one only with bigger departure heights in order to obtain larger strains in the sagbend and to simulate a possible loss of tension scenario.

The natural frequency of the pipeline was also investigated. The results show that the applied tension force and water depth had a small effect on the frequency. However, if the pipeline had been oscillating for a longer period of time the measuring would probably become more accurate, and a bigger variation would most likely occur. Further analyses of this were not carried out due to time shortage, but as future work it would be interesting to perform an investigation to see what waves and current conditions the pipeline could have been installed in without the risk of getting into resonance with waves and vortices shed by the current flow.

It would also be of interest to try the test with different stinger radiuses in order to see how the departure angle and strains develop for the larger laying heights.

Another scenario can involve placing a soft material at the span shoulders in order to study the burying of the pipeline as it oscillates during the installation phase.

# References:

(1)    NOU 1974,40, "Rørledninger på dypt vann". Universitetsforlaget.

(2)    Young Bai,"Pipelines and Risers". Elsevier Ocean Engineering Book Series, Vol. 3, 2001.

(3)    A. H. Mousselli, "Offshore Pipeline Design, Analysis and Methods". Pennwell Publishing Company, Tulsa, Oklahoma, 1981.

(4)    Design code: "DNV-OS-F101 Submarine Pipeline Systems". Det Norske Veritas, Oslo, October 2007, amended in April 2008.

(5)    Braestrup, M.W., J.B. Andersen, L.W. Andersen, M.B. Bryndum, C.J. Christensen and N. Rishøj, "Design and Installation of Marine Pipelines". Blackwell Science Ldt., Oxford, 2005

(6)    Ersland, A., "Pipeline Installation in Deep Water". Master thesis at the Department of Offshore Technology, the Stavanger University College, Stavanger, Norway, 2000

(7)    Lecture notes for the course Marine Operations at the University of Stavanger

(8)    Lecture notes for the course Pipelines and Risers at the University of Stavanger

(9)    Stava, I., "Design of Arctic Offshore Pipelines in Areas Subjected to Ice Ridge Gouging". Master thesis at the Department of Mechanical and Structural Engineering and Materials Science, the University of Stavanger, Stavanger, Norway, 2007

(10)   Personal conversation with Ove Tobias Gudmestad, Professor at the University of Stavanger.

(11)   Personal conversation with Loic Meignan, engineer at IKM Ocean Design.

(12)   Personal conversation with Jiong Guan, engineer at IKM Ocean Design.

(13)   http://www.isope.org/publications/journals/ijope-02-2/abst-2-2-p157-RH-3-Skomedal.pdf (last checked 10.06.09)

       Skomedal, E.," Static Calculation of Pipeline Free Spans". International Journal of Offshore and Polar Engineering, Vol. 2, No. 2, Høvik, Norway, 1992.

(14)   http://e-book.lib.sjtu.edu.cn/otc-2005/pdfs/otc17627.pdf (last checked 10.06.09)

E.P Heerema, "Recent Achievements and Present Trends in Deepwater Pipe-lay Systems". Presented at the 2005 Offshore Technology Conference (OTC), Houston, Texas, USA: OTC

(15)     http://www.hse.gov.uk/research/rrpdf/rr053.pdf (Last checked 10.06.09)

Robson, J.K., "Ship/Platform Collision Incident Database (2001)". Prepared by Serco Assurance for the Health and Safety Executive, England, 2003.

(16)     Design code: "DNV-RP-F105 Free Spanning Pipelines". Det Norske Veritas, Oslo, February 2006.

(17)     Personal conversations with Kenneth Macdonald, professor at the University of Stavanger

(18)     Johannesen, M. J. "Installasjon av rørledninger på dypt vann".  Master thesis at the Department of Mechanical and Structural Engineering and Materials Science, the University of Stavanger, Stavanger, Norway, 2001.

(19)     www.hbm.com
         HBM product information, HBM (Last checked 10.06.09)

# List of Appendixes

## Appendix A; Calculation of required tension force in order to avoid plastic deformations in the sagbend

Equation 6.15 has been rewritten here since there was no water in the experiments. The last term has been neglected and the weight of the pipeline in air has been used.

DNV states that the yielding point of pipeline is when the strain exceeds 0.5%.

$$T = w \cdot (\frac{r}{\varepsilon_0} + D)$$

## For a height of 3.08 meters:

$$T = 0.186 \cdot (\frac{0.004}{0.005} + 3.08)$$
$$T = 0.72 \, kg$$

**The conservative calculation using yield strain of copper:**

Yield Strength: $365 \, \frac{N}{mm^2}$

Young's modulus: $1.2 \cdot 10^5 \, \frac{N}{mm^2}$

The yield strain for copper:

$$\varepsilon_p = \frac{365}{1.2 \cdot 10^5}$$

$$\varepsilon_p = 0.003$$

$$T = 0.186 \cdot (\frac{0.004}{0.003} + 3.08)$$

$$T = 0.82 \, kg$$

## For a height of 4.97 meters:

$$T = w \cdot (\frac{r}{\varepsilon_0} + Z)$$

$$T = 0.186 \cdot (\frac{0.004}{0.005} + 4.97)$$

$$T = 1.1 \, kg$$

**The conservative calculation:**

$$T = 0.186 \cdot (\frac{0.004}{0.003} + 4.97)$$

$$T = 1.2 \, kg$$

## Appendix B; Calculation of required stinger radius in order to avoid plastic deformations in the overbend

Even though DNV states that the yield point is at a strain of 0.5%, the DNV criteria for a pipeline of steel quality X65 was chosen as it was conservative. This criterion gives an allowable strain of 0.25%.

$$R = \frac{r}{\varepsilon}$$

$$R = \frac{0.004}{0.0025}$$

$$\boldsymbol{R = 1.6 \ meters}$$

Since this was the minimum allowable radius, a larger radius was chosen.

When using yield stress of copper (Equation 4.2):

$$R = \frac{120000 \cdot 0.008 \cdot 10^3}{2 \cdot 365 \cdot 0.85}$$

$$\boldsymbol{R = 1.55 \ meters}$$

Since this was the minimum allowable radius, a larger radius was chosen.

# Appendix C; Calculation of friction coefficients

Figures C-1 – C-6 show the forces required order to make the pipe slide on the concrete floor and the stinger:
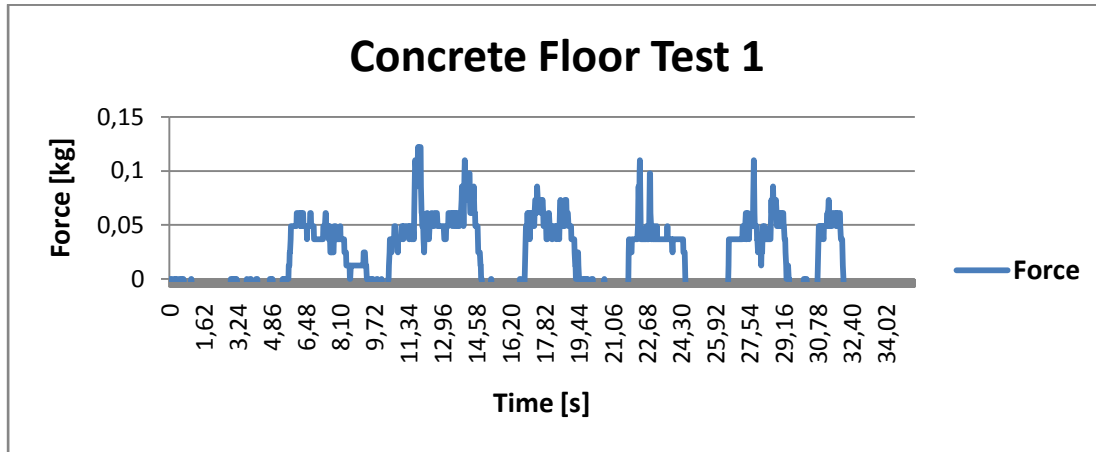


**Figure C-1. Friction test number one on concrete floor.**
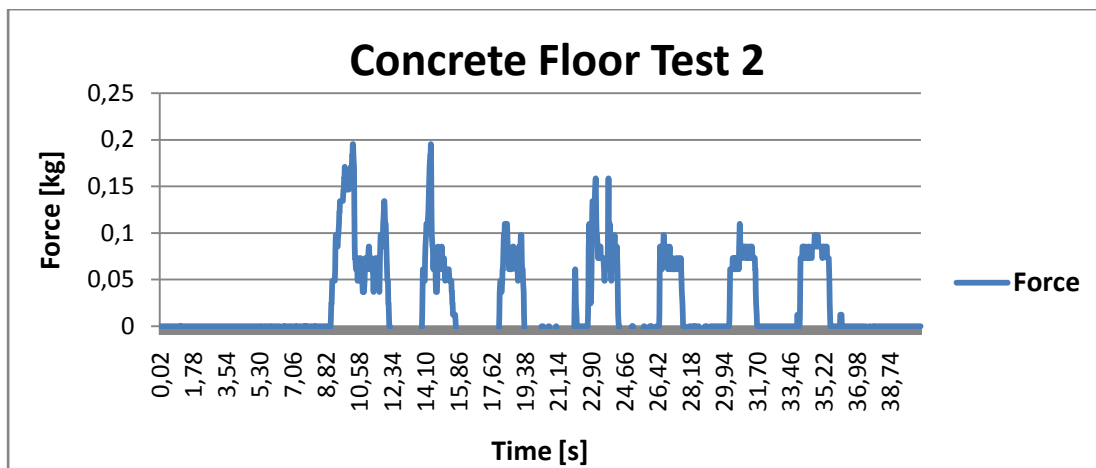


**Figure C-2. Friction test number two on concrete floor.**
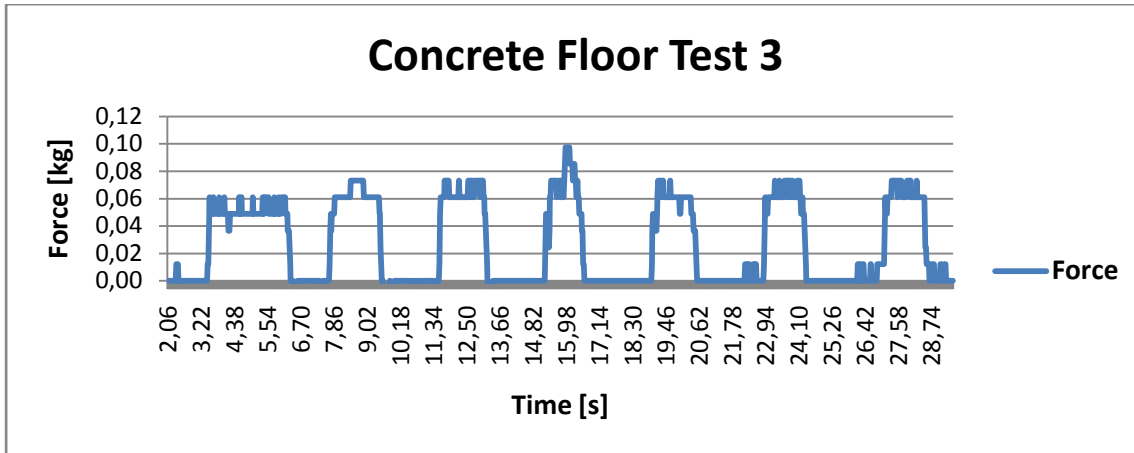
**Figure C-3. Friction test number three on concrete floor.**

Based on the three graphs the average force required in order to make the piece of pipe slide on the concrete floor was 0.13 kg.

The weight of the one meter long pipe was 0.186 kg

This gives:

$$\mu = \frac{F_f}{N}$$

$$\mu = \frac{0.130 kg}{0.186 kg}$$

$$\mathbf{\mu = 0.70}$$
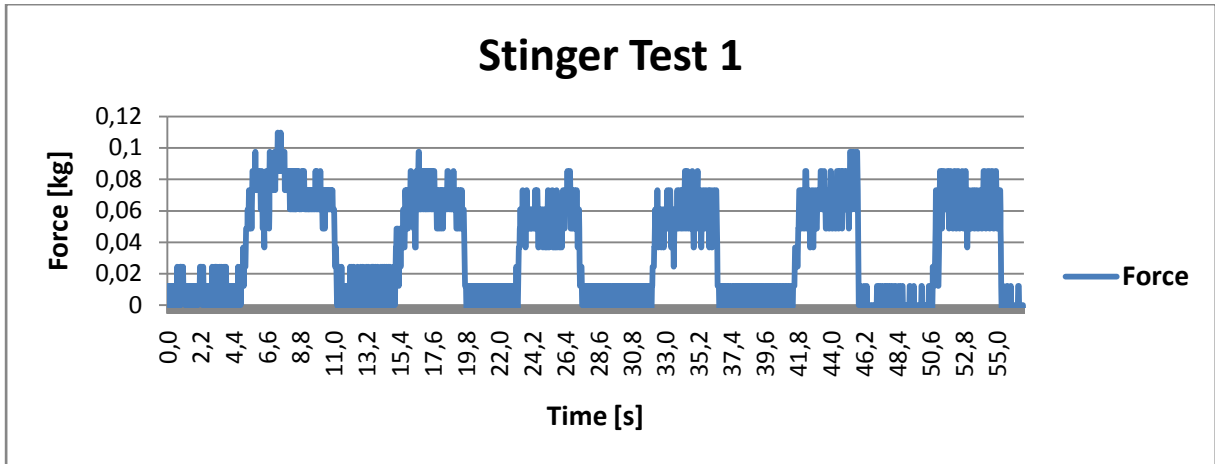
**Figure C-4. Friction test number one on concrete floor.**
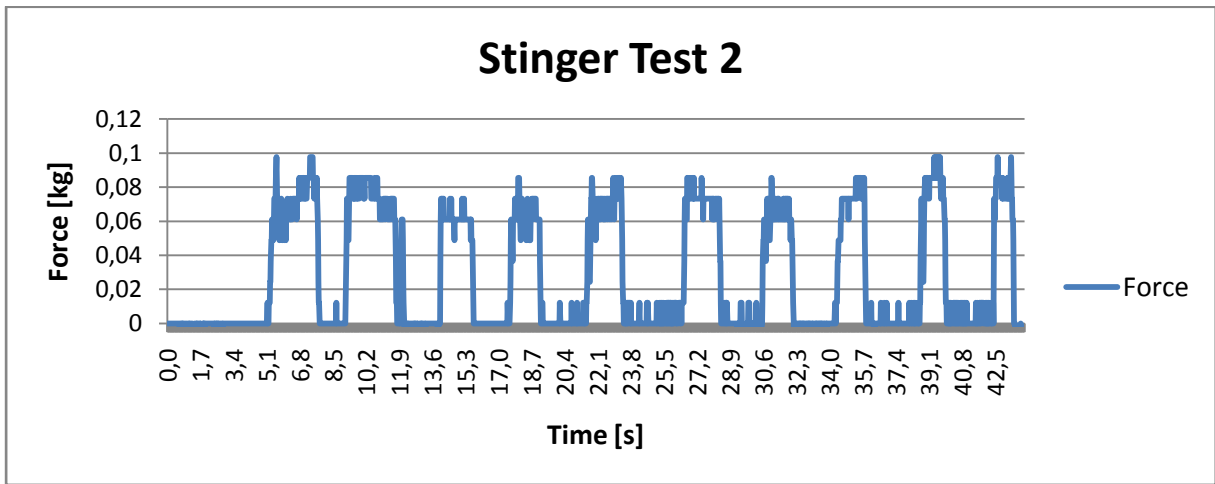


**Figure C-5. Friction test number one on concrete floor.**
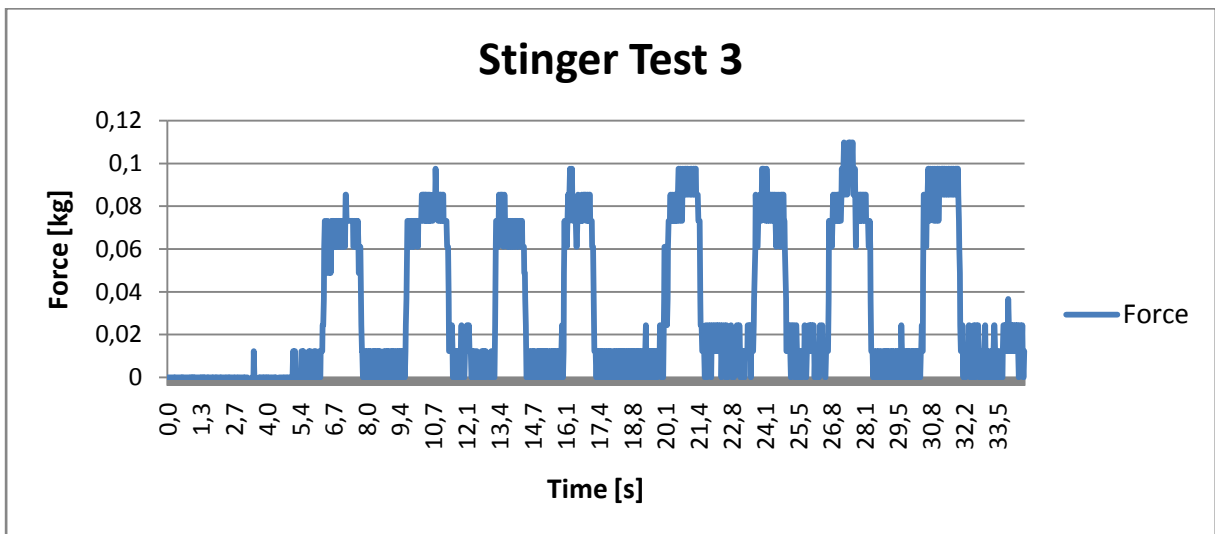


**Figure C-6. Friction test number one on concrete floor.**

Based on the three graphs the average force required in order to make the piece of pipe slide on the stinger was 0.09 kg.

The weight of the one meter long pipe was 0.186 kg

This gives:

$$\mu = \frac{F_f}{N}$$

$$\mu = \frac{0.09kg}{0.186kg}$$

$$\mathbf{\mu = 0.48}$$

## Appendix D; Calculation of the horizontal span lengths from OrcaFlex

Figure D-1 shows the horizontal length of the pipeline as a function of the actual arc length of the pipeline. The graph is different for every single test scenario, however only this one is used as an example. The calculations have been done using the respective graphs.

Figures D-2 – D-37 show the contact force between the pipeline and seabed/stinger as a function of arc length of the pipeline. By using these graphs it is possible to calculate the horizontal span lengths of the pipeline.
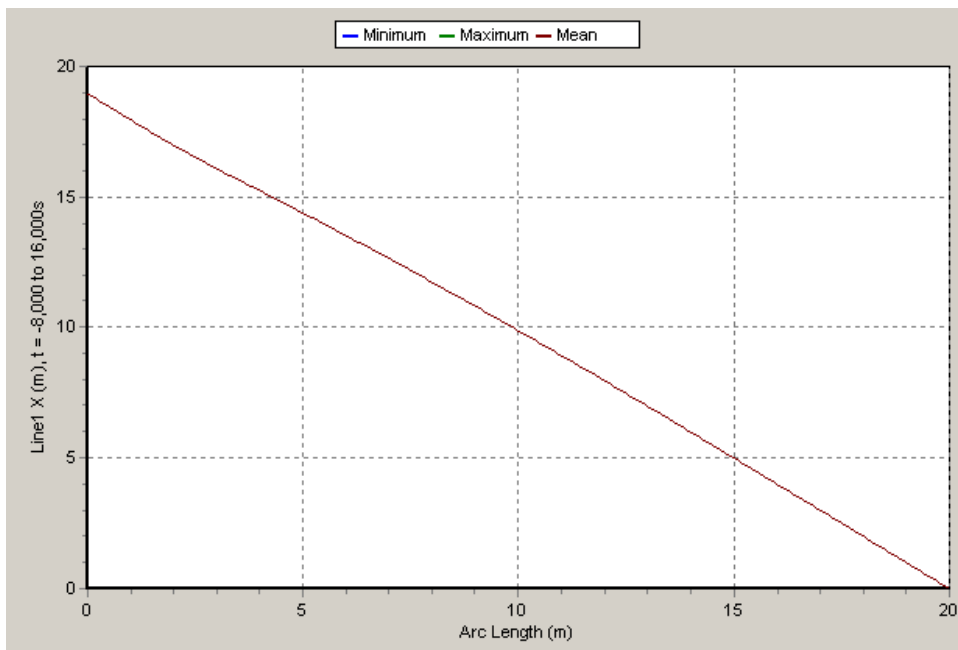


**Figure D-1. The horizontal x-coordinate as a function of the arc length of the pipeline from OrcaFlex**

## Laying height 4.97 meters, Long Span Model:
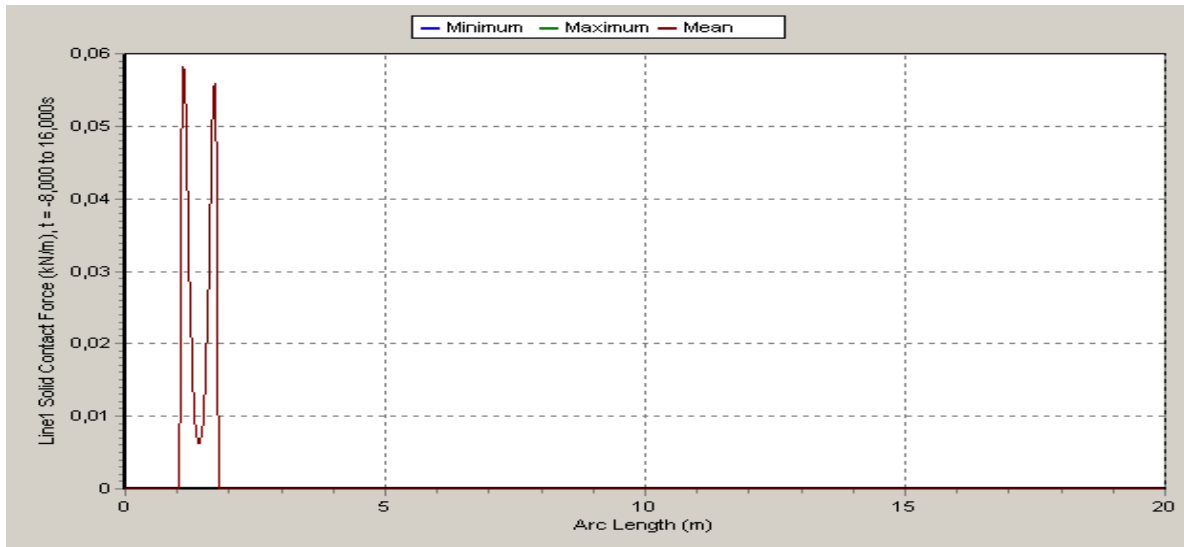
### 3kg tension force:
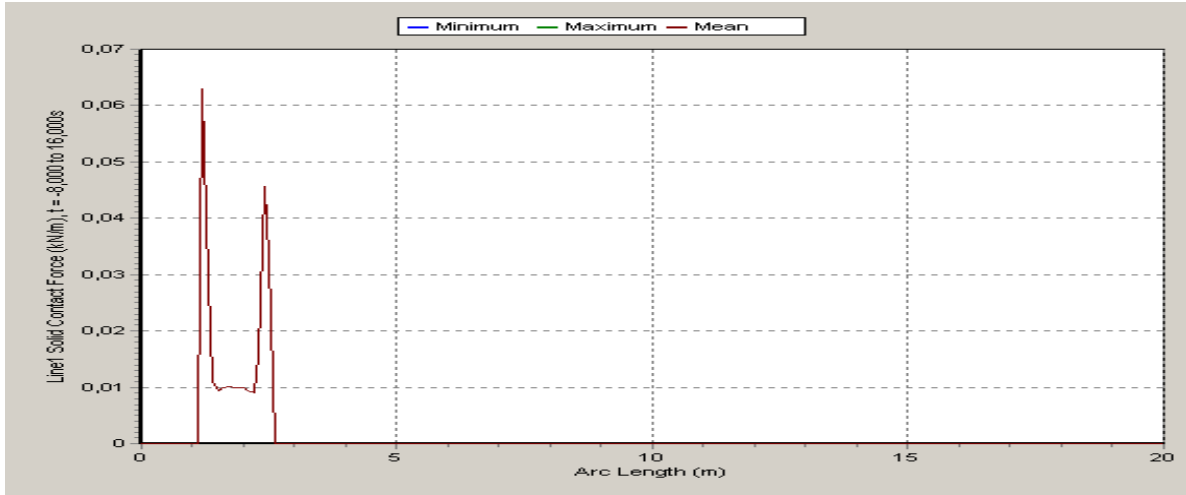


**Figure D-2. Contact force between pipeline and stinger for a tension force of 3 kg**
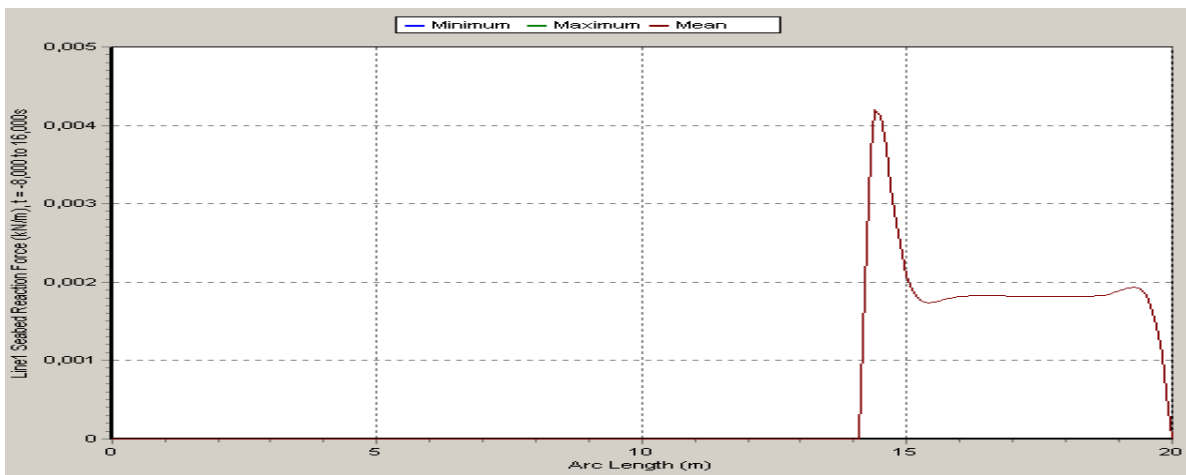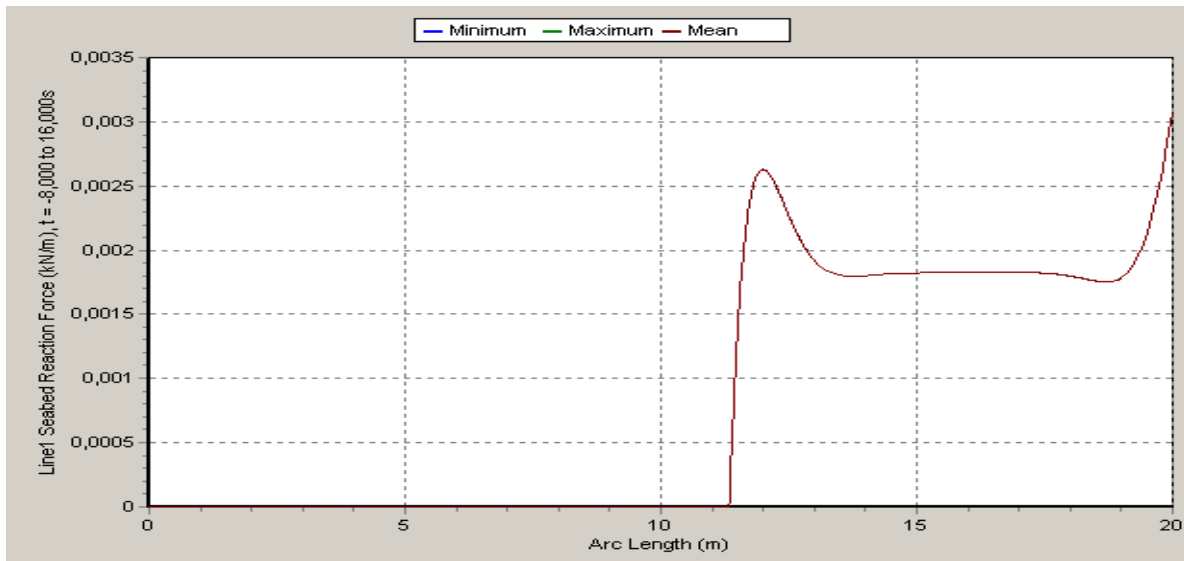


**Figure D-3. Contact force between pipeline and seabed for a tension force of 3 kg.**

Distance to departure point:      261 m      →      Hor. distance:  16.18 m
Distance to touchdown point:     1.09 m →     Hor. distance:  5.89 m

Hor. span length:      $16.18 - 5.89 = \mathbf{10.29\ m}$
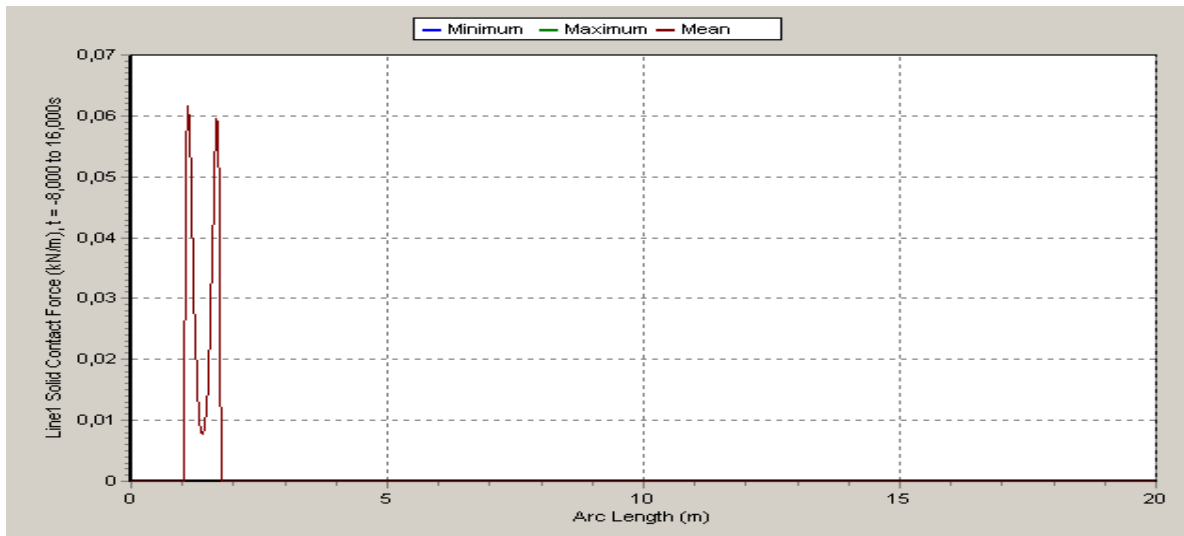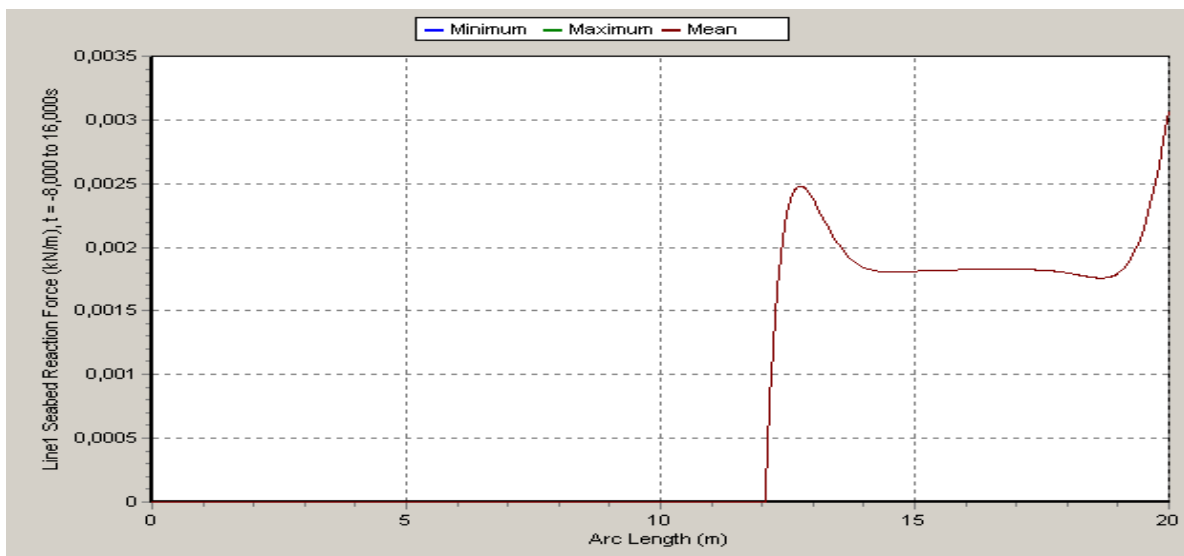
## 3.5 kg tension force:
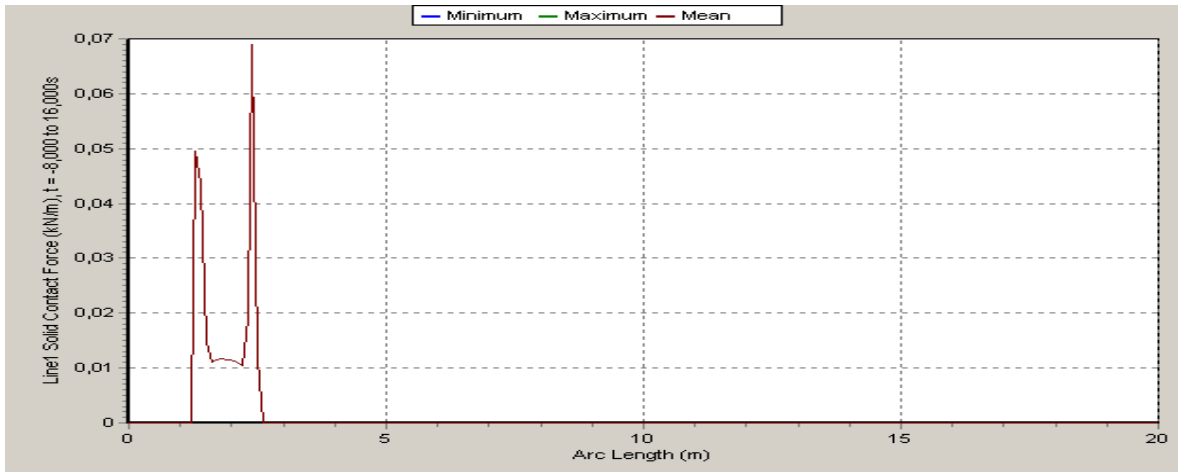


**Figure D-4. Contact force between pipeline and stinger for a tension force of 3.5 kg.**
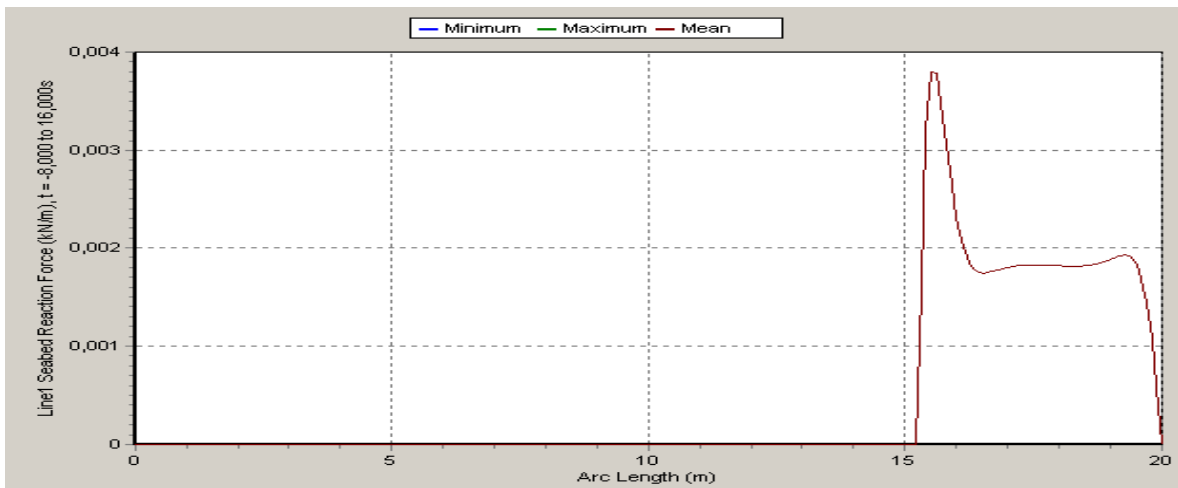


**Figure D-5. Contact force between pipeline and seabed for a tension force of 3.5 kg**

| | | | |
|---|---|---|---|
| Distance to departure point: | 2.60m | → | Hor. distance: 16.32 m |
| Distance to touchdown point: | 15.20m | → | Hor. distance: 4.83 m |

Hor. span length:  $16.32 - 4.83 = \mathbf{11.49\ m}$
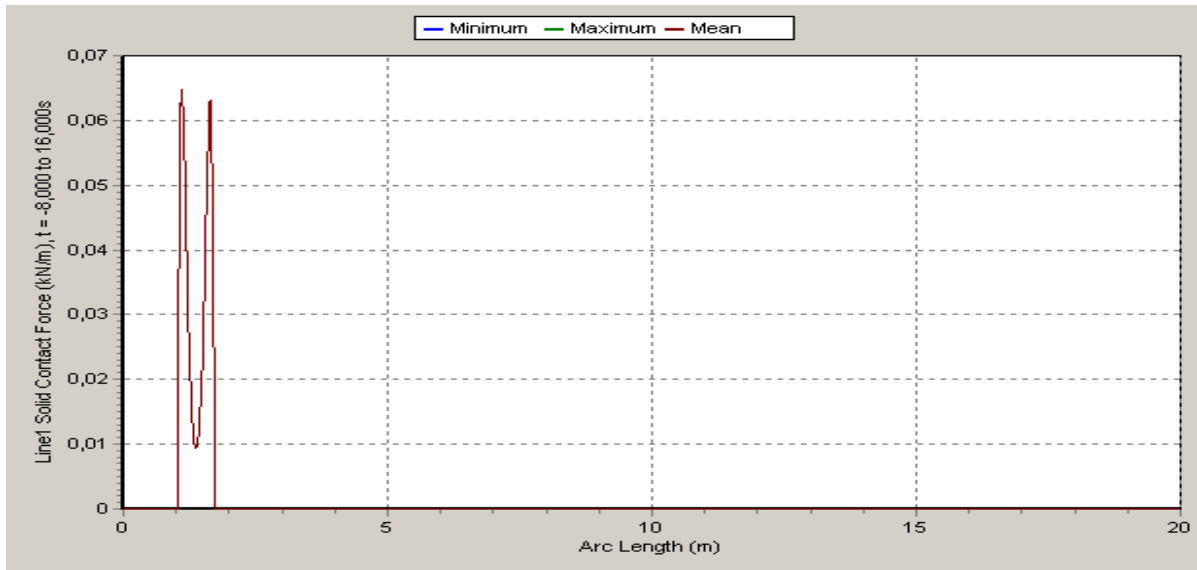
**4 kg tension force:**
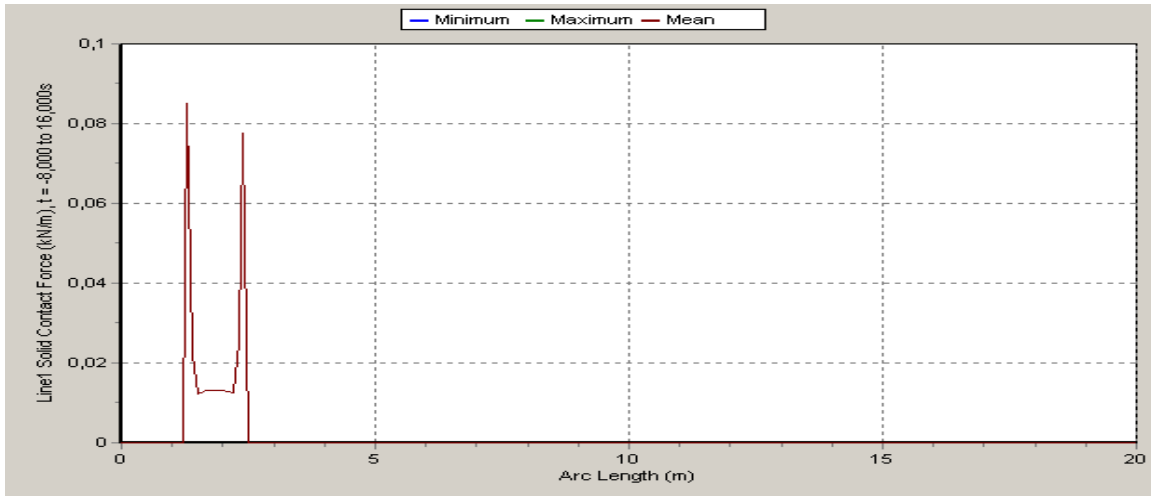


**Figure D-6. Contact force between pipeline and stinger for a tension force of 4 kg**
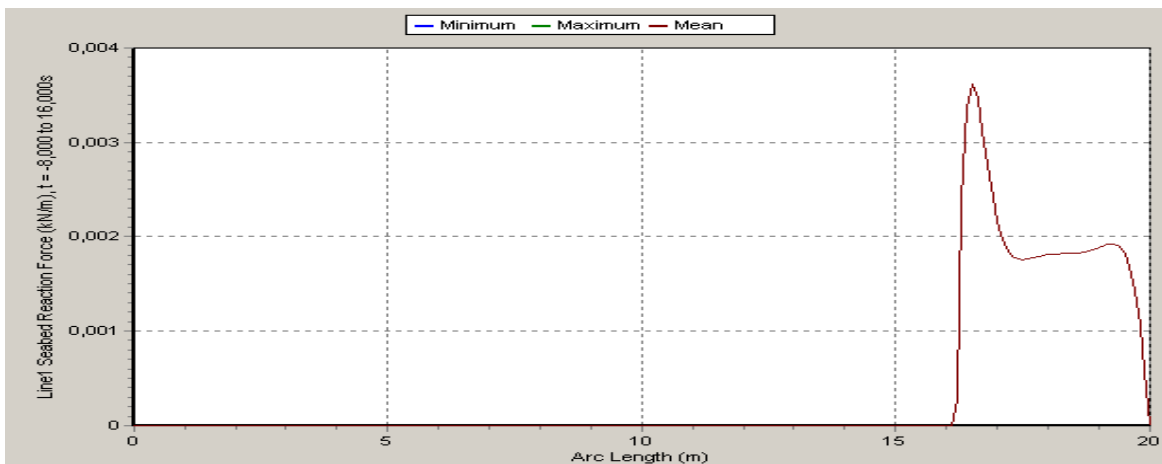


**Figure D-7. Contact force between pipeline and seabed for a tension force of 4 kg**

| | | | |
|---|---|---|---|
| Distance to departure point: | 2.48 m | → | Hor. distance: 16.48 m |
| Distance to touchdown point: | 16.1 m | → | Hor. distance: 3.93 m |

Hor. span length:     $16.48 - 3.93 = \mathbf{12.55\ m}$

## 4.5 kg tension force:
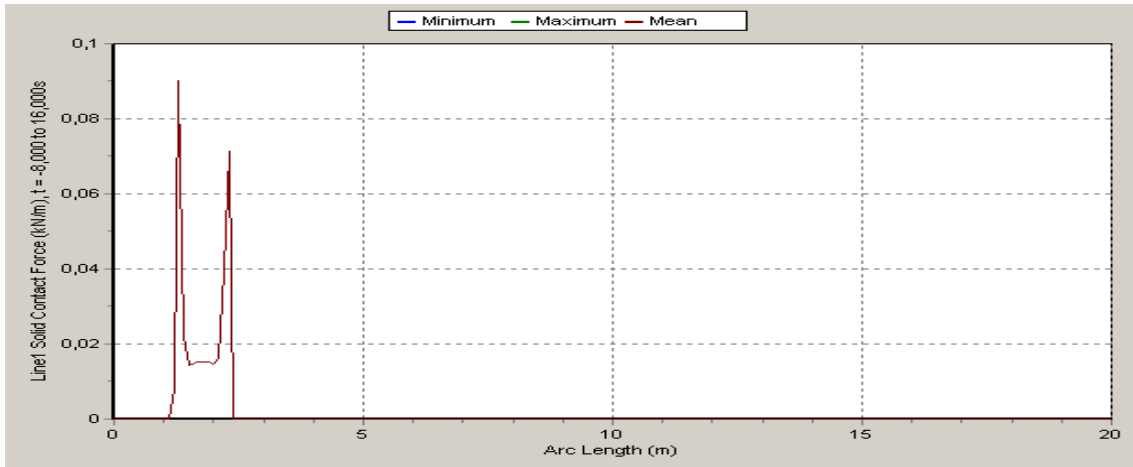


**Figure D-8. Contact force between pipeline and stinger for a tension force of 4.5 kg**
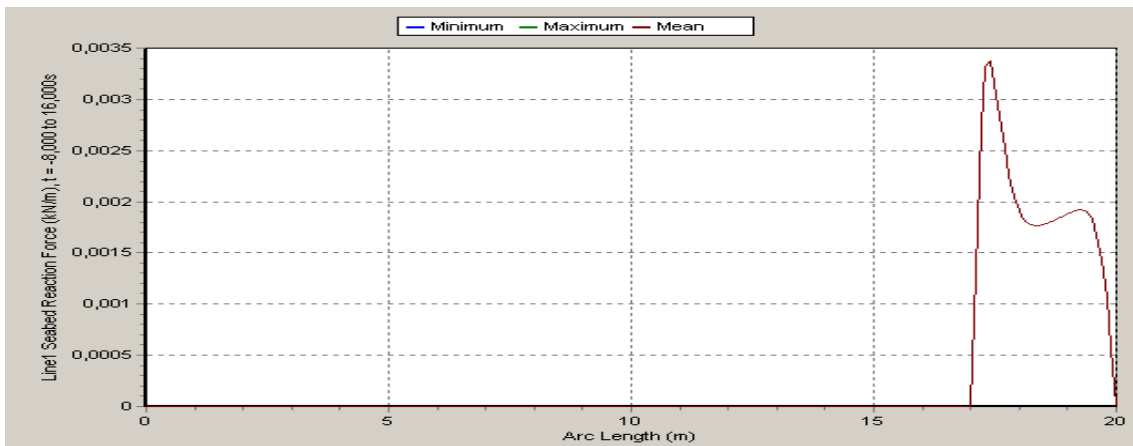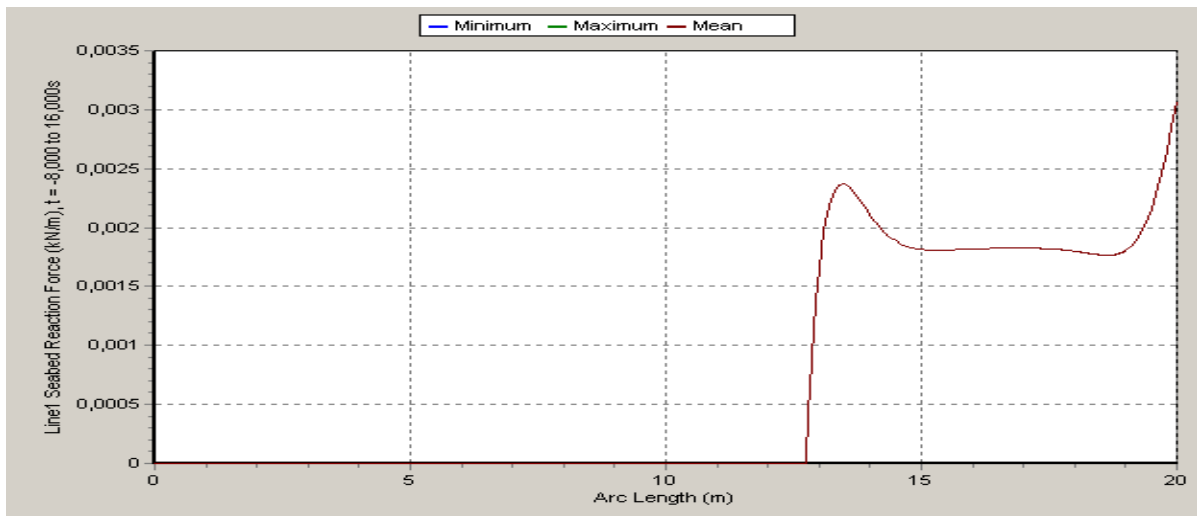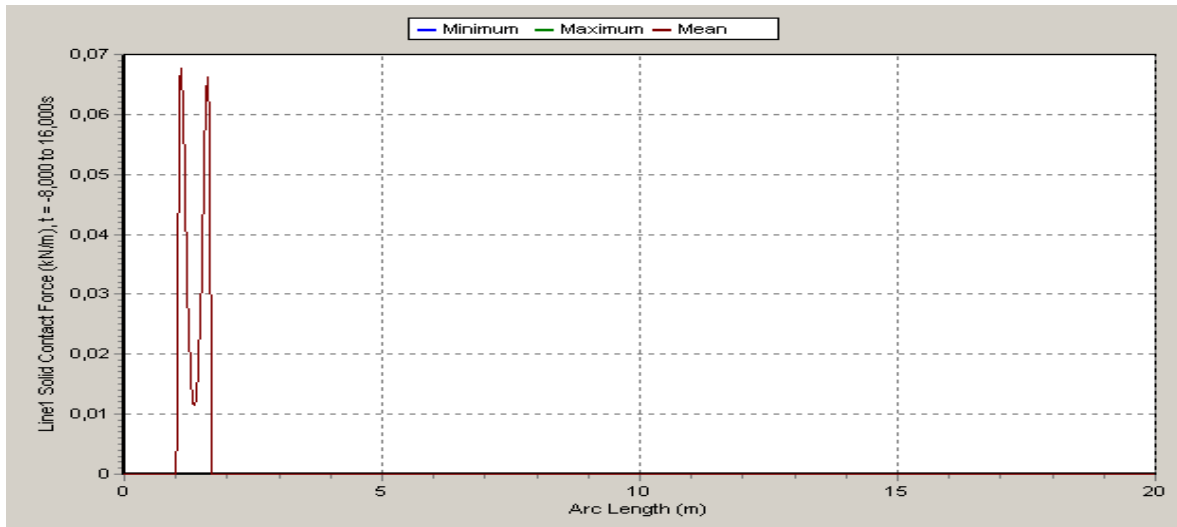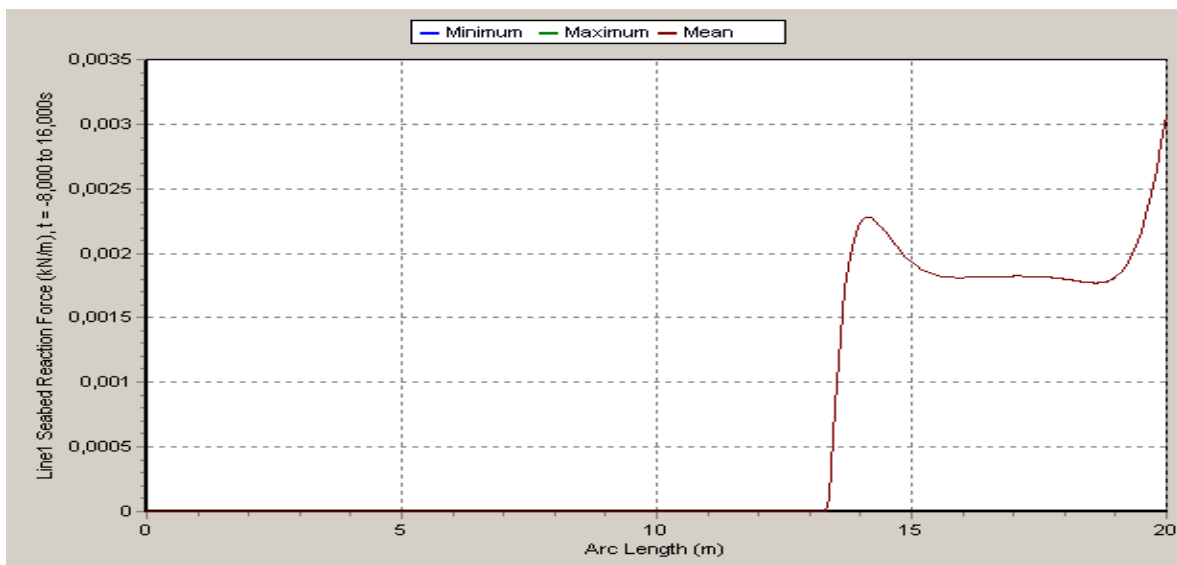


**Figure D-9. Contact force between pipeline and seabed for a tension force of 4.5 kg**

Distance to departure point:       2.40 m       →      Hor. distance: 16.60 m
Distance to touchdown point:     16.99m      →      Hor. distance:  3.01 m

Hor. span length:     $16.60 - 3.01 = \mathbf{13.59\ m}$

# Laying height 4.97 meters, Short Span Model

## 3 kg tension force:
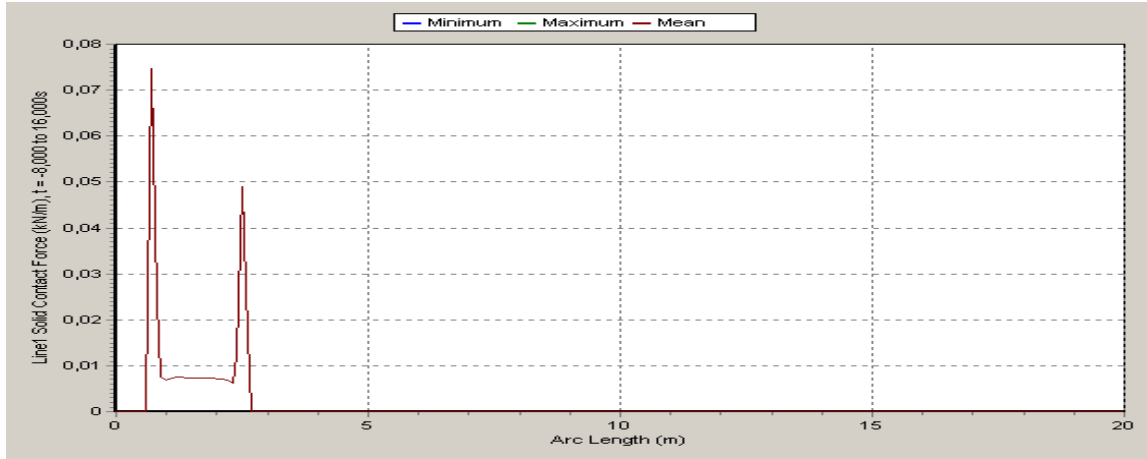


**Figure D-10. Contact force between pipeline and stinger for a tension force of 3 kg**
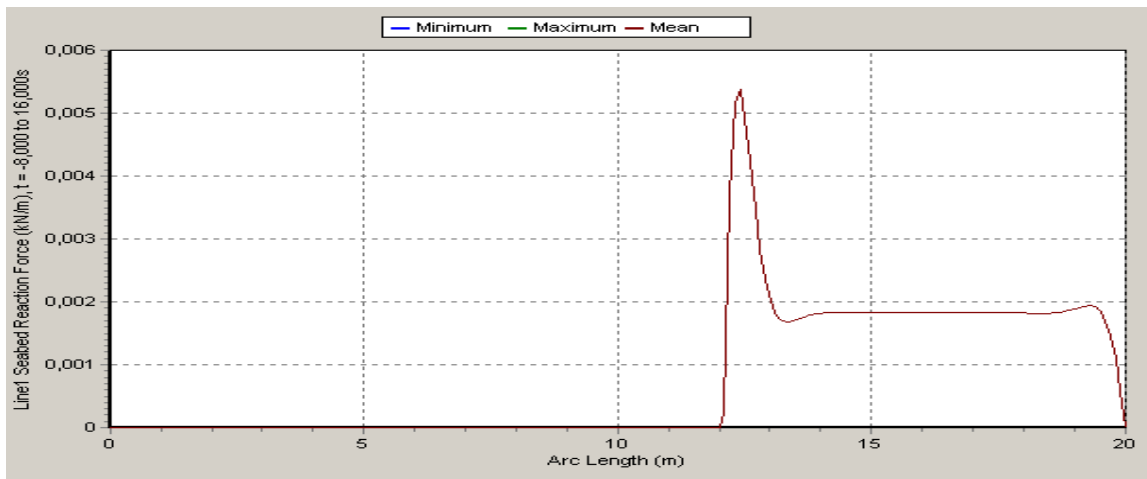


**Figure D-11. Contact force between pipeline and seabed for a tension force of 3 kg**

| | | | |
|---|---|---|---|
| Distance to departure point: | 2.70 m | → | Hor. distance: 15.96 m |
| Distance to touchdown point: | 12.0  m | → | Hor. distance:  8.0 m |

Hor. span length:     $15.96 - 8.0 = \mathbf{7.96\ m}$
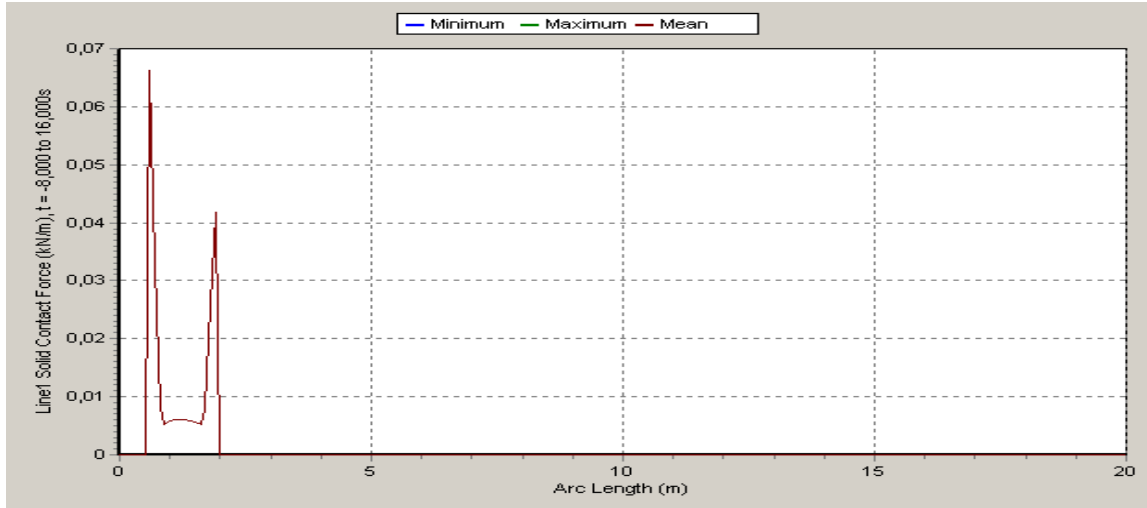
## 3.5 kg tension force:
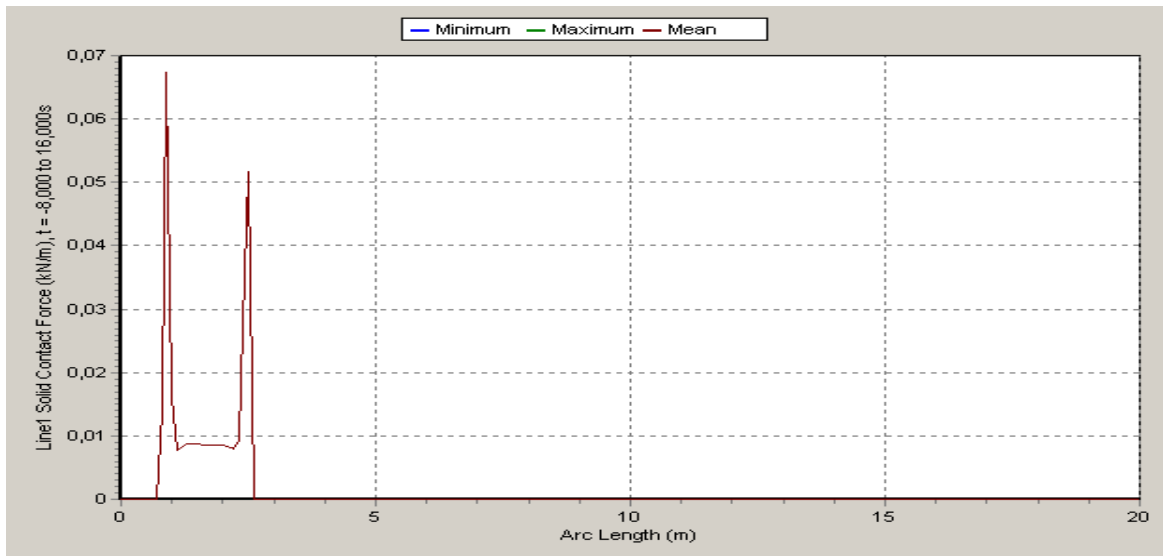


**Figure D-12. Contact force between pipeline and stinger for a tension force of 3.5 kg**
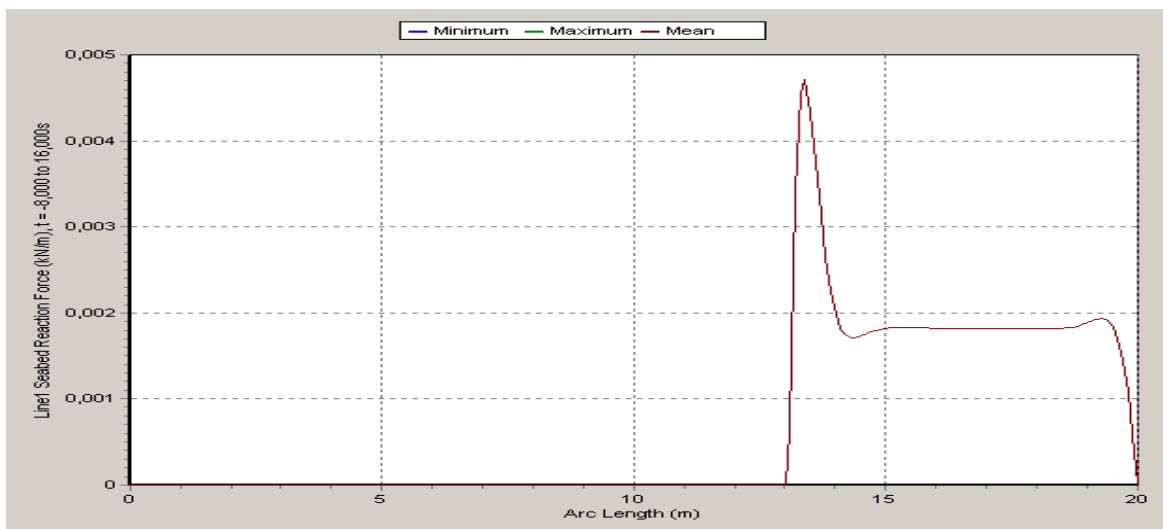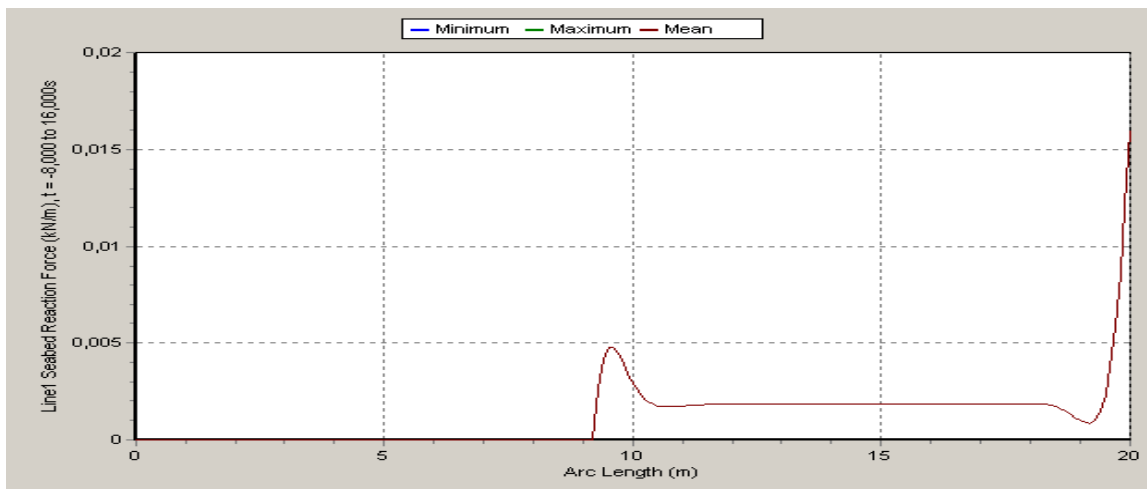


**Figure D-13. Contact force between pipeline and seabed for a tension force of 3.5 kg**

Distance to departure point:    2.59 m    →    Hor. distance: 16.17 m
Distance to touchdown point:    12.96 m    →    Hor. distance:  7.04 m

Hor. span length:    $16.17 - 7.04 = \mathbf{9.13\ m}$
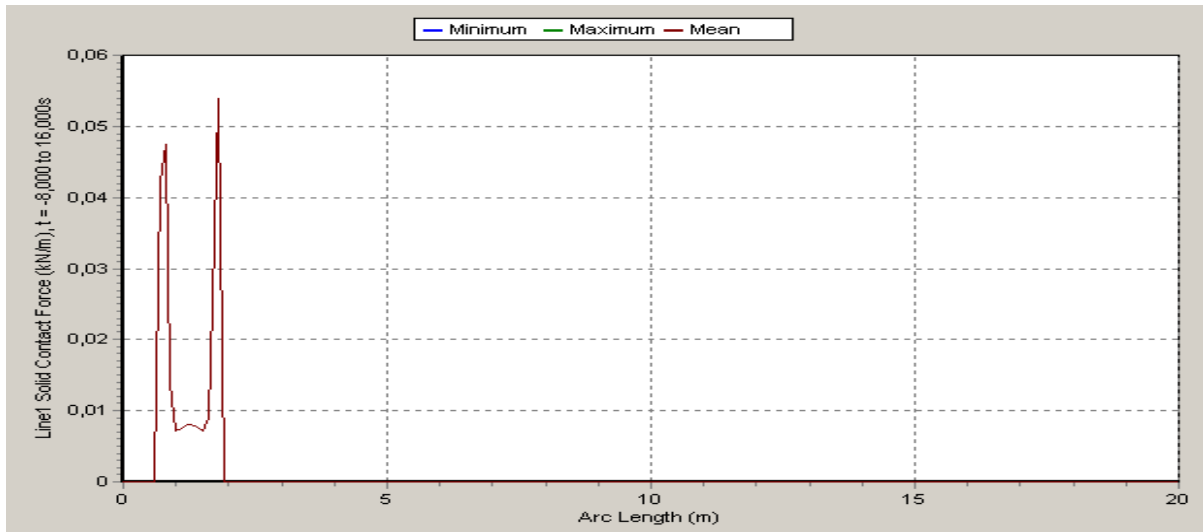
## 4 kg tension force:
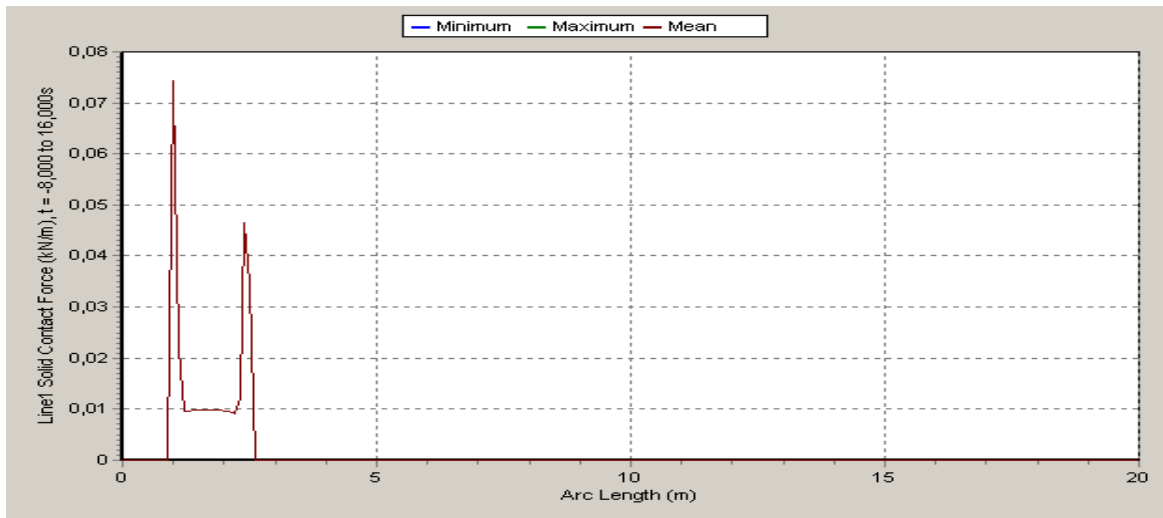


**Figure D-14. Contact force between pipeline and stinger for a tension force of 4 kg**
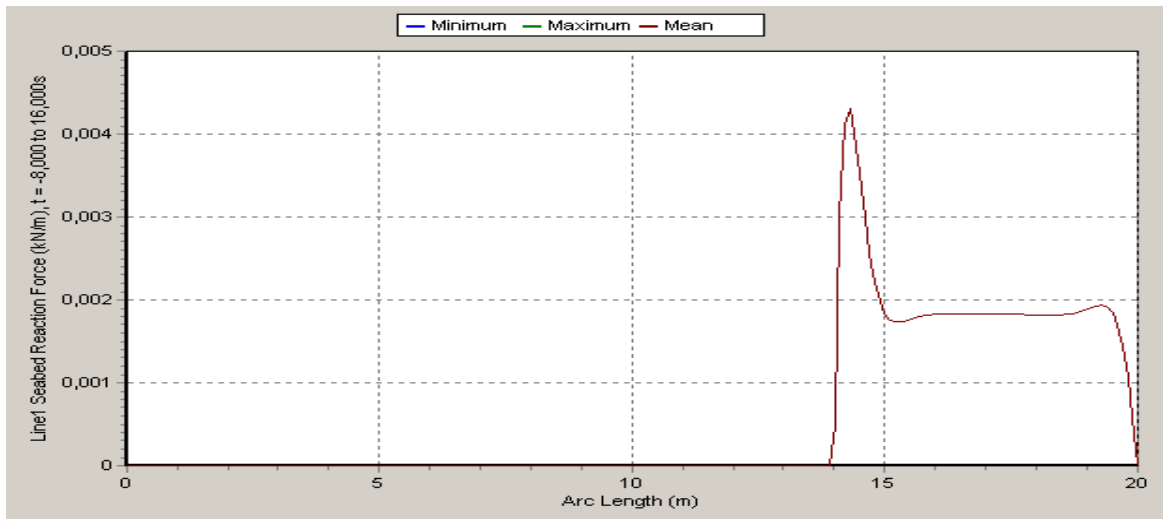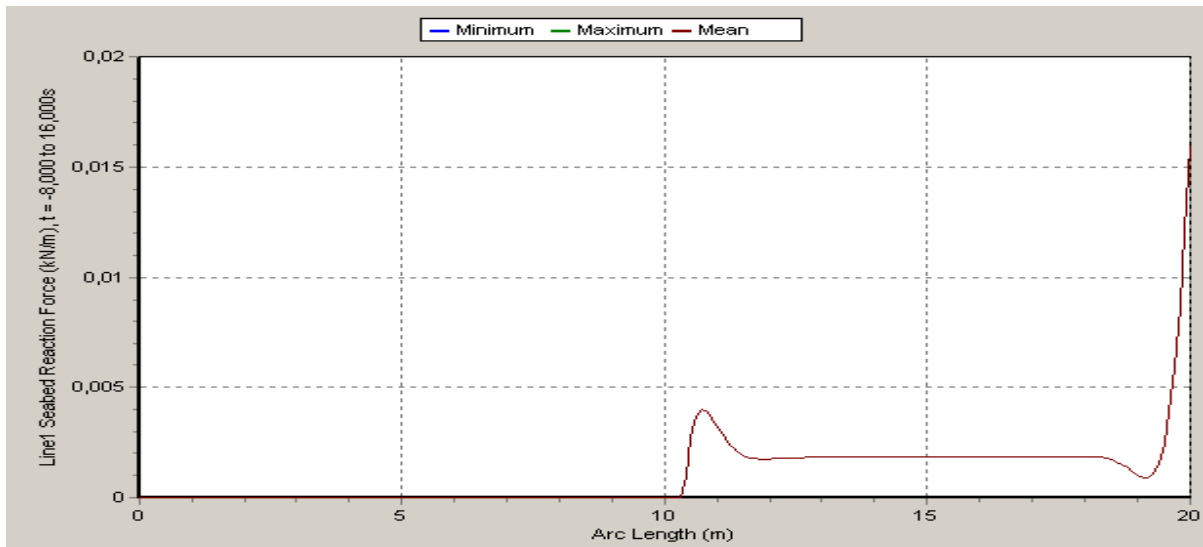


**Figure D-15. Contact force between pipeline and seabed for a tension force of 4 kg**

Distance to departure point: 2.58 m → Hor. distance: 16.25 m
Distance to touchdown point: 13.88 m → Hor. distance: 6.14 m

Hor. span length: $16.25 - 6.14 = \textbf{10.11} \, \textbf{\textit{m}}$

## 4.5 kg tension force:
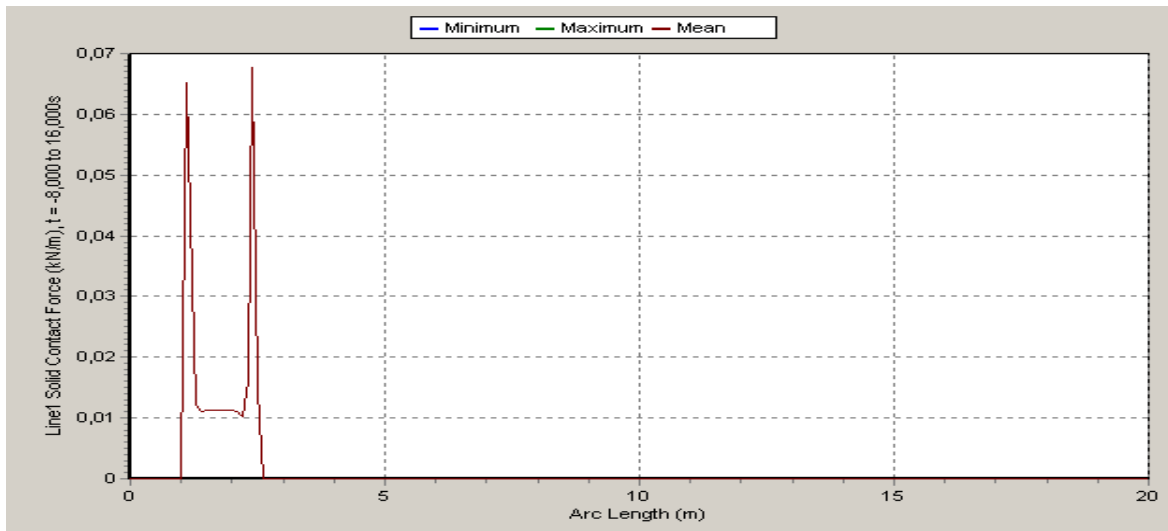


**Figure D-16. Contact force between pipeline and stinger for a tension force of 4.5 kg**
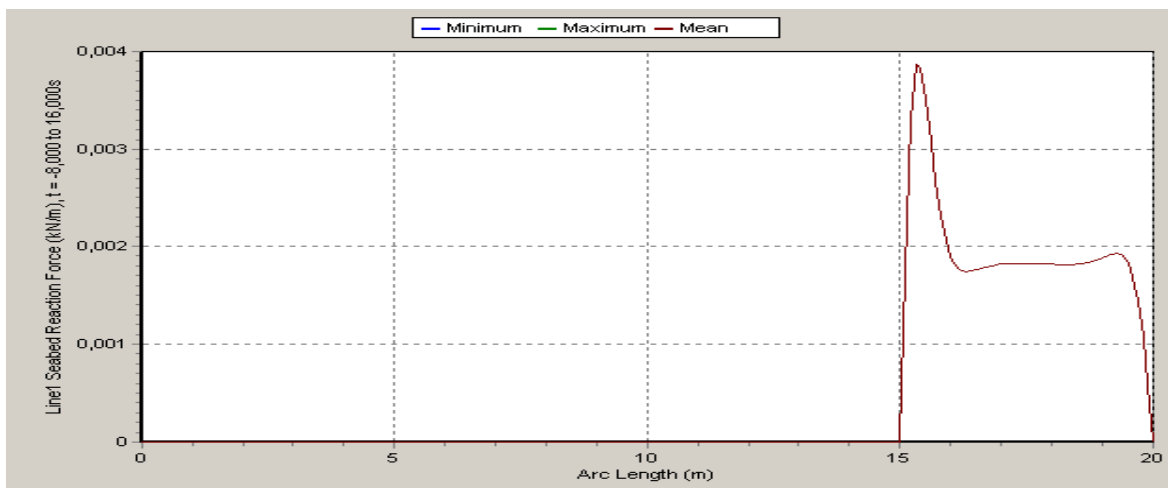


**Figure D-17. Contact force between pipeline and seabed for a tension force of 4.5 kg**

| | | | |
|---|---|---|---|
| Distance to departure point: | 2.57 m | → | Hor. distance: 16.3 m |
| Distance to touchdown point: | 14.99 m | → | Hor. distance: 5.06 m |

Hor. span length: $16.30 - 5.06 = \mathbf{11.24\ m}$

## Laying height 3.08 meters, Long Span Model
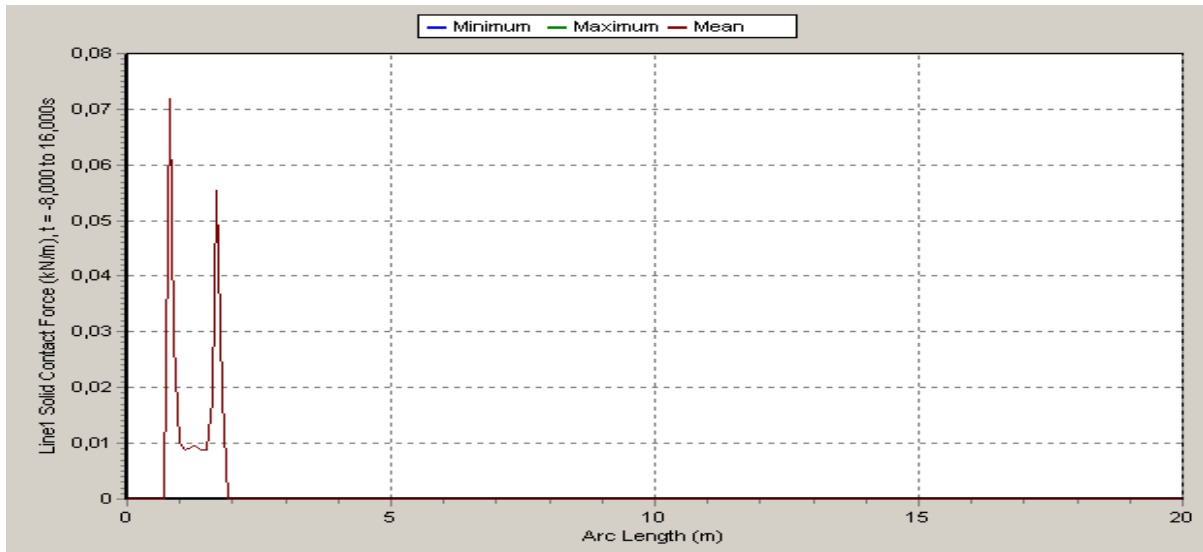
**2 kg tension force:**
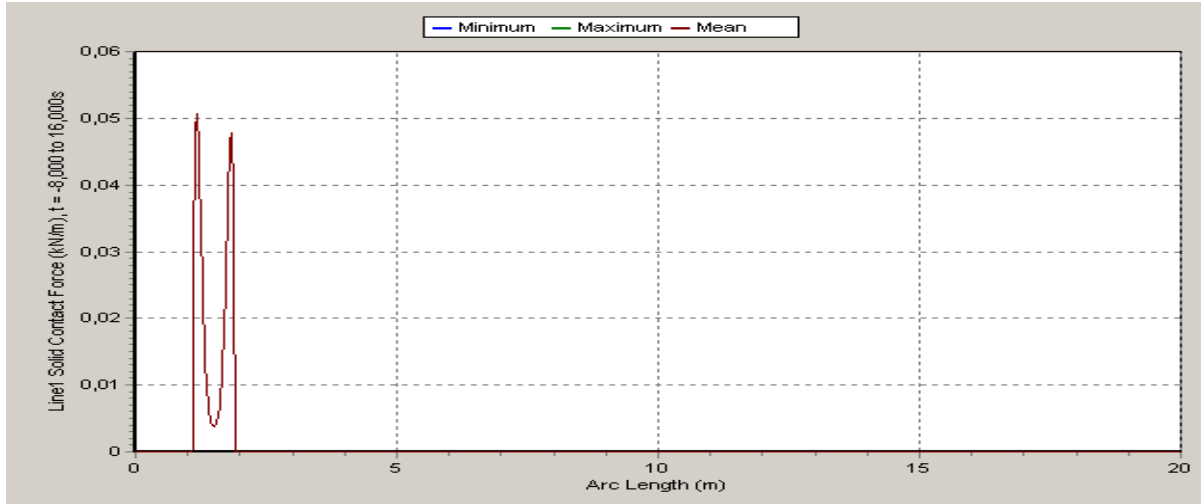


**Figure D-18. Contact force between pipeline and stinger for a tension force of 2 kg**
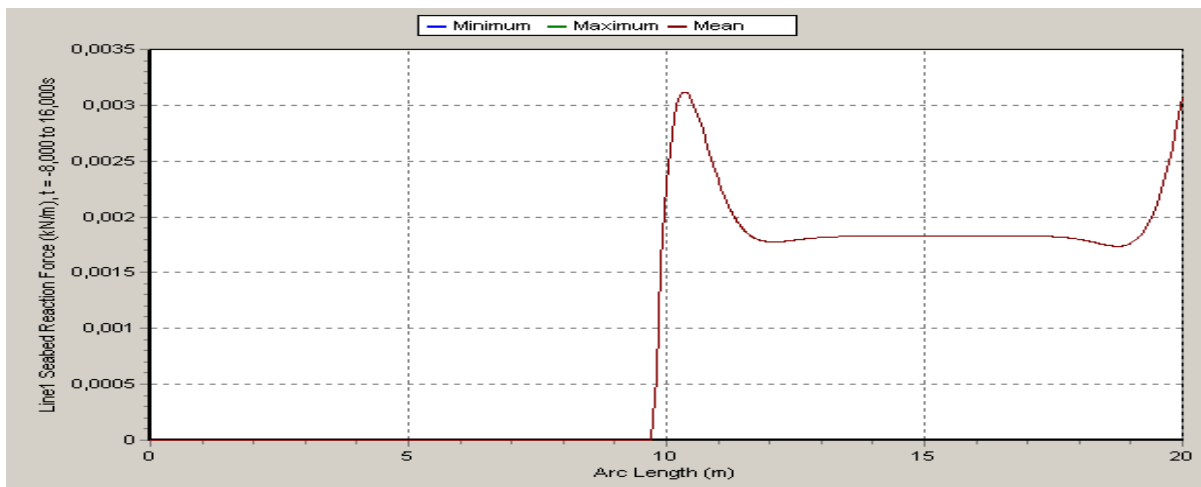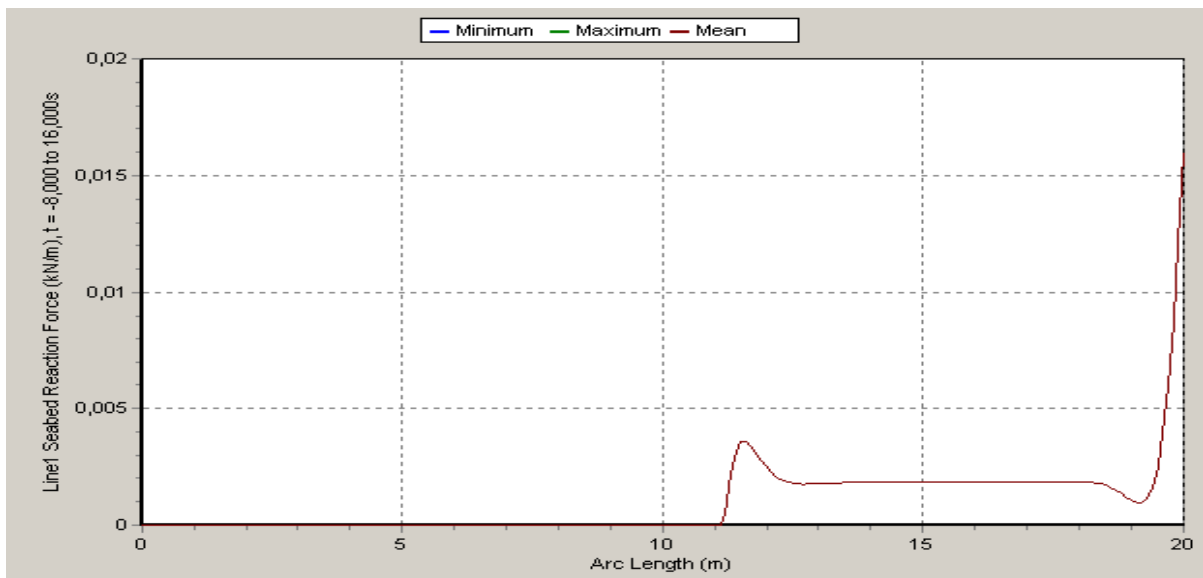


**Figure D-19. Contact force between pipeline and seabed for a tension force of 2 kg**

Distance to departure point:        1.90 m        →        Hor. distance: 17.49 m
Distance to touchdown point:        9.70 m        →        Hor. distance:  10.33 m

Hor. span length:      $17.49 - 10.33 = \mathbf{7.16\ m}$
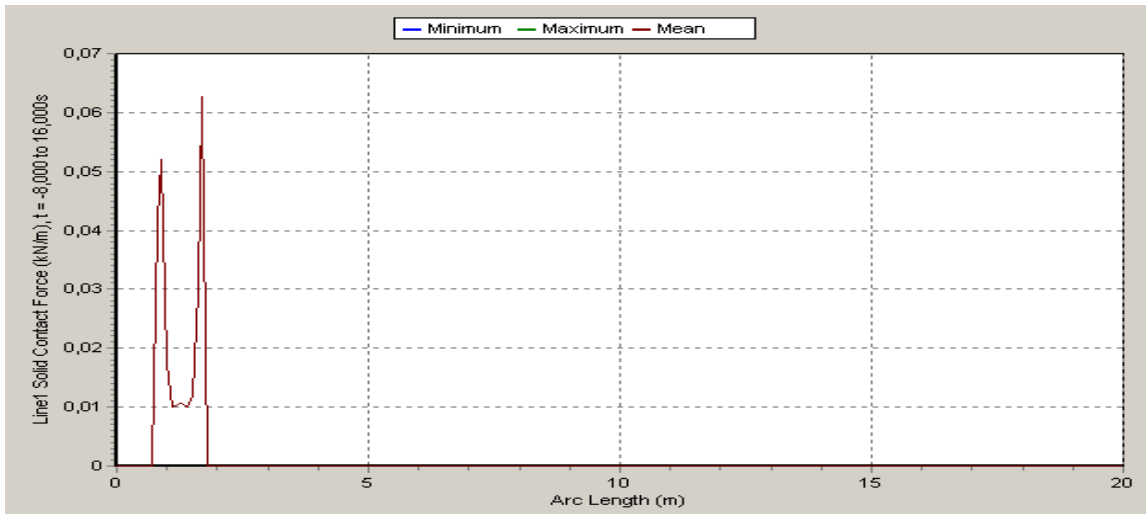
**3 kg tension force:**



**Figure D-20. Contact force between pipeline and stinger for a tension force of 3 kg**
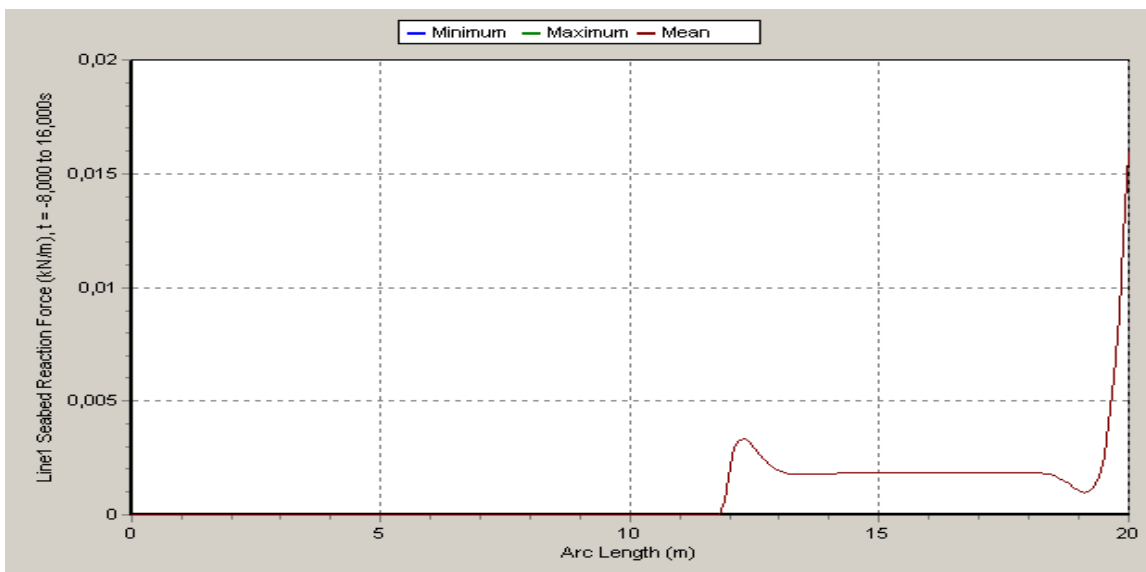


**Figure D-21. Contact force between pipeline and seabed for a tension force of 3 kg**

Distance to departure point:    1.79m        →    Hor. distance: 17.69 m
Distance to touchdown point:    11.32 m      →    Hor. distance:  8.69 m

Hor. span length:    $17.69 - 8.69 = \mathbf{9.0\ m}$

## 3.5 kg tension force:



**Figure D-22. Contact force between pipeline and stinger for a tension force of 3.5 kg**



**Figure D-23. Contact force between pipeline and seabed for a tension force of 3.5 kg**

Distance to departure point:        1.76 m     →     Hor. distance: 17.70 m
Distance to touchdown point:     12.03 m    →     Hor. distance:  7.98 m

Hor. span length:     $17.70 - 7.98 = \mathbf{9.72\ m}$
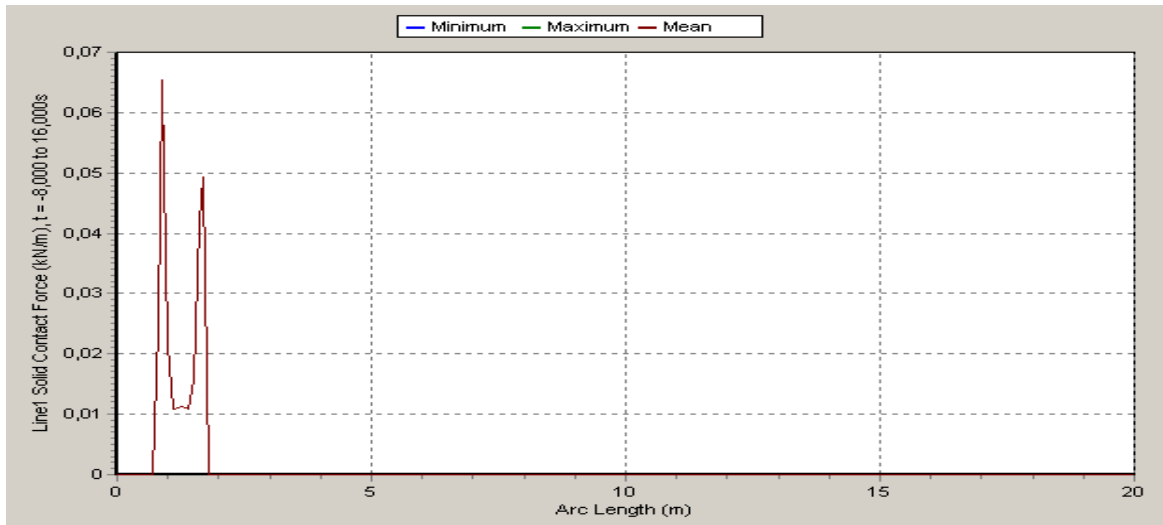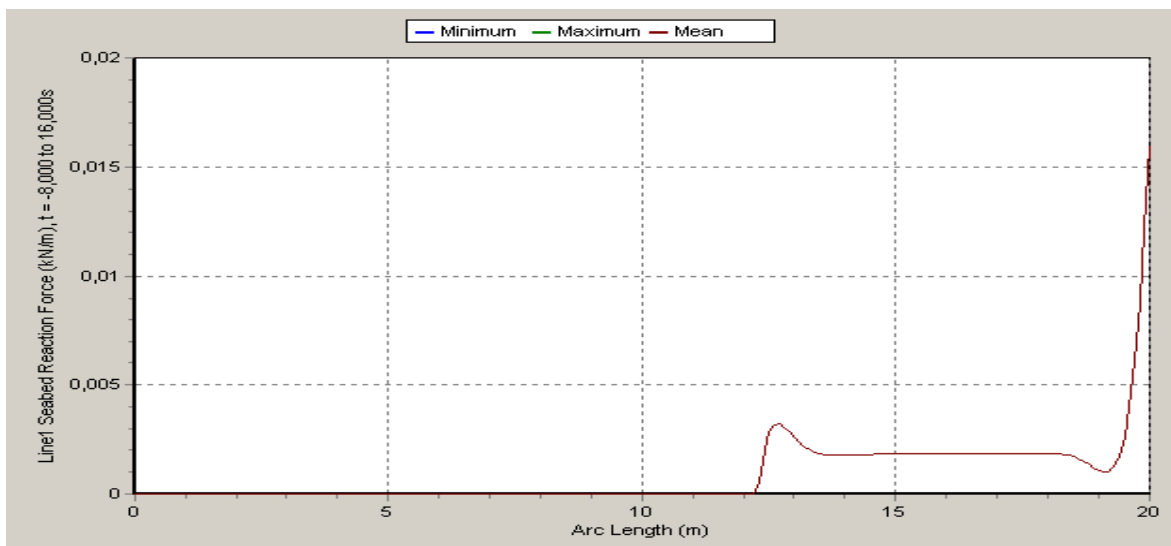
## 4 kg tension force:



**Figure D-24. Contact force between pipeline and stinger for a tension force of 4 kg**



**Figure D-25. Contact force between pipeline and seabed for a tension force of 4 kg**

| | | | |
|---|---|---|---|
| Distance to departure point: | 1.71 m | → | Hor. distance: 17.78 m |
| Distance to touchdown point: | 12.75 m | → | Hor. distance: 7.28 m |

Hor. span length:     $17.78 - 7.28 = \mathbf{10.50\ m}$

## 4.5 kg tension force:



**Figure D-26. Contact force between pipeline and stinger for a tension force of 4.5 kg**



**Figure D-27. Contact force between pipeline and seabed for a tension force of 4.5 kg**

Distance to departure point:        1.68 m      →    Hor. distance: 17.88 m
Distance to touchdown point:    13.30 m      →    Hor. distance:  6.70 m

Hor. span length:    $16.30 - 5.06 = \mathbf{11.18\ m}$

## Laying height 3.08 meters, Short Span Model

**2 kg tension force:**



**Figure D-28. Contact force between pipeline and stinger for a tension force of 2 kg**



**Figure D-29. Contact force between pipeline and seabed for a tension force of 2 kg**

| | | | | |
|---|---|---|---|---|
| Distance to departure point: | 2.00 m | → | Hor. distance: | 17.30 m |
| Distance to touchdown point: | 9.20 m | → | Hor. distance: | 10.77 m |

Hor. span length:     $17.30 - 10.77 = \mathbf{6.53\ m}$

## 3 kg tension force:



**Figure D-30. Contact force between pipeline and stinger for a tension force of 3 kg**



**Figure D-31. Contact force between pipeline and seabed for a tension force of 3 kg**

Distance to departure point:      1.90 m      →      Hor. distance: 17.51 m
Distance to touchdown point:      10.30 m      →      Hor. distance:  9.72 m

Hor. span length:      $17.51 - 9.72 = \mathbf{7.79\ m}$

## 3.5 kg tension force:



**Figure D-32. Contact force between pipeline and stinger for a tension force of 3.5 kg**



**Figure D-33. Contact force between pipeline and seabed for a tension force of 3.5 kg**

Distance to departure point:      1.89 m    →    Hor. distance: 17.53 m
Distance to touchdown point:     11.11 m    →    Hor. distance:  8.90 m

Hor. span length:    $17.53 - 8.90 = \mathbf{8.63\ m}$

**4 kg tension force:**



**Figure D-34. Contact force between pipeline and stinger for a tension force of 4 kg**



**Figure D-35. Contact force between pipeline and seabed for a tension force of 4 kg**

| | | | |
|---|---|---|---|
| Distance to departure point: | 1.79 m | → | Hor. distance: 17.69 m |
| Distance to touchdown point: | 11.81 m | → | Hor. distance: 8.20 m |

Hor. span length:     $17.69 - 8.20 = \mathbf{9.49\ m}$

## 4.5 kg tension force:



**Figure D-36. Contact force between pipeline and stinger for a tension force of 4.5 kg**



**Figure D-37. Contact force between pipeline and seabed for a tension force of 4.5 kg**

Distance to departure point:        1.79 m        →      Hor. distance: 17.71 m
Distance to touchdown point:     12.21 m     →      Hor. distance:  7.82 m

Hor. span length:     $17.71 - 8.82 = \mathbf{9.89\ m}$

# Appendix E;     Simulations done in OrcaFlex

Figures E-1 – E-26 show the simulations done in OrcaFlex when the pipeline was laid onto an uneven seabed. Some of the geometries of the pipeline in these figures were used to describe the strains in chapter 17.

## Pipeline laid from 3.08 meters height:

**Long Span Model**
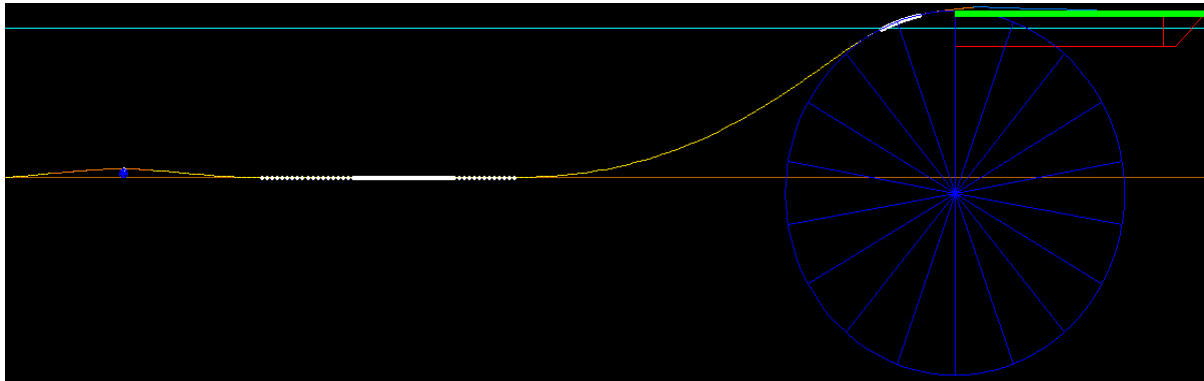
One obstacle:



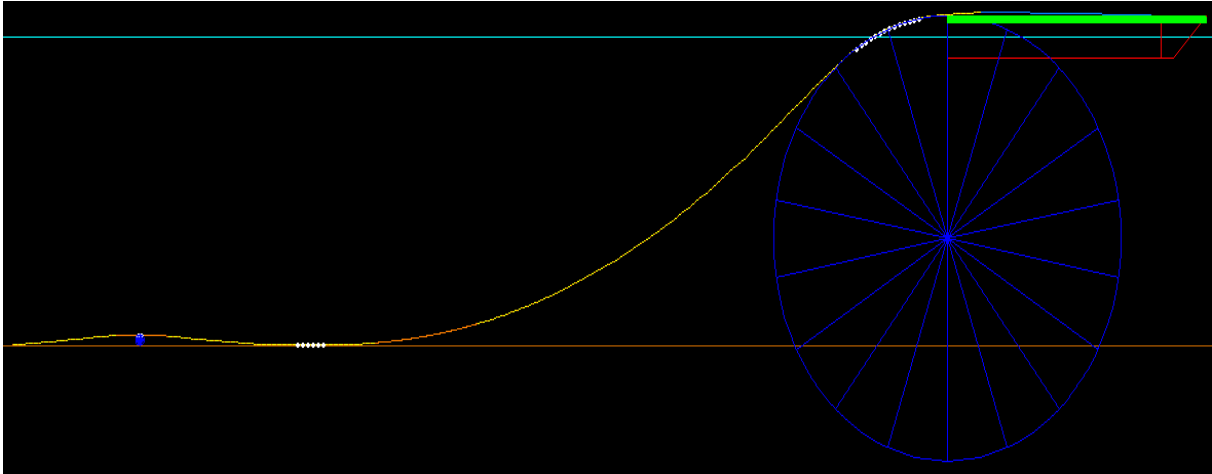**Figure E-1. Simulation in OrcaFlex when the pipeline was laid onto one obstacle with a tension force of 2 kg.**
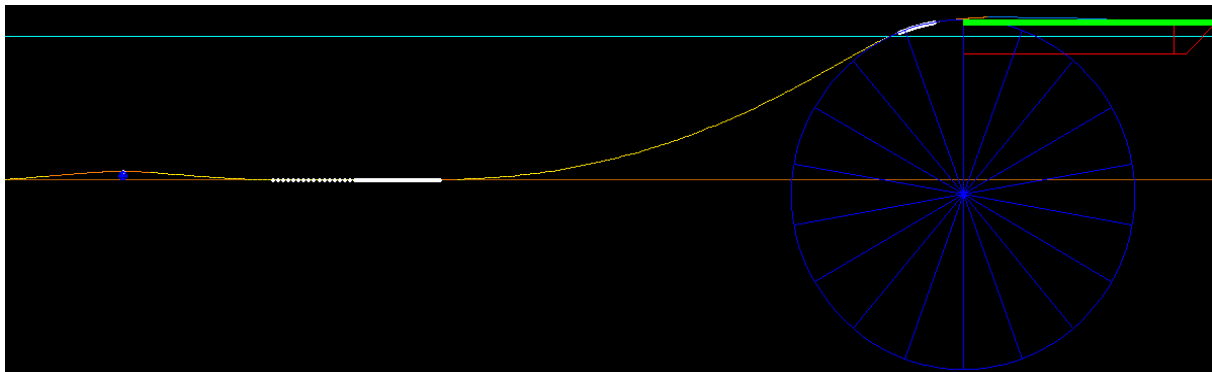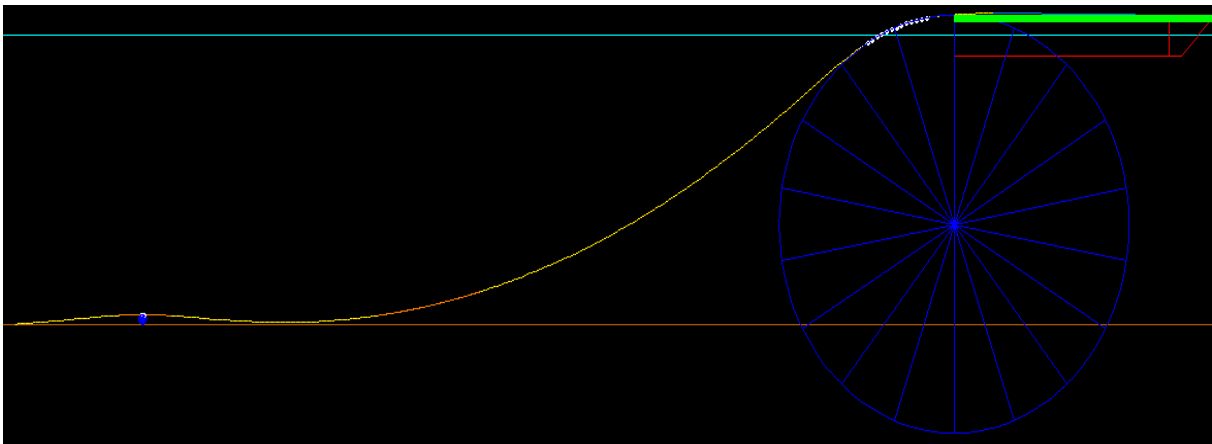


**Figure E-2. Simulation in OrcaFlex when the pipeline was laid onto one obstacle with a tension force of 3 kg.**
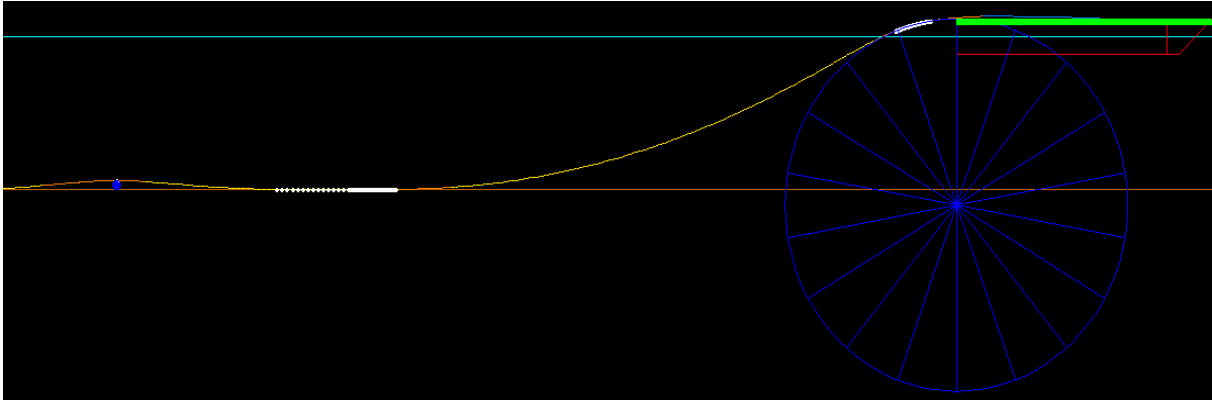
**Figure E-3. Simulation in OrcaFlex when the pipeline was laid onto one obstacle with a tension force of 3.5 kg.**
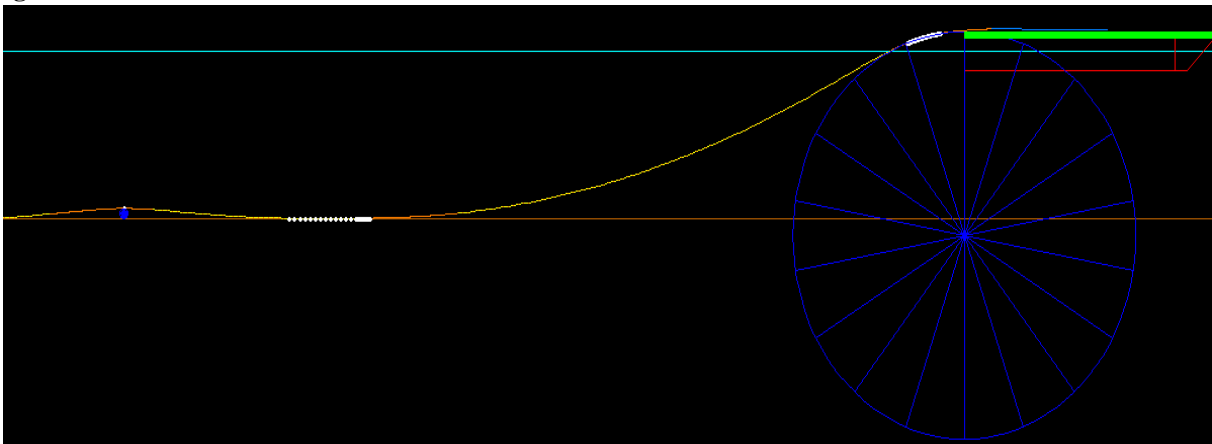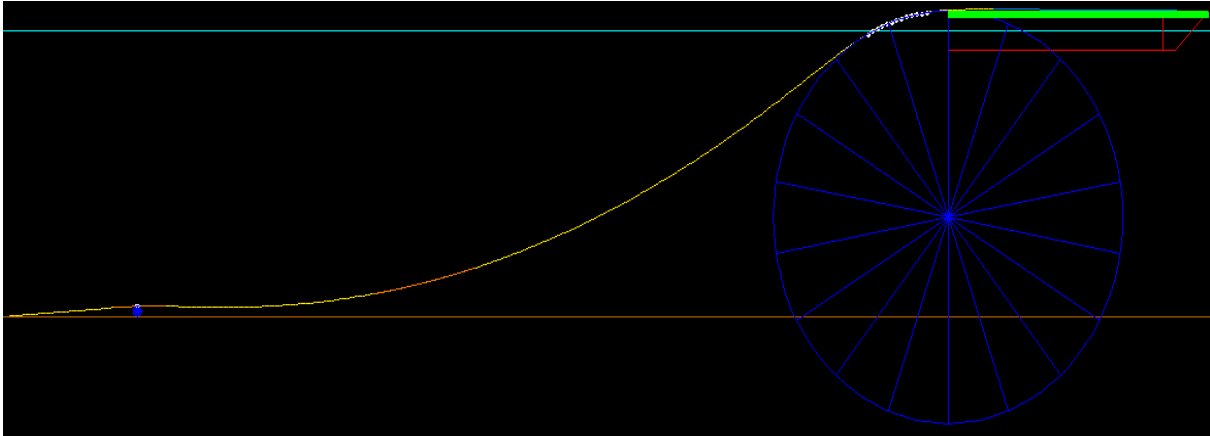


**Figure E-4. Simulation in OrcaFlex when the pipeline was laid onto one obstacle with a tension force of 4 kg.**
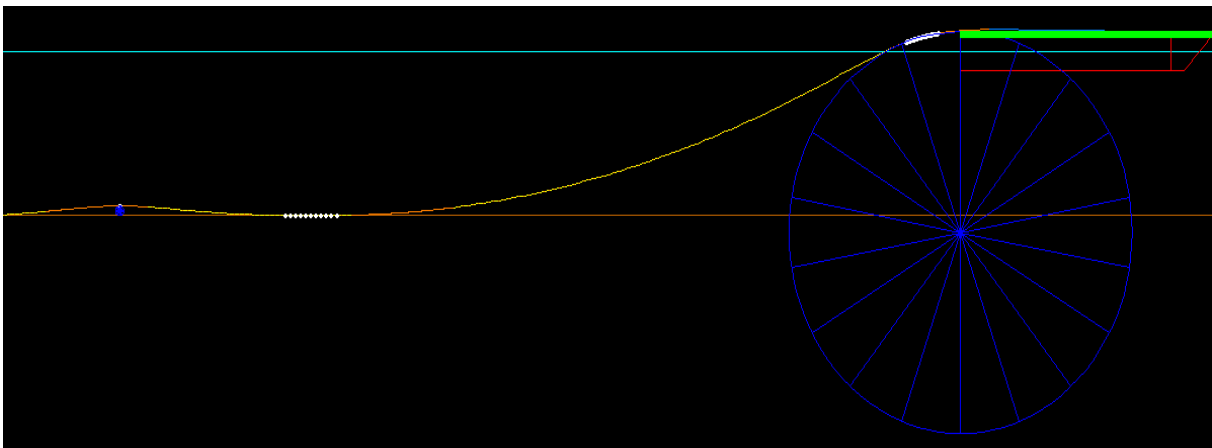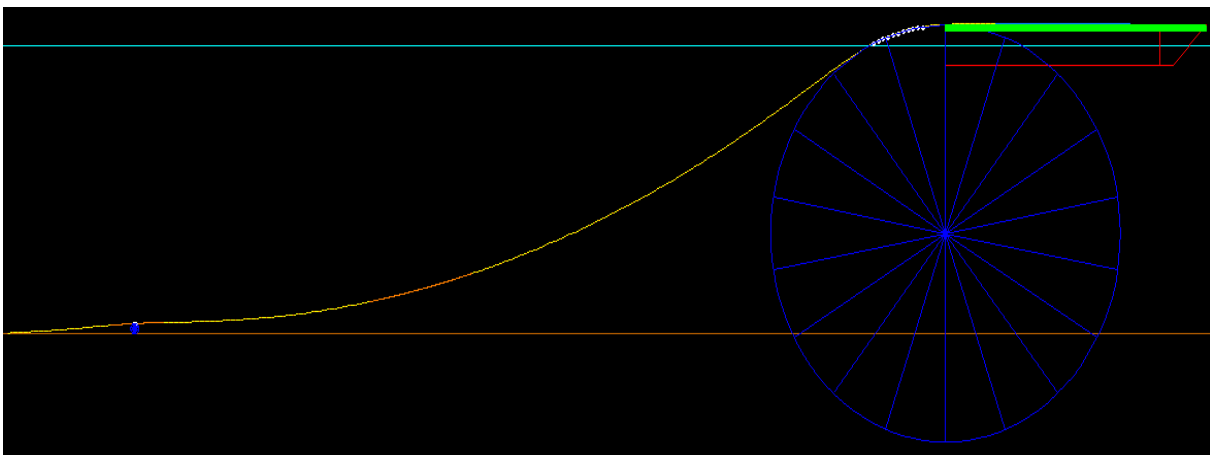


**Figure E-5. Simulation in OrcaFlex when the pipeline was laid onto one obstacle with a tension force of 4.5 kg.**
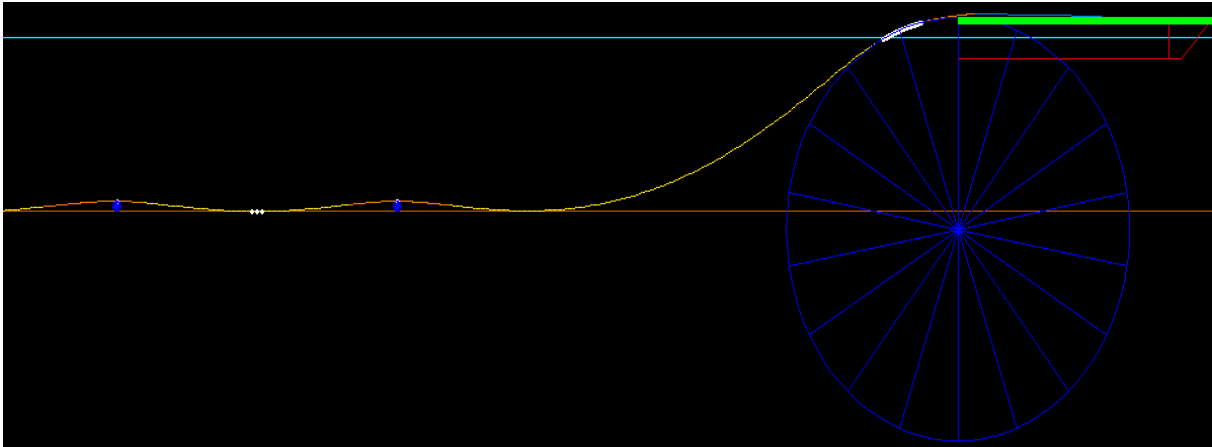
Two obstacles:



**Figure E-6. Simulation in OrcaFlex when the pipeline was laid onto two obstacles with a tension force of 2 kg.**
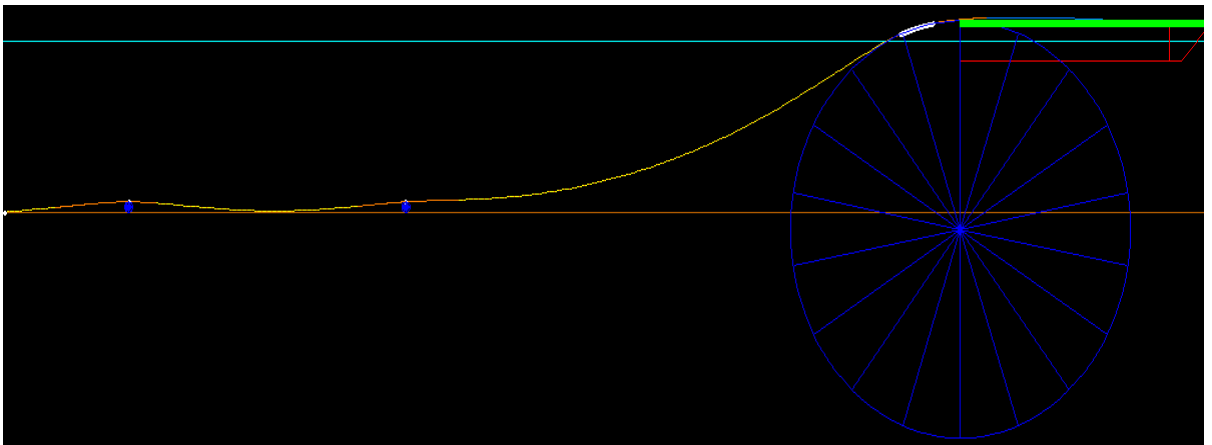


**Figure E-7. Simulation in OrcaFlex when the pipeline was laid onto two obstacles with a tension force of 3 kg.**
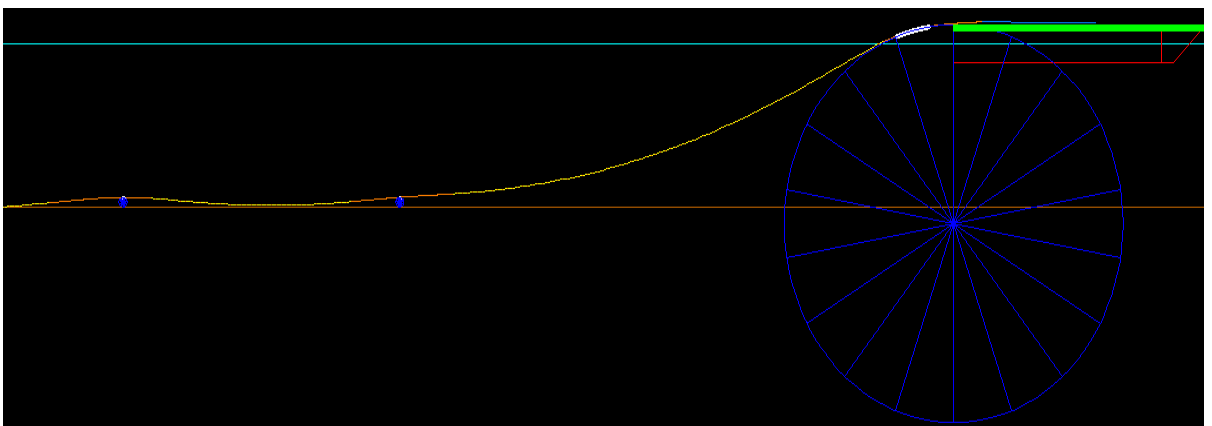


**Figure E-8. Simulation in OrcaFlex when the pipeline was laid onto two obstacles with a tension force of 3.5 kg.**
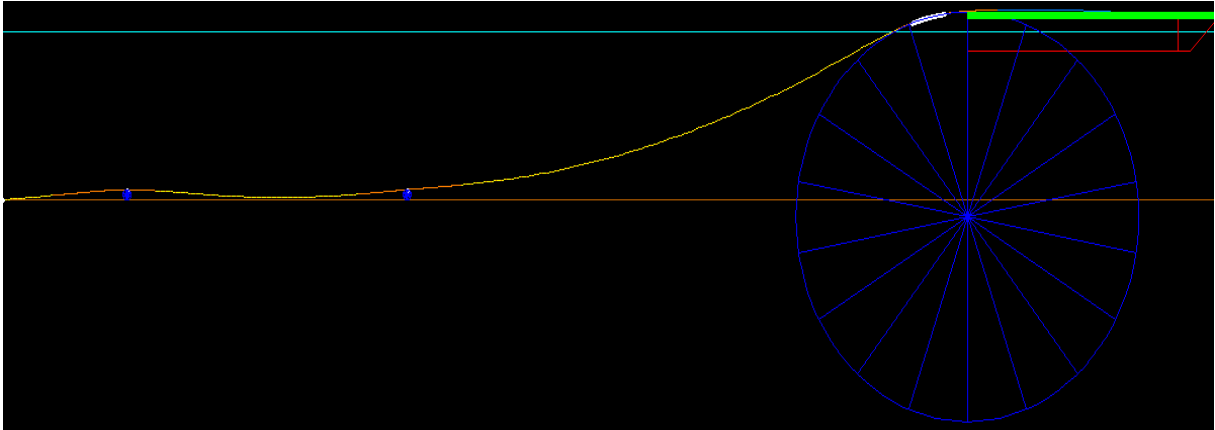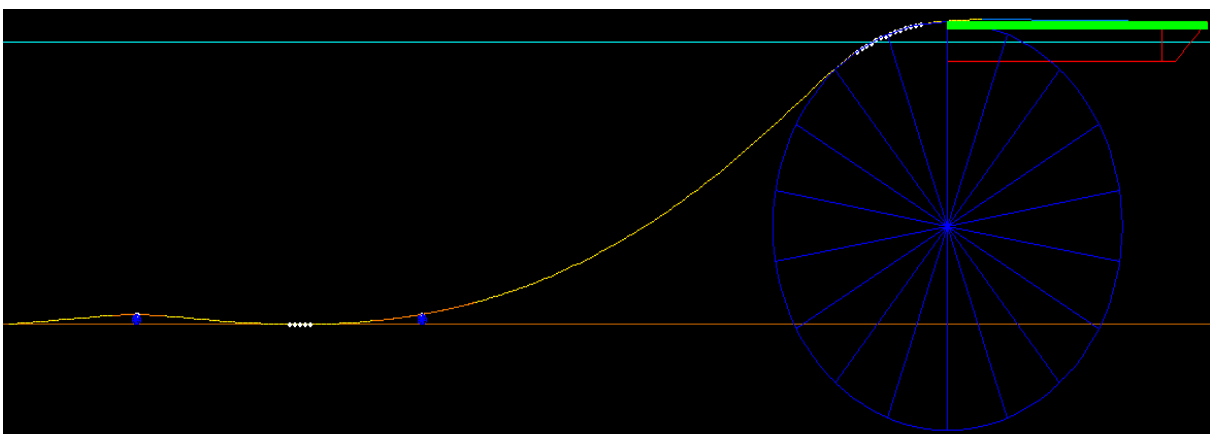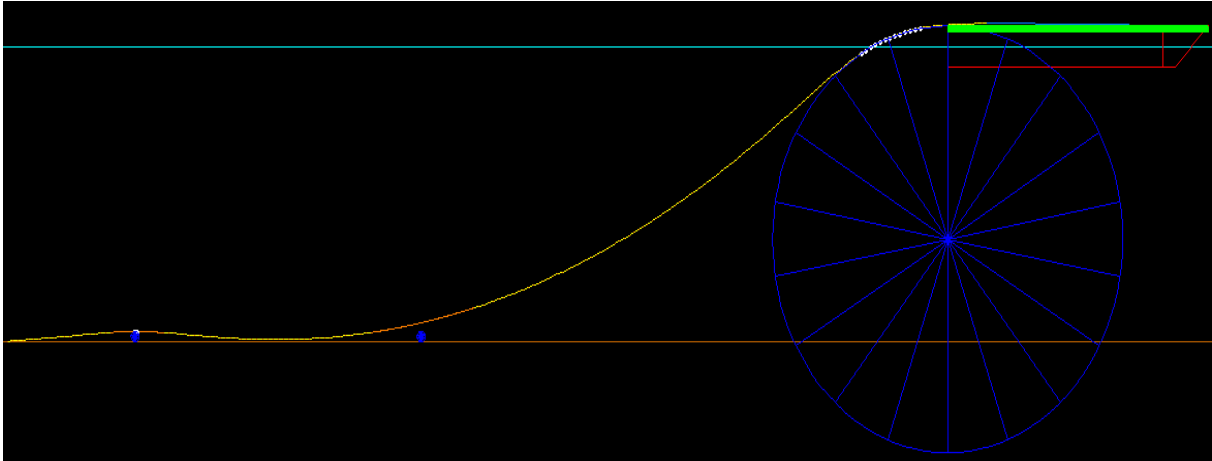
**Figure E-9. Simulation in OrcaFlex when the pipeline was laid onto two obstacles with a tension force of 4 kg.**
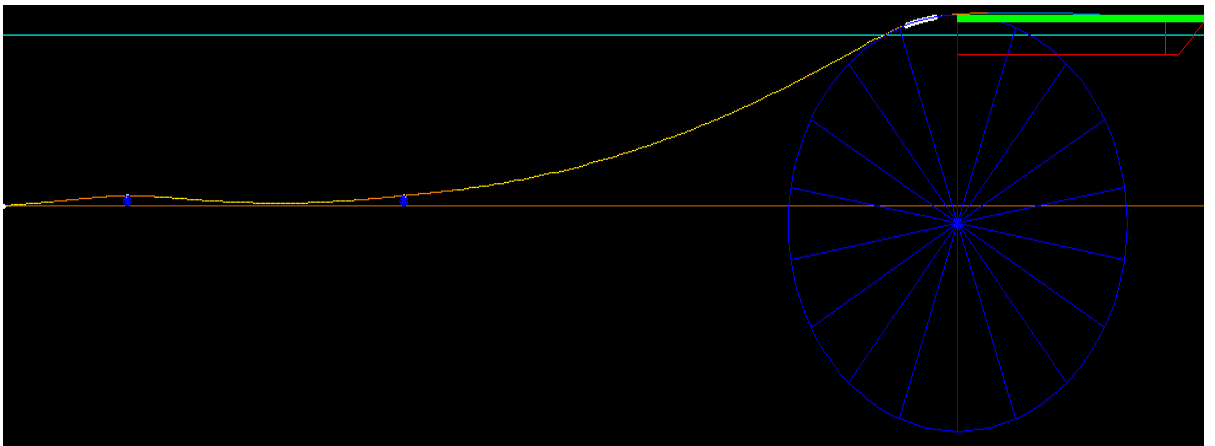


**Figure E-10. Simulation in OrcaFlex when the pipeline was laid onto two obstacles with a tension force of 4.5 kg.**

# Pipeline laid from 4.97 meters height:

## Long Span Model

One obstacle:



**Figure E-11. Simulation in OrcaFlex when the pipeline was laid onto one obstacle with a tension force of 3 kg.**



**Figure E-12. Simulation in OrcaFlex when the pipeline was laid onto one obstacle with a tension force of 3.5 kg.**
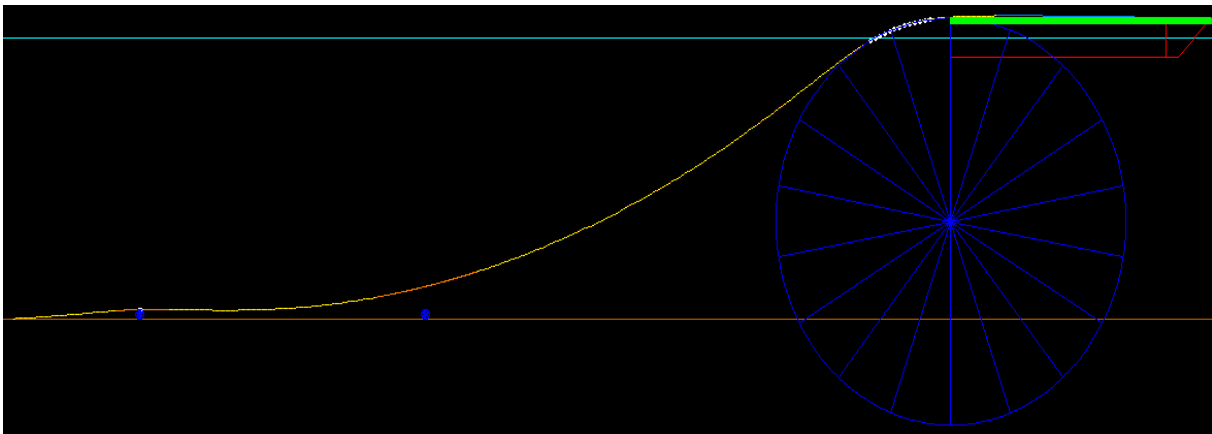
**Figure E-13. Simulation in OrcaFlex when the pipeline was laid onto one obstacle with a tension force of 4 kg.**



**Figure E-14. Simulation in OrcaFlex when the pipeline was laid onto one obstacle with a tension force of 4.5 kg.**

Two obstacles:



**Figure E-15.  Simulation in OrcaFlex when the pipeline was laid onto two obstacles with a tension force of 3 kg.**

**Figure E-16. Simulation in OrcaFlex when the pipeline was laid onto two obstacles with a tension force of 3.5 kg.**



**Figure E-17. Simulation in OrcaFlex when the pipeline was laid onto two obstacles with a tension force of 4 kg.**
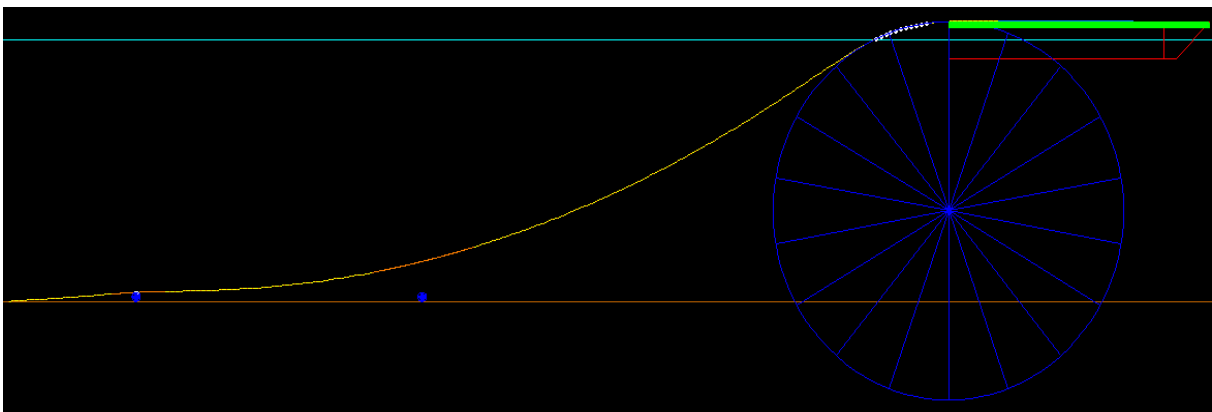


**Figure E-18. Simulation in OrcaFlex when the pipeline was laid onto two obstacles with a tension force of 4.5 kg.**
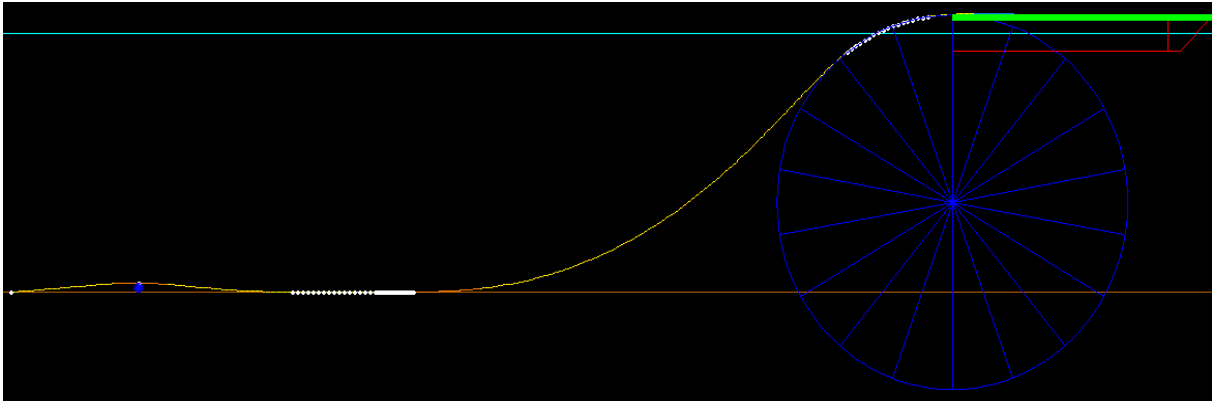
## Short Span Model:

One obstacle:



**Figure E-19. Simulation in OrcaFlex when the pipeline was laid onto one obstacle with a tension force of 3 kg.**
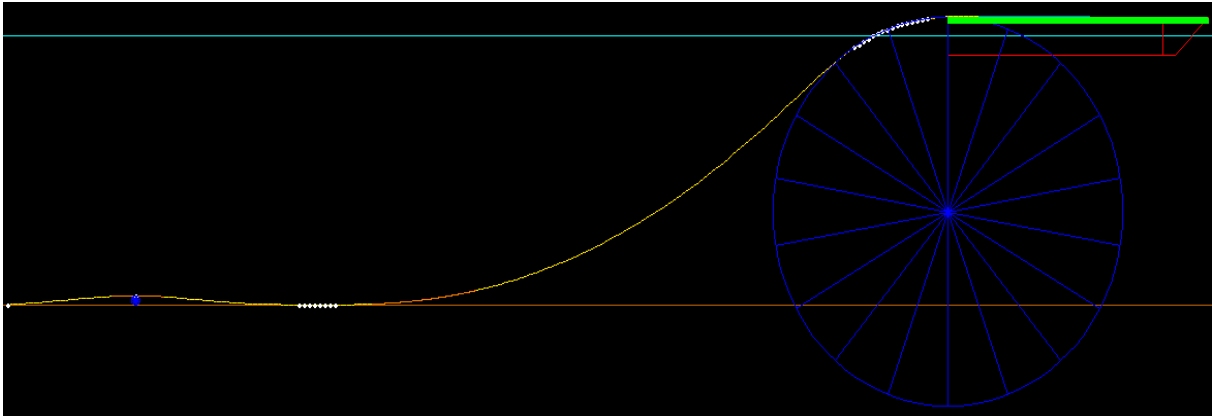


**Figure E-20. Simulation in OrcaFlex when the pipeline was laid onto one obstacle with a tension force of 3.5 kg.**
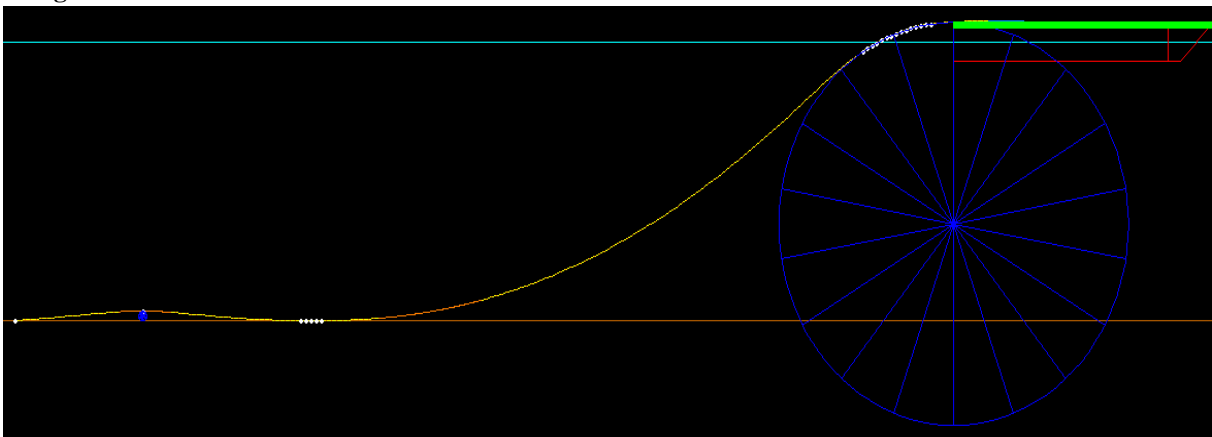


**Figure E-21. Simulation in OrcaFlex when the pipeline was laid onto one obstacle with a tension force of 4 kg.**
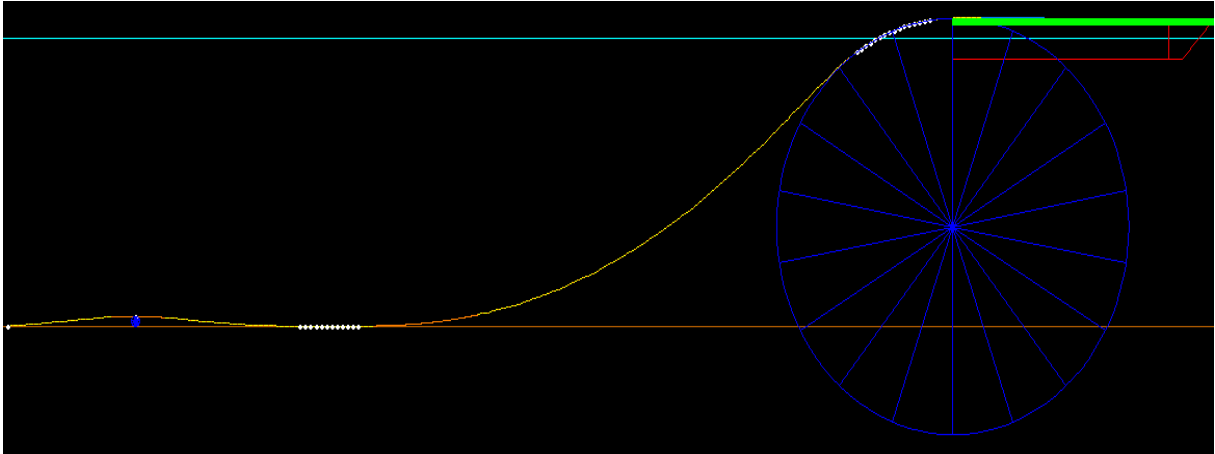
**Figure E-22. Simulation in OrcaFlex when the pipeline was laid onto one obstacle with a tension force of 4.5 kg.**
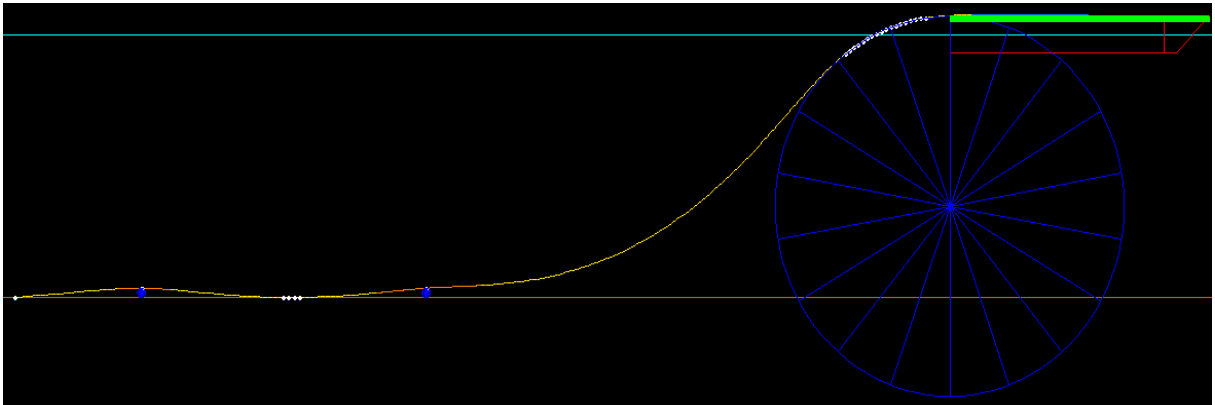
Two obstacles:



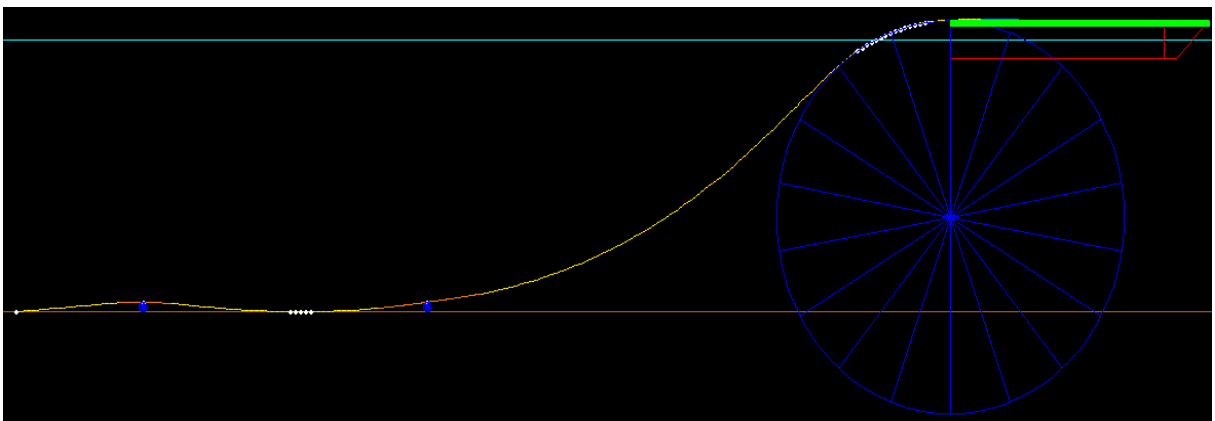**Figure E-23. Simulation in OrcaFlex when the pipeline was laid onto two obstacles with a tension force of 3 kg.**



**Figure E-24. Simulation in OrcaFlex when the pipeline was laid onto two obstacles with a tension force of 3.5 kg.**
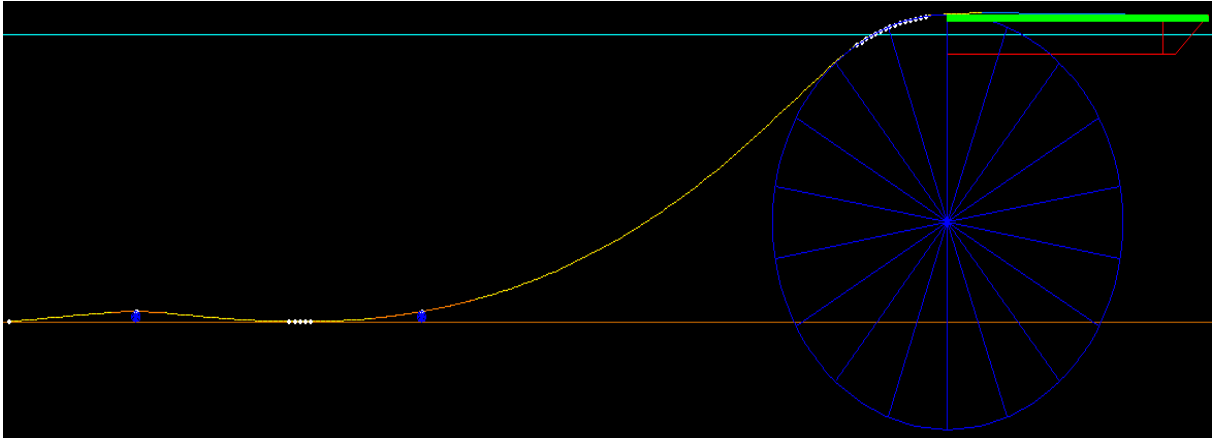
XXXVI

**Figure E-25. Simulation in OrcaFlex when the pipeline was laid onto two obstacles with a tension force of 4 kg.**
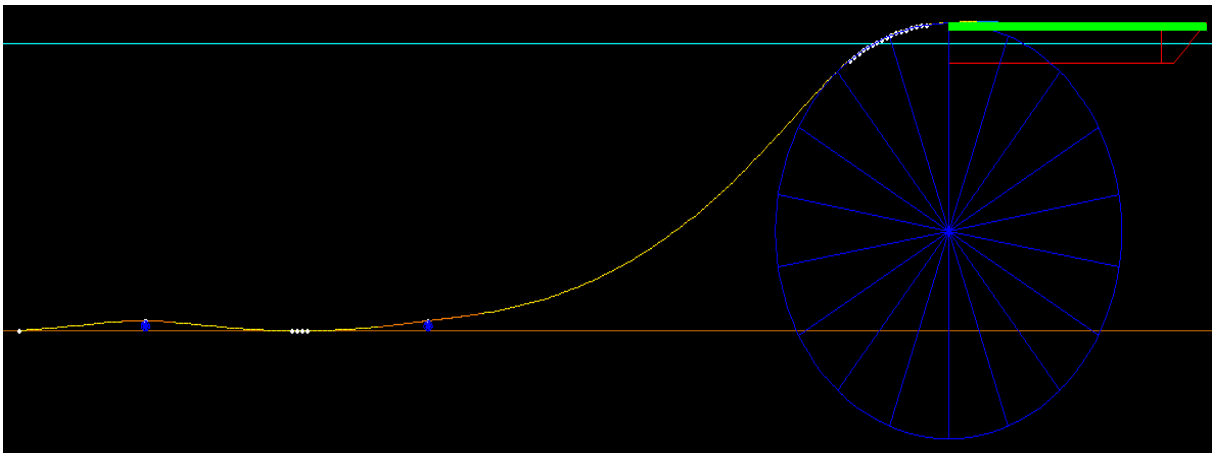


**Figure E-26. Simulation in OrcaFlex when the pipeline was laid onto two obstacles with a tension force of 4.5 kg.**

## Appendix F;        Scaling calculations

## For a 36 inch steel pipe:

| | |
|---|---|
| Scaling ratio: | 1:114 |
| Young's Modulus copper: | $1.2 \cdot 10^{11} \frac{N}{m^2}$ |
| Young's Modulus Steel: | $2.1 \cdot 10^{11} \frac{N}{m^2}$ |
| Length of copper pipe: | 20 m |
| Length of steel pipe: | 2280 m (20 m*114) |
| External diameter of copper pipe: | 0.008 m |
| External diameter of steel pipe: | 0.91 m |
| Wall thickness of copper pipe: | 0.001 m |
| Wall thickness of steel pipe: | 0.0312268 m |
| Density steel: | $7850 \frac{kg}{m^3}$ |
| Density water: | $1025 \frac{kg}{m^3}$ |

**Condition:**

$\frac{w \cdot L^3}{E \cdot t \cdot D^3}$  has to be approximately the same for both models.

For copper pipe used in test:

$$\frac{0.186 \cdot 20^3}{1.2 \cdot 10^{11} \cdot 0.001 \cdot 0.008^3} = 24.2188$$

Since it is a relation between two terms it does not matter if the weight of the pipeline is in kg or Newton.

Cross-sectional area of the steel pipe:

$$A = \pi \cdot (\frac{0.91}{2})^2 - \pi \cdot (\frac{0.91}{2} - 0.0312268)^2$$
$$A = 0.0862 \, m^2$$

Weight of steel pipe:

$$w = 0.0862 \cdot 7850$$
$$w = 676.74 \; \frac{kg}{m}$$

Submerged weight of steel pipe:

$$w = 676.74 - 1025 \cdot \pi \cdot \left(\frac{0.91^2}{2}\right)$$
$$w = 10.095 \; \frac{kg}{m}$$

$$\frac{10.095 \cdot 2280^3}{2.1 \cdot 10^{11} \cdot 0.0312268 \cdot 0.91^3} = 24.2128 \approx 24.2188$$

One can see that for a 36 inch steel pipeline with wall thickness of approximately 31 millimetres the similarity of the condition between the steel model and the copper pipe was quite good.
It is worth noticing that for the copper model the weight of the pipeline in air is used and not submerged weight since the experiments were done in air.

## For a 20 inch steel pipe:

Scaling ratio:                     1:63.5
External diameter of steel pipe:   0.508 m
Wall thickness:                    0.017655 m
Length of steel pipe:              1270 m (20 m·63.5)

Cross-sectional area of the steel pipe:

$$A = \pi \cdot \left(\frac{0.508}{2}\right)^2 - \pi \cdot \left(\frac{0.508}{2} - 0.017655\right)^2$$
$$A = 0.0272 \; m^2$$

Weight of steel pipe:

$$w = 0.0272 \cdot 7850$$

$$w = 213.496 \ \frac{kg}{m}$$

Submerged weight of steel pipe:

$$w = 213.496 - 1025 \cdot \pi \cdot \left(\frac{0.508^2}{2}\right)$$

$$w = 5.746 \ \frac{kg}{m}$$

$$\frac{5.746 \cdot 1270^3}{2.1 \cdot 10^{11} \cdot 0.017655 \cdot 0.508^3} = 24.2140 \approx 24.2188$$

This means that for a 20 inch steel pipeline, the condition will fit quite well when the wall thickness is 17.7 millimetres.

## Appendix G;    Calculation of axial and bending stiffness of the pipeline

Bending stiffness:

$$S_b = E \cdot I$$

$$I = \frac{\pi}{64}(D_o^4 - D_i^4)$$

Where,
$D_0$ = External diameter of pipeline
$D_i$ = Internal diameter of pipeline

$$I = \frac{\pi}{64}(0.008^4 - 0.006^4)$$

$$I = 1.374 \cdot 10^{-10} m^4$$

$$S_b = 1.2 \cdot 10^{11} \cdot 1.374 \cdot 10^{-10}$$

$$\boldsymbol{S_b = 16.49\ Nm^2}$$

Axial stiffness:

$$S_a = E \cdot A$$

$$S_a = 1.2 \cdot 10^{11} \cdot \pi \cdot 0.004^2 - \pi \cdot 0.003^2$$

$$\boldsymbol{S_a = 2638.9\ KN}$$

## Appendix H;    Calculations of theoretical bending strain in the overbend

According to Equation 4.1 the bending strain can be calculated by:

$$\varepsilon = \frac{D}{2R}$$

$$\varepsilon = \frac{0.008\ m}{2 \cdot 3.36\ m}$$

$$\boldsymbol{\varepsilon = 0.119\ \%}$$